

HUMBOLDT-UNIVERSITÄT ZU BERLIN



LEBENSWISSENSCHAFTLICHE FAKULTÄT  
INSTITUT FÜR BIOLOGIE

BACHELORARBEIT

ZUM ERWERB DES AKADEMISCHEN GRADES BACHELOR OF  
SCIENCE

A physiologically based pharmacokinetic (PBPK) model of the probe drug talinolol for the characterization of intestinal P-glycoprotein

Ein physiologisch basiertes pharmakokinetisches (PBPK) Modell von Talinolol zur Charakterisierung des intestinalen P-Glykoproteins

vorgelegt von

**Beatrice Amelie Stemmer Mallol**

Matrikelnummer: 584955

E-Mail: stemallb@hu-berlin.de

Geburtsdatum und -ort: 07.05.1998 Paris

angefertigt in der Arbeitsgruppe Systems Medicine of the Liver  
am Institut für Theoretische Biologie  
Berlin, im Juli 2023

Erstprüfer: **Dr. Matthias König**

Zweitprüfer: **Prof. Dr. Hanspeter Herz**

# Contents

|                   |                                                              |           |
|-------------------|--------------------------------------------------------------|-----------|
| <b>1</b>          | <b>Introduction</b>                                          | <b>5</b>  |
| 1.1               | Talinolol . . . . .                                          | 5         |
| 1.2               | P-glycoprotein (P-gp) . . . . .                              | 5         |
| 1.3               | Talinolol pharmacokinetics . . . . .                         | 5         |
| 1.4               | Intestinal architecture . . . . .                            | 7         |
| 1.5               | Genotypes and genetic variants . . . . .                     | 8         |
| 1.5.1             | P-glycoprotein . . . . .                                     | 8         |
| 1.5.2             | OATP2B1 . . . . .                                            | 9         |
| 1.5.3             | OATP1B1 . . . . .                                            | 9         |
| 1.6               | Physiologically based pharmacokinetic (PBPK) model . . . . . | 10        |
| 1.7               | Question, scope and hypotheses . . . . .                     | 10        |
| <b>2</b>          | <b>Methods</b>                                               | <b>11</b> |
| 2.1               | Literature research . . . . .                                | 11        |
| 2.2               | Data curation . . . . .                                      | 11        |
| 2.3               | Pharmacokinetic parameters . . . . .                         | 11        |
| 2.4               | Physiologically based pharmacokinetic (PBPK) model . . . . . | 12        |
| 2.5               | Parameter fitting . . . . .                                  | 13        |
| <b>3</b>          | <b>Results</b>                                               | <b>14</b> |
| 3.1               | Talinolol data . . . . .                                     | 14        |
| 3.2               | Computational model of talinolol . . . . .                   | 16        |
| 3.2.1             | Physiologically based pharmacokinetic (PBPK) model . . . . . | 16        |
| 3.2.2             | Intestinal model . . . . .                                   | 17        |
| 3.2.3             | Kidney model . . . . .                                       | 21        |
| 3.2.4             | Liver model . . . . .                                        | 21        |
| 3.2.5             | Model of cirrhosis and renal impairment . . . . .            | 22        |
| 3.3               | Parameter fitting . . . . .                                  | 23        |
| 3.4               | Model performance . . . . .                                  | 25        |
| 3.4.1             | Single dose intravenous . . . . .                            | 25        |
| 3.4.2             | Single dose oral . . . . .                                   | 26        |
| 3.4.3             | Multiple dose oral . . . . .                                 | 29        |
| 3.5               | Model application . . . . .                                  | 31        |
| 3.5.1             | Effect of P-glycoprotein activity . . . . .                  | 31        |
| 3.5.2             | Effect of OATP1B1 activity . . . . .                         | 34        |
| 3.5.3             | Effect of OATP2B1 activity . . . . .                         | 35        |
| 3.5.4             | Effect of renal function . . . . .                           | 37        |
| 3.5.5             | Site-dependency of intestinal absorption . . . . .           | 39        |
| 3.6               | Summary . . . . .                                            | 41        |
| <b>4</b>          | <b>Discussion</b>                                            | <b>42</b> |
| 4.1               | Data . . . . .                                               | 42        |
| 4.2               | Model . . . . .                                              | 42        |
| 4.3               | Genetic variants . . . . .                                   | 44        |
| 4.4               | Disease . . . . .                                            | 44        |
| <b>5</b>          | <b>Outlook</b>                                               | <b>45</b> |
| 5.1               | Drug-drug interactions . . . . .                             | 45        |
| 5.2               | Drug formulations . . . . .                                  | 45        |
| 5.3               | Gastrointestinal surgery . . . . .                           | 45        |
| <b>6</b>          | <b>Supplement</b>                                            | <b>47</b> |
| <b>References</b> |                                                              | <b>53</b> |

## **Acronym**

|                |                                                          |
|----------------|----------------------------------------------------------|
| <b>ABCB1</b>   | ATP Binding Cassette B1                                  |
| <b>AUC</b>     | Area Under the Curve                                     |
| <b>Cl</b>      | Clearance                                                |
| <b>Cmax</b>    | Maximum concentration                                    |
| <b>CR</b>      | Controlled-Release Tablet                                |
| <b>CYP3A4</b>  | Cytochrome P450 3A4                                      |
| <b>IR</b>      | Immediate-Release Tablet                                 |
| <b>IV</b>      | Intravenous                                              |
| <b>Kel</b>     | Elimination rate                                         |
| <b>MRP2</b>    | Multidrug Resistance-Associated Protein 2                |
| <b>OATP</b>    | Organic Anionic Transport Polypeptide                    |
| <b>OATP1B1</b> | Organic Anionic Transport Polypeptide 1B1                |
| <b>OATP2B1</b> | Organic Anionic Transport Polypeptide 2B1                |
| <b>ODE</b>     | Ordinary Differential Equation                           |
| <b>PBPK</b>    | Physiologically Based Pharmacokinetic                    |
| <b>P-gp</b>    | P-glycoprotein                                           |
| <b>PO</b>      | Per Oral                                                 |
| <b>SBML</b>    | Systems Biology Markup Language                          |
| <b>SLCO1B1</b> | Solute Carrier Organic Anion Transporter Polypeptide 1B1 |
| <b>SLCO2B1</b> | Solute Carrier Organic Anion Transporter Polypeptide 2B1 |
| <b>SNP</b>     | Single Nucleotide Polymorphism                           |
| <b>Thalf</b>   | Half-Life                                                |

# **Abstract**

## **English**

Talinolol is a cardioselective beta-blocker used for the treatment of various cardiovascular diseases and tachyarrhythmia. The gastrointestinal absorption of talinolol is determined via its uptake in the intestine via the organic anion transporting polypeptide 2B1 (OATP2B1) and its efflux via the P-glycoprotein (P-gp). After intestinal absorption talinolol can be transported into the liver via OATP1B1 talinolol where it undergoes enterohepatic circulation. Talinolol is excreted unchanged in the urine and feces.

In addition to its clinical application, talinolol is widely used as a probe drug for the intestinal efflux transporter P-glycoprotein. P-gp plays a crucial role in the human body as it is expressed in various tissues to protect against potentially toxic substances, facilitating the elimination of xenobiotics. The application of talinolol for P-gp phenotyping enables evaluation of factors influencing P-gp-mediated transport *in vivo* such as genetic polymorphisms of P-gp as well as the distribution of P-gp along the intestine.

Within this thesis, an extensive dataset of talinolol pharmacokinetics was established and used to develop a physiologically based pharmacokinetic (PBPK) model for talinolol. The model was applied to investigate the influence of various factors on the pharmacokinetics of talinolol, including: (i) genetic variants of P-gp; (ii) enzymatic activity of the transporters OATP2B1 and OATP1B1; (iii) site-specific distribution of P-gp and OATP2B1 proteins in the intestine, and (iv) the impact of diseases such as liver cirrhosis and renal dysfunction.

The model enables precise predictions of the concentration-time profile of talinolol in various tissues following oral or intravenous administration. Furthermore, the model accurately describes the effect of genetic variants of P-gp on the pharmacokinetics of talinolol. The detailed description of the limiting intestinal absorption of intestinal provided by the model, along with the precise prediction of talinolol's pharmacokinetics in different renal functions, holds significant clinical relevance.

## **German**

Talinolol ist ein kardioselektiver Betablocker, der zur Behandlung verschiedener kardiovaskulärer Erkrankungen und Tachyarrhythmien eingesetzt wird. Die gastrointestinale Absorption von Talinolol erfolgt über die Aufnahme im Darm über das organische anionische Transportpeptid 2B1 (OATP2B1) und den Efflux über das P-Glykoprotein (P-gp). Nach der intestinalen Absorption kann Talinolol über OATP1B1 in die Leber transportiert werden, wo es einem enterohepatischen Kreislauf unterliegt. Talinolol wird unverändert über den Urin und den Stuhl ausgeschieden.

Neben seiner klinischen Anwendung wird Talinolol häufig als Testsubstanz für den intestinalen Effluxtransporter P-Glykoprotein verwendet. P-gp spielt eine entscheidende Rolle im menschlichen Körper, da es in verschiedenen Geweben exprimiert wird, um vor potenziell toxischen Substanzen zu schützen und die Eliminierung von Xenobiotika zu erleichtern. Die Anwendung von Talinolol zur Phänotypisierung von P-gp ermöglicht die Bewertung von Faktoren, die den P-gp-vermittelten Transport *in vivo* beeinflussen, wie genetische Polymorphismen von P-gp sowie die Verteilung von P-gp entlang des Darms.

Im Rahmen dieser Arbeit wurde ein umfangreicher Datensatz zur Pharmakokinetik von Talinolol erstellt und zur Entwicklung eines physiologisch basierten Pharmakokinetik (PBPK)-Modells für Talinolol verwendet. Das Modell wurde angewendet, um den Einfluss verschiedener Faktoren auf die Pharmakokinetik von Talinolol zu untersuchen, einschließlich: (i) genetische Varianten von P-gp; (ii) enzymatische Aktivität der Transporter OATP2B1 und OATP1B1; (iii) ortspezifische Verteilung von P-gp- und OATP2B1-Proteinen im Darm und (iv) Auswirkungen von Krankheiten wie Leberzirrhose und Nierenfunktionsstörungen.

Das Modell ermöglicht präzise Vorhersagen des Konzentrations-Zeit-Verlaufs von Talinolol in verschiedenen Geweben nach oraler oder intravenöser Verabreichung. Darüber hinaus ist das Modell in der Lage den Effekt von genetischen Varianten des P-gp auf die Pharmakokinetik Talinolols wieder zu geben. Von großer klinischer Bedeutung ist die detaillierte Beschreibung der limitierenden intestinalen Absorption durch das Modell sowie die genaue Vorhersage der Pharmakokinetik von Talinolol für unterschiedlichen Nierenfunktionen.

# 1 Introduction

The beta-blocker talinolol is used in the treatment of cardiovascular diseases, including arterial hypertension and coronary heart failure. In addition, talinolol is an important probe drug for the intestinal P-glycoprotein (P-gp) and organic anion transporter proteins (OATP).

## 1.1 Talinolol

Talinolol is a highly cardioselective antagonist of  $\beta 1$ -adrenoceptors. By blocking these receptors, beta-blockers can reduce heart rate, blood pressure, and cardiac output, thereby decreasing the heart's workload. This can be beneficial in conditions such as hypertension, heart failure and angina pectoris [15]. A daily dose of 50 - 300 mg is recommended [54, 24, 15, 49]. In 1975, talinolol (Cordanum, Arzneimittelwerk Dresden GmbH, Dresden, Germany) was introduced in Germany and Eastern Europe [18].

Talinolol consists of a 1:1 racemate mixture of R- and S-talinolol [6, 91, 97]. However, it is not undergoing enantiomer specific kinetic behavior. Talinolol shows low plasma protein binding [83], minor enterohepatic recirculation [77, 91], and no significant first pass metabolism [81] which makes it a very good model substrate for phenotyping enzymes involved in talinolol pharmacokinetics such as P-gp and OATP transporters [82, 68].

## 1.2 P-glycoprotein (P-gp)

The efflux transporter P-gp, also known as multi-drug resistance protein 1 (MDR1), is part of the ATP-binding cassette (ABC) transporter superfamily and is encoded by the ABCB1 gene [8]. P-gp is localized in the enterocytes of the small intestine, the canalicular membrane of the liver, the proximal renal tubular cells and the blood-brain barrier [16, 79]. P-gp transports numerous substances out of the cell along the apical side under ATP consumption [16]. Thus, it causes both limited absorption and excretion of substances and detoxification of organs. P-gp plays an important role in the outward transport of talinolol in the small intestine [18].

## 1.3 Talinolol pharmacokinetics

The main processes affecting talinolol pharmacokinetics are absorption, distribution, metabolism and excretion, in short: ADME.

**Absorption** Talinolol can be administered via different routes, either orally, intravenously, or by intestinal infusion. The most common form of administration is a tablet that dissolves in the stomach. Different formulations of talinolol tablets exist, which can be distinguished in immediate- and controlled-released. These formulations have different release kinetics, with immediate-release tablets releasing almost the entire dose within three hours. In contrast, controlled-release tablets have slower release times and significantly reduced bioavailability [83]. Due to the long half-life of 10-32 h, talinolol can be taken once daily [83, 89].

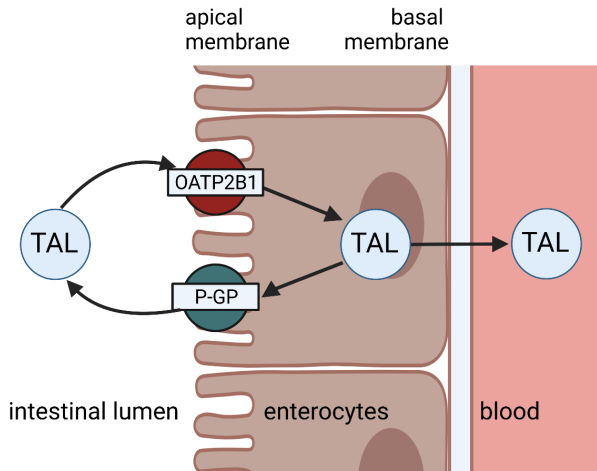


**Figure 1: Absorption of talinolol.** In the intestine, talinolol is taken up via the OATP2B1 transporter into the enterocytes from which it is further transported into the bloodstream. P-gp functions as an efflux transporter of talinolol which exports part of the talinol back into the intestinal lumen. The interplay between OATP2B1 and P-gp and the site-dependent distributions of these transporters influence the amount of talinol absorbed in the systemic circulation. Created with <https://biorender.com>.

Once talinolol reaches the small intestine, it is absorbed across the apical membrane of the enterocytes by the uptake transporter OATP2B1 (Fig. 1). OATP2B1 belongs to the family of organic anion-transporting polypeptides (OATP), which are key transporters not only in the intestine but also in the kidney and liver. Their substrates include a wide range of xenobiotics such as talinolol, endogenous molecules, and food components.

Talinolol is an important substrate of the P-gp [82] and can consequently be applied as a probe drug to characterize P-gp by the use of talinolol pharmacokinetics. P-gp can export talinolol from the enterocytes to the intestine across the apical membrane. This reverse efflux transport leads to limited absorption and pre-systemic elimination, resulting in an oral availability of 55 - 75 % for talinolol [81, 18, 17, 5, 64].

The activity of the transporters, P-gp and OATP2B1, have a decisive impact on the disposition of talinolol, see Fig. 1. Genetic variants of these transporters and drug-drug interactions can have a particular influence on their activity. For instance, rifampicin and St. Johns wort have been identified as substrates of the pregnant X receptor (PXR) which positively affects the expression of P-gp due to the resulting ligand-activated transcription process [4, 11, 23]. In contrast, drugs, such as erythromycin, inhibit P-gp activity [66].

A second protein which could play a role in the reverse transport from enterocytes is the multi-drug resistance-associated protein 2 (MRP2) [17].

**Distribution and Metabolism** Blood from the intestine enters the liver via the portal vein. Here, the liver-specific uptake transporter OATP1B1 in the sinusoidal membrane of hepatocytes is involved in the uptake of talinolol [5]. In the liver, a small amount of talinolol undergoes metabolism (< 1 %) via CYP3A4 dependent hydroxylation of talinolol to 2-cis, 3-cis, 3-trans, and 4-trans talinolol with 4-trans talinolol accounting for the largest fraction of metabolites [5, 62, 81, 97].

Talinolol is removed from the liver via biliary excretion. P-gp is not only localized at the apical membranes of intestinal enterocytes, but also at the bile canalicular side of the hepatocytes, responsible for the efflux of talinolol from the liver into the bile which is secreted into the intestinal lumen. Consequently, talinolol can be reabsorbed from the

intestine, a process called enterohepatic circulation. *Terhaag et al.* (1989) [77], *Wetterich et al.* (1996) [91], and *Haustein et al.* (1981) [24] showed that around 10 % of a talinolol dose are excreted via the bile. I.e., enterohepatic circulation is an important, but minor route of excretion.

**Excretion** Talinolol is eliminated from the body after oral administration via urinary excretion which contributes approximately 60 % and via feces contributing around 40 % [81, 83] (unabsorbed talinolol and talinolol via the enterohepatic circulation). Consequently, renal elimination is the major route of excretion and elimination of talinolol via the kidney is highly dependent on renal function [49]. In addition to the unchanged talinolol, minor quantities of talinolol metabolites can be found in urine and feces, with amounts in each being comparable but very low [5, 81, 62].

## 1.4 Intestinal architecture

Significant parameters affecting oral drug absorption include the anatomy and enzyme distribution of uptake and efflux transporters within the intestine.

The intestine, along with the esophagus, stomach, liver, and bile, is part of the gastrointestinal tract and can be divided into the small intestine and colon, whereby the small intestine plays a central role in the absorption of substances. With a length of 4.45 - 6.6 m, the small intestine comprises the longest section of the gastrointestinal tract which can be differentiated into three sections: duodenum, jejunum, and ileum, see Fig. 2.

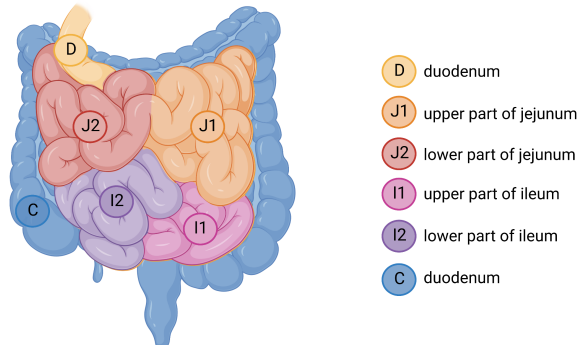


**Figure 2: Intestinal anatomy.** The intestine is divided into the duodenum, the upper and lower part of the jejunum, the upper and lower part of the ileum, and the colon. Created with <https://biorender.com>.

The intestine is lined with enterocytes, in whose membrane the transporters relevant for talinolol disposition are localized. Whereas the mRNA expression and protein amount of OATP2B1 is constant along the small intestine, a significant increase in both mRNA expression and protein amount of P-gp can be observed from duodenum, over the jejunum to the ileum [10]. The transporter distribution along the intestine forms an absorption window for talinolol in the upper region of the small intestine.

Important experiments to determine the absorption of talinolol in different regions of the intestine are site-specific infusions of talinolol. For instance, the results of *Gramatte et al.* (1996) [18] supported the assumption of a regioselective absorption of talinolol.

## 1.5 Genotypes and genetic variants

Genetic polymorphisms which alter the enzyme activity P-gp in the intestine and liver and the OATP isoforms OATP2B1 in the intestine and OATP1B1 could have a major effect on talinolol pharmacokinetics. Most genetic polymorphisms are due to single nucleotide polymorphisms (SNPs), which can affect the expression and protein's function.

### 1.5.1 P-glycoprotein

Large variability of P-gp expression and activity exists between individuals [5]. P-gp is encoded by the gene ABCB1 with an important SNP being 3435C>T [28]. Other SNPs are on exon 12 (1236C>T) and 21 (2677G>T/A) [28, 52].

The wobble polymorphism 3435C>T and 1236C>T have no impact on the amino acid sequence, whereas 2677G>T/A results in the incorporation of Thr or Ala, respectively, instead of Ser at position 893 [3]. The mutations of 1236C>T and 2677G>T on exon 12 and 21, respectively, are inherited more frequently than expected by chance with the mutations 3435C>T on exon 26 and are thereby in linkage equilibrium [96, 29, 38]. This suggests that there may exist a correlation between these specific genetic variants.

The genetic polymorphism of ABCB1 may affect the mRNA expression, protein amount and protein activity of P-gp resulting in altered pharmacokinetics of talinolol.

*Schwarz et al.* (2007) [64] found a correlation between SNPs of ABCB1 and its reduced duodenal mRNA expression, for 1236C>T, 2677G>T/A individually, and in combination with the 3435C>T polymorphic genotype. However, contrasting findings from other studies suggest that the homozygous 3435TT genotype is responsible for the reduction in P-gp expression [28, 38], and that none of the three polymorphisms have an effect on the expression of P-glycoprotein [70]. Therefore, there is conflicting evidence regarding the impact of these SNPs on P-glycoprotein expression. Nonetheless, there is a clear consensus in the literature that there is a positive correlation between the expression of duodenal ABCB1 mRNA and the bioavailability of orally administered talinolol [5, 6, 64].

Similarly, the influence of these SNPs on pharmacokinetics is also inconclusive. Several studies have found no significant effect of the genetic variants 3435C>T and the combination 2677G>T/A and 3435C>T on the pharmacokinetics of talinolol [5, 6, 22, 70, 96]. However, a trend has been observed in the literature that with an increasing number of SNPs in exons 12, 21, or 26, the AUC of talinolol decreases [26, 64]. Particularly comprehensive results were presented by *Schwarz et al.* (2007) [64]: For the 1236CC genotype, AUC of  $1012 \pm 510$  ng·h/ml were measured, for CT  $692 \pm 407$  ng·h/ml; for 2677GG,  $1012 \pm 510$  ng·h/ml was measured, for GT  $715 \pm 466$  ng·h/ml, and for TA  $597$  ng·h/ml; for 3435CC,  $1281 \pm 701$  ng·h/ml was measured, for CT  $730 \pm 359$  ng·h/ml, and for TT  $564$  ng·h/ml. This trend is supported by the combination of polymorphisms in exons 12/21/26, which exhibit lower AUC compared to the wild type. In comparison to most studies, *Schwarz et al.* (2005) [64] and *Wang et al.* (2013) [87] not only observed generally lower plasma concentrations of talinolol but also found no difference or lower concentrations for the wild-type 3435CC compared to 3435TT (cmax  $584.9 \pm 115.2$  vs.  $500.3 \pm 96.2 \frac{ng}{ml}$ , p<0.05 und auc.inf  $12681.2 \pm 4828.2$  vs.  $9000.8 \pm 3153.2$  ng·h/ml, p<0.05). This observation regarding the AUC of talinolol in the blood was further supported by *Siegmund et al.* (2002) [70] for the 2677TT/AT genotype compared to the wild-type.

### 1.5.2 OATP2B1

OATP2B1 (Organic Anion Transporting Polypeptide 2B1), encoded by the gene SLCO2B1, is a protein that belongs to the solute carrier organic anion transporter family [76].

*Kobayashi et al.* (2003) [40] showed that OATP2B1 is localized at the apical membrane of enterocytes in the intestine, in addition to the liver [86] and other tissues [50]. The studies by *Drozdik et al.* (2014, 2019) [10, 9] and *Meier et al.* (2007) [53] led to the finding that mRNA expression and protein levels of OATP2B1 differ slightly between segments of the intestine.

Besides some endogenous molecules, xenobiotics are among the main substrates of OATP2B1. For instance statins, antibiotics, and besides talinolol also, other probe drugs of P-gp (e.g., fexofenadine) are transported via OATP2B1 [39]. Polymorphisms in the SLCO2B1 gene can lead to variations in the expression and function of OATP2B1, which can influence the pharmacokinetics and pharmacodynamics of drugs transported by this transporter [55].

The nucleotide exchanges C1457C>T and G935G>A lead to a change in the amino acid Ser486Phe and Arg312Gln, respectively [39].

Not much has been reported about the effect of polymorphisms of OATP2B1 on the absorption of talinolol. For other substrates, such as fexofenadine [33] and the beta-blocker celiprolol [32], the genetic variant SLCO2B1\*3 with mutation c.1457C>T was associated with reduced transport activity compared with wild-type SLCO2B1\*1. The opposite was shown by *Akamine et al.* (2010) [2].

The high allele frequency of 31 % of the SLCO2B1\*3 genotype in Japan [61] is especially remarkable. In contrast, the allele frequency of 2.8 % in Finns [51] is much lower.

It should be further noted that OATP2B1 has similar but lower substrate selectivity than the liver-specific OATP1B1. In addition, the expression and amount of OATP2B1 transporter is over 10-fold smaller in the basolateral membrane of hepatocytes compared to OATP1B1 [60, 9].

As mentioned by *Nakaishi et al.* (2012) [57], OATP2B1 is likely important for drug absorption from the small intestine, while OATP1B1 plays a determinant role in hepatic basolateral uptake.

### 1.5.3 OATP1B1

The findings of *Bernsdorf et al.* (2006) [5] provide evidence that OATP1B1 plays a crucial role in the hepatic uptake of talinolol. OATP1B1, encoded by the SLCO1B1 gene [1], is a liver-specific uptake transporter [44], and various SNPs exist for this gene, similar to ABCB1.

Of particular interest are the SNPs 388A>G and 521T>C, which result in amino acid substitutions of Asn to Asp and Val to Ala, respectively. The wild-type allele is denoted as \*1a for the 388A-521T genotype. The other polymorphisms are described by the following alleles: \*1b (388G-521T), \*5 (388A-521C), and \*15 (388G-521C) [72, 80].

Interestingly, individuals with the SLCO1B1\*1b allele exhibit increased protein activity and higher fecal excretion compared to the wild-type SLCO1B1a/\*1a genotype. Consequently, talinolol is more efficiently absorbed into the liver in individuals with the \*1b allele, resulting in a significantly reduced half-life when compared to the wild-type genotype ( $12.2 \pm 1.6$  h vs.  $14.5 \pm 1.4$  h,  $p = 0.01$ ) [5].

These findings highlight the importance of genetic variations in SLCO1B1 and their impact on talinolol pharmacokinetics, providing insights into interindividual variability in drug response.

## 1.6 Physiologically based pharmacokinetic (PBPK) model

Physiologically based pharmacokinetic (PBPK) models allow mathematical description and simulation of drug pharmacokinetics based on coupled ordinary differential equations (ODE). For this purpose, physiological and pharmacokinetic parameters and biochemical reactions are included in the model enabling a precise description of the respective compartments and transport via the blood via the systemic circulation. This serves as a basis for the generation of predictive simulations.

Such models are a unique tool to study medical questions and test hypotheses *in silico*. Not only is it a useful method for predicting the pharmacokinetics of a drug, but also a great tool for studying metabolic phenotyping using test compounds (e.g. dextromethorphan [21], caffeine [19], or ICG [42]).

## 1.7 Question, scope and hypotheses

Within this project a PBPK model of the P-gp probe talinolol was developed and used to study the effect of P-gp and OATP activity on talinolol pharmacokinetics. Two applications are the study of the effect of genetic polymorphisms of these transporters or drug-drug interactions with P-gp and OATPs. Specifically, a PBPK model of talinolol was developed to systematically analyse the following questions:

- (i) What are the effects of genetic variants of P-glycoprotein, OATP2B1 and OATP1B1 on talinolol pharmacokinetics?
- (ii) What are the effects of changes in P-glycoprotein protein amount on talinolol pharmacokinetics?
- (iii) What is the role of enzyme distribution of OATP2B1 and P-gp within the intestine?
- (iv) How does hepatic and renal impairment affect talinolol pharmacokinetics?

The main objective was to describe the influence of P-gp on the talinolol pharmacokinetics and apply the model to clinically relevant questions such as: How is phenotyping via talinolol affected by changes in P-gp activity (genotypes, protein amounts)?

## 2 Methods

The main methods applied in this work were literature research, curation of pharmacokinetics data, calculation of pharmacokinetic parameters, and development of a PBPK model of talinolol, using parameter fitting for parameter optimization.

### 2.1 Literature research

For an overview of the available pharmacokinetic literature for talinolol, an initial search via PKPDAI for 'talinolol' was performed, a web service providing pharmacokinetic articles (<https://pkpdai.com/pkdocsearch>). The search results were extended via a Pubmed search with the search terms 'talinolol AND pharmacokinetics' (<https://pubmed.ncbi.nlm.nih.gov/?term=talinolol+AND+pharmacokinetics>).

The resulting publications were screened and filtered based on the following criteria: the clinical trials had to contain pharmacokinetic parameters or time-course data for talinolol. Data had to be for human subjects (i.e. other species were excluded such as rat or mouse). Main focus was on data in healthy subjects but data for renal impairment and hepatic impairment was included. Concerning the intervention, it was ensured that talinolol was administered at least once alone or as a co-medication with another substance. Also of high interest were studies that published information on genotypes of P-gp, OATP1B1, and OATP2B1 and associated mRNA or protein data. The literature corpus was extended by additional literature available in the primary references.

### 2.2 Data curation

Data regarding study design and pharmacokinetic parameters were extracted from the relevant studies and tabulated using LibreOffice based on established data curation workflows [20]. The study design provided information on the subjects, groups (genetic variants of enzymes), and intervention. Information about the subjects was anthropometric data (e.g., height and BMI), ethnicity, health status, lifestyle (e.g., non-smoking), and medication, such as oral contraceptives. In addition to the substance and dose administered, the intervention also indicates the route of administration (oral, intravenous, intestinal infusion) and the treatment course. Data on genetic variants and type of tablets (immediate- or slow release) were included when available. The numerical data contained in the charts and tables was manually extracted using the "PlotDigitizer" tool and digitized into spreadsheets. After creation of a standardized JSON file encoding the meta-data of the study, the curated data reviewed by a second curator and uploaded to the open database PK-DB (<https://pk-db.com>).

### 2.3 Pharmacokinetic parameters

The following pharmacokinetic parameters were calculated and used for evaluation of the predicted pharmacokinetics:

**Maximum concentration,  $c_{\max}$  [ $\mu\text{M}$ ]**  $c_{\max}$  is calculated from the maximum of the concentration curve.

**Area under the curve, AUC [ $\frac{\text{ng}\cdot\text{hr}}{\text{ml}}$ ]** AUC is proportional to the bioavailable amount of the drug of the administered dose and is calculated using the trapezoidal rule.  $AUC_{\text{end}}$  describes AUC up to the end time of measurement and can be described by the following equation 1:

$$AUC_{end} = \frac{1}{2} \sum_{i=1}^{n-1} ((t_{i+1} - t_i)(C_i - C_{i+1})) \quad (1)$$

$AUC_{inf}$  is the extrapolation of the  $AUC_{end}$  assuming mono-exponential decrease.

**Bioavailability, F [ % ]** The bioavailability expresses the proportion of the available amount of the drug to the administered dose. Accordingly, there is a bioavailability of 100 % when administered intravenously.

**Elimination rate,  $k_{el}$  [  $\frac{l}{min}$  ]**  $k_{el}$  describes the rate at which a drug is eliminated from the blood. Assuming that the elimination is exponential, the log-transformed equation 2 yields equation 3, from which  $k_{el}$  can be calculated using linear regression.

$$C_{tal}(t) = C_{tal}(0) \cdot e^{-k_{el} \cdot t} \quad (2)$$

$$\log(C_{tal}(t)) = \log(C_{tal}(0)) - k_{el} \cdot t \quad (3)$$

**Half-life,  $t_{half}$  [hr]**  $t_{half}$  is the time in which the drug concentration falls by 50 %. This can be calculated from the elimination rate by the following formula 4:

$$t_{half} = \frac{\ln(2)}{k_{el}} \quad (4)$$

**Volume of distribution,  $V_d$  [l]**  $V_d$  describes a fictitious volume required to obtain the same concentration with the amount of drug available in the body as in the blood.

$$V_d = AUC \cdot k_{el} \quad (5)$$

**Clearance, Cl [  $\frac{ml}{min}$  ]** Clearance describes the volume which can be cleared from the drug per unit of time. Cl is calculated via equation 6

$$Cl = k_{el} \cdot V_d \quad (6)$$

Clearance takes place via various organs, in the case of talinolol via the kidneys and the liver. The total clearance is the sum of all excretion fractions, equation 7.

$$Cl_{total} = Cl_{hepatic} + Cl_{renal} + Cl_{nonrenal} \quad (7)$$

Renal and fecal clearance can be calculated by dividing the measured amount of talinolol excreted in urine and feces, respectively, by the plasma AUC. Cl<sub>renal</sub> and Cl<sub>fecal</sub> is reflected in the equation 6 and 9, respectively.

$$Cl_{renal} = A_{urine} \cdot AUC \quad (8)$$

$$Cl_{fecal} = A_{feces} \cdot AUC \quad (9)$$

## 2.4 Physiologically based pharmacokinetic (PBPK) model

A physiologically based pharmacokinetic (PBPK) model is a computational model in the form of ordinary differential equations (ODEs). The developed PBPK model consists of a whole body model and submodels representing the organs and tissues. The individual models contain the compartments, physiological properties, pharmacokinetic parameters, and biochemical reactions of the respective organ or tissue. The PBPK model follows a

hierarchical structure, with the parent whole-body model connected to the submodels via blood flow. In the context of this work, an existing template of the whole body for the blood transport was used in which the submodels of the liver, kidney, and with special focus, the intestine were developed.

The PBPK model of talinolol was encoded in the Systems Biology Markup Language (SBML) [31, 37]. For development and visualization, sbmlutils [46] and cy3sbml [47, 48] were used. The model utilizes ordinary differential equations (ODE) which were numerically solved by sbmlsim [45] based on the high-performance SBML simulator libroadrunner [73, 88]. The model is available in SBML under CC-BY 4.0 license from <https://github.com/matthiaskoenig/talinolol-model>. Within this work, version 0.9.2 of the model was used [74].

## 2.5 Parameter fitting

Parameter fitting was used to minimize the distance between experimental data and model predictions by optimizing a subset of parameters of the model. The fitting procedure was performed in a two step procedure: (i) first parameters relevant for the intravenous application of talinolol were optimized using the subset of intravenous data (such as the tissue-plasma partition coefficient of talinolol). (ii) With the intravenous parameters the parameters for oral administration of talinolol were optimized using a subset of talinolol data after oral application (e.g., absorption rate of talinolol).

In the cost function the sum of the quadratic weighted residuals  $r_{i,k}$  for all time courses  $k$  and data points  $i$  were minimized, equation 10. Time courses were weighted by the participants in the respective study  $w_k$  and individual time points with the error associated with the measurement  $w_{i,k}$ .

$$F(\vec{p}) = \frac{1}{2} \sum_{i,k} (w_k \cdot w_{i,k} \cdot r_{i,k})^2 \quad (10)$$

Multiple optimization runs based on a local optimizer were performed for (i) and (ii) with the optimal parameters used in the final model.

### 3 Results

The main objective of this thesis was to develop a physiologically based pharmacokinetic (PBPK) model for talinolol and apply it to study the research questions from Sec. 1.7.

To this end, extensive data collection and curation was performed (Sec. 3.1), which served as the basis for model development (Sec. 3.2). In Sec. 3.4, the model performance is analyzed and model simulations are compared with experimental data. The developed model was applied to study various questions, Sec. 3.5.

#### 3.1 Talinolol data

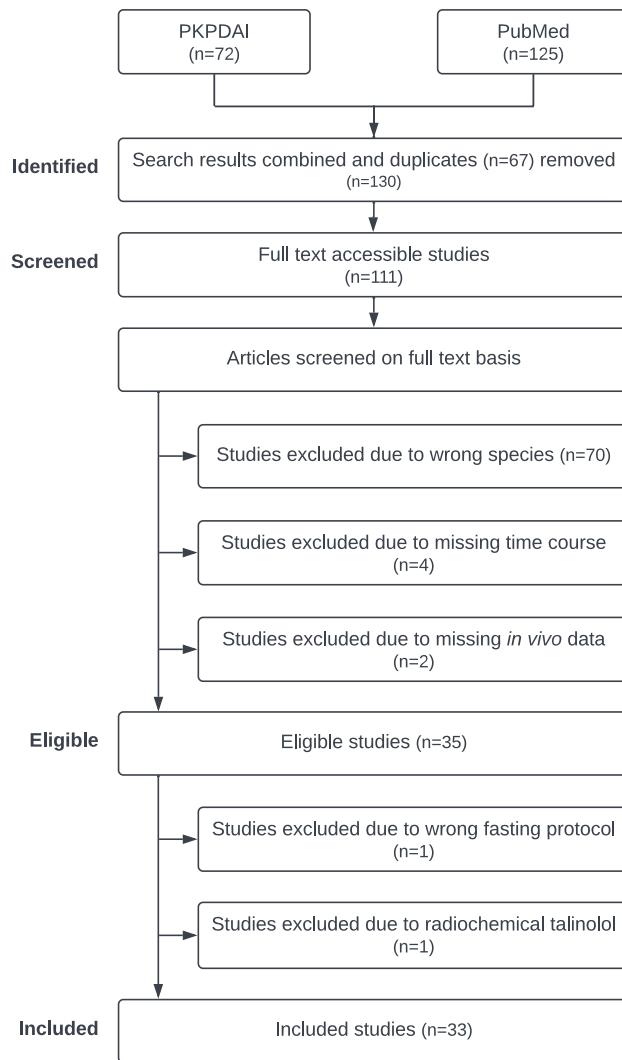


**Figure 3: PRISMA flow diagram.** Overview of data selection for the pharmacokinetics dataset of talinolol established in this work. PubMed and PKPDAI were used for the literature search on the pharmacokinetics of talinolol. Application of the eligibility criteria resulted in 35 studies, of which 34 were curated for this work (see Tab. 1). The procedure is described in detail in the Materials and Methods Sec. 2.1.

A large number of studies with data and information on the pharmacokinetics of talinolol were retrieved via the literature research. As depicted in the PRISMA flow diagram, Fig. 3, the 130 studies were filtered, with duplicates and studies that did not contain available

fulltext PDFs being the first to be excluded. The remaining 111 studies were screened for criteria such that they studied human subjects, and that they included time course and in vivo data. In addition to healthy subjects, studies involving patients with renal dysfunction andcholecystectomy were included. Via a T-drain bile could be collected in cholecystectomy patients, which provided essential information about the enterohepatic circulation of talinolol. A single study was excluded because of an incorrect fasting protocol, and another study was excluded because radioisotopic talinolol was administered. This resulted in 33 clinical studies which were curated and formed the data basis for the development and evaluation of the PKDB model. Tab. 1 provides an overview of the curated studies, such as the number of subjects (n), health status, dosing protocol, route of administration, and genetic variants. All data was uploaded in the pharmacokinetics database PK-DB and can be freely accessed via the respective PBPK-ID.

**Table 1: Overview of curated clinical trials.** From the number of subjects (n), health status, dosing protocol, information on the route, iv: intravenous, po: oral, and dosing can be obtained.

| PMID     | PKDB      | Study               | n  | Healthy | Patient | Fit | Dosing protocol                                          | Multiple dose | Genotype         |
|----------|-----------|---------------------|----|---------|---------|-----|----------------------------------------------------------|---------------|------------------|
| 16542205 | PKDB0016  | Bernsdorf2006 [5]   | 18 | ✓       |         | ✓   | iv (solution): 30 mg<br>po (tablet): 100 mg              |               |                  |
| 15637528 | PKDB00565 | Bogman2005 [6]      | 9  | ✓       |         | ✓   | intraintestinal (solution): 50 mg                        |               |                  |
| 8606523  | PKDB00564 | DeMey1995 [54]      | 12 | ✓       |         | ✓   | po (capsule): 25, 50, 100, 400 mg                        |               |                  |
| 19280523 | PKDB00566 | Fan2009a [13]       | 12 | ✓       |         | ✓   | po (tablet): 100 mg                                      |               |                  |
| 19401473 | PKDB00608 | Fan2009b [14]       | 10 | ✓       |         | ✓   | po (tablet): 100 mg                                      |               |                  |
| 15371980 | PKDB00609 | Giessmann2004 [17]  | 8  | ✓       |         | ✓   | iv (solution): 30 mg<br>po (IR tablet): 100 mg           | ✓             |                  |
| 8646825  | PKDB00610 | Gramatte1996 [18]   | 6  | ✓       |         |     | intraintestinal (solution): 100 mg                       |               |                  |
| 19555315 | PKDB00555 | Han2009 [22]        | 18 | ✓       |         | ✓   | po (tablet): 100 mg                                      |               |                  |
| 17466606 | PKDB00569 | He2007 [25]         | 12 | ✓       |         | ✓   | po (tablet): 50 mg                                       |               |                  |
| 22725663 | PKDB00611 | He2012 [26]         | 18 | ✓       |         | ✓   | po (tablet): 100 mg                                      |               | C3435T           |
| 17468862 | PKDB00561 | Juan2007 [36]       | 12 | ✓       |         | ✓   | po (tablet): 50 mg                                       |               |                  |
| 11270803 | PKDB00704 | Krueger2001 [49]    | 32 | ✓       |         | ✓   | po (NR): 100 mg                                          | ✓             |                  |
| 24472704 | PKDB00612 | Nguyen2014 [59]     | 10 | ✓       |         |     | po (FC tablet): 100 mg                                   |               |                  |
| 25486333 | PKDB00705 | Nguyen2015 [58]     | 10 | ✓       |         | ✓   | po (FC tablet): 100 mg                                   |               |                  |
| 21312289 | PKDB00572 | Ruijke2010 [63]     | 12 | ✓       |         | ✓   | po (tablet): 50 mg                                       |               |                  |
| 10096260 | PKDB00613 | Schwarz1999 [65]    | 9  | ✓       |         | ✓   | po (tablet): 50 mg                                       |               |                  |
| 10783825 | PKDB00706 | Schwarz2000 [66]    | 9  | ✓       |         | ✓   | po (tablet): 50 mg                                       |               |                  |
| 15903127 | PKDB00563 | Schwarz2005 [67]    | 24 | ✓       |         | ✓   | po (tablet): 50 mg                                       |               |                  |
| 17392718 | PKDB00614 | Schwarz2007 [64]    | 9  | ✓       |         | ✓   | iv (solution): 30 mg<br>po (tablet): 50 mg               |               |                  |
| 12587122 | PKDB00615 | Siegmund2003 [69]   | 36 | ✓       |         | ✓   | po (SC tablet): 2X50, 100 mg<br>(FC tablet): 100, 200 mg |               |                  |
| 6688879  | PKDB00707 | Terhaag1983 [78]    | 3  | ✓       |         | ✓   | po (NR): 200 mg                                          |               |                  |
| 2565889  | PKDB00708 | Terhaag1989 [77]    | 6  | ✓       | ✓       | ✓   | iv (solution): 20, 30 mg                                 |               |                  |
| 8527689  | PKDB00619 | Trausch1995 [81]    | 12 | ✓       |         | ✓   | iv (solution): 30 mg<br>po (NR): 50 mg                   |               |                  |
| 16713700 | PKDB00556 | Tubic2006a [83]     | 7  | ✓       |         | ✓   | po (IR tablet): 100 mg<br>(CR tablet) 100, 200 mg        |               |                  |
| 23422925 | PKDB00567 | Wang2013 [87]       | 18 | ✓       |         |     | po (NR): 100 mg                                          |               |                  |
| 10945310 | PKDB00562 | Westphal2000a [89]  | 10 | ✓       |         | ✓   | iv (solution): 30 mg                                     |               |                  |
| 11061574 | PKDB00620 | Westphal2000b [90]  | 8  | ✓       |         | ✓   | po (tablet): 100 mg                                      | ✓             |                  |
| 8710739  | PKDB00709 | Wetterich1996 [91]  | 6  | ✓       | ✓       | ✓   | iv (solution): 30 mg<br>po (tablet): 100 mg              |               |                  |
| 21943317 | PKDB00570 | Xiao2012 [92]       | 18 | ✓       |         | ✓   | po (tablet): 100 mg                                      |               |                  |
| 22983284 | PKDB00571 | Yan2013 [94]        | 14 | ✓       |         | ✓   | po (tablet): 100 mg                                      |               |                  |
| 19845435 | PKDB00617 | Zeng2009 [95]       | 16 | ✓       |         | ✓   | po (tablet): 100 mg                                      |               |                  |
| 16170863 | PKDB00568 | Zhang2005 [96]      | 27 | ✓       |         | ✓   | po (tablet): 100 mg                                      |               |                  |
| 11835190 | PKDB00618 | Zschiesche2002 [97] | 8  | ✓       |         | ✓   | iv (solution): 30 mg<br>po (FC tablet): 100 mg           | ✓             | G2677T/A, C3435T |

NR: not reported, SC: sugar-coated tablet, FC: film-coated tablet, IR: immediate-release tablet, CR: controlled-release tablet

### 3.2 Computational model of talinolol

#### 3.2.1 Physiologically based pharmacokinetic (PBPK) model

Based on the curated data PBPK model of talinolol was developed, see Fig.4. The PBPK model follows a hierarchical structure, with the whole-body model describing the systemic circulation of talinolol which connects the tissue submodels via the blood flow. An existing template of a whole-body PBPK model was adapted to talinolol and extended with the submodels for the small intestine, liver, and the kidneys. The submodels describe (i) intestinal dissolution, absorption, and excretion of talinolol in the feces (ii) liver uptake and biliary excretion, and (iii) kidney excretion.

An overview of the model, fit, and scan parameters is provided in Tab. 2.

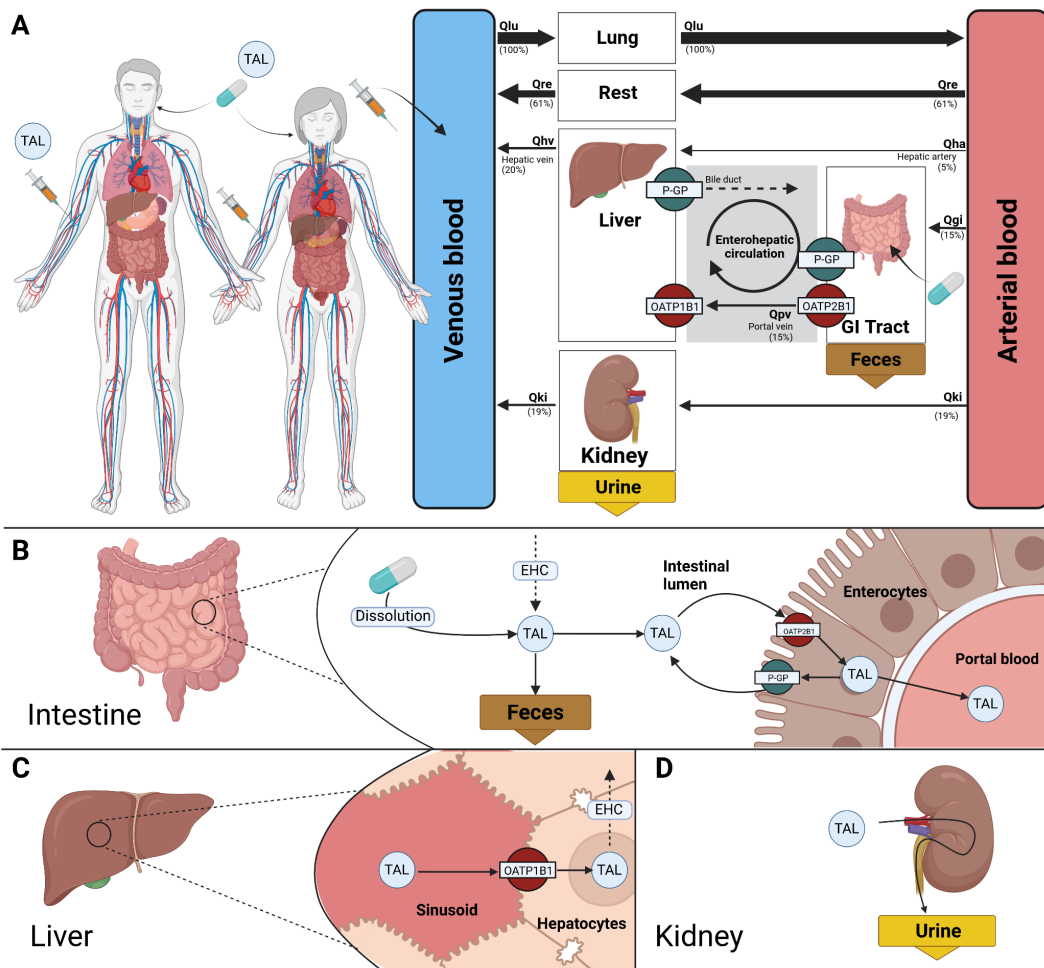


**Figure 4: PBPK model of talinolol (TAL).** (A) The whole body model representing the blood flow through the circulation connection the organs. Only organs of relevance were modeled; the remaining organs were pooled in the rest compartment. Talinolol can either be administered intravenously or orally. (B) Dissolution, absorption, and excretion via feces in the intestine model. Talinolol can be absorbed via OATP2B1 from the intestine. Absorption is reduced due to the efflux transport of talinolol via P-gp from enterocytes. (C) Within the liver model talinolol can be taken up via OATP1B1 from the blood into hepatocytes and be eliminated via the bile and the enterohepatic circulation (EHC). (D) Urinary excretion of talinolol via the kidney model. Created with <https://biorender.com>.

**Table 2: Overview of model, fit, and scan parameters.** The Prefixes GU, LI, and KI are used for the intestinal, liver, and kidney model, respectively.

| Model parameter     | Description                                                                            | Value   | Unit                        | References                                                      |
|---------------------|----------------------------------------------------------------------------------------|---------|-----------------------------|-----------------------------------------------------------------|
| BW                  | Body weight                                                                            | 75      | kg                          | ICRP (2002) [84]                                                |
| HEIGHT              | Body height                                                                            | 170     | cm                          | ICRP (2002) [84] [84]                                           |
| COWB                | Cardiac output per body weight                                                         | 0.83    | $\frac{ml}{kg \cdot s}$     | <i>de Simone et al.</i> (1997) [71]; ICRP (2002) [84]           |
| HCT                 | Hematocrit                                                                             | 0.51    | -                           | <i>Vander et al.</i> (2001) [85]; <i>Herman</i> (2016) [27]     |
| Fblood              | Fraction of organ volume that is blood vessels                                         | 0.02    | -                           |                                                                 |
| FVgu                | Fractional tissue volume gut                                                           | 0.0171  | $\frac{l}{kg}$              | ICRP (2002) [84]; <i>Jones and Rowland-Yeo</i> (2013) [35] [35] |
| FVki                | Fractional tissue volume kidney                                                        | 0.0044  | $\frac{l}{kg}$              | ICRP (2002) [84]; <i>Jones and Rowland-Yeo</i> (2013) [35]      |
| FVli                | Fractional tissue volume liver                                                         | 0.021   | $\frac{l}{kg}$              | ICRP (2002) [84]; <i>Jones and Rowland-Yeo</i> (2013) [35]      |
| FVlu                | Fractional tissue volume lung                                                          | 0.0297  | $\frac{l}{kg}$              | ICRP (2002) [84]; <i>Jones and Rowland-Yeo</i> (2013) [35]      |
| FVve                | Fractional tissue volume venous blood                                                  | 0.0514  | $\frac{l}{kg}$              | ICRP (2002) [84]; <i>Jones and Rowland-Yeo</i> (2013) [35]      |
| FVar                | Fractional tissue volume arterial blood                                                | 0.0257  | $\frac{l}{kg}$              | ICRP (2002) [84]; <i>Jones and Rowland-Yeo</i> (2013) [35]      |
| FVbi                | Fractional tissue volume bile                                                          | 0.00071 | $\frac{l}{kg}$              | ICRP (2002) [84]; <i>Jones and Rowland-Yeo</i> (2013) [35]      |
| FVpo                | Fractional tissue volume portal vein                                                   | 0.001   | $\frac{l}{kg}$              | ICRP (2002) [84]; <i>Jones and Rowland-Yeo</i> (2013) [35]      |
| FVhv                | Fractional tissue volume hepatic vein                                                  | 0.001   | $\frac{l}{kg}$              | ICRP (2002) [84]; <i>Jones and Rowland-Yeo</i> (2013) [35]      |
| FQgu                | Fractional blood flow gut                                                              | 0.18    | -                           | ICRP (2002) [84]; <i>Jones and Rowland-Yeo</i> (2013) [35]      |
| FQki                | Fractional blood flow kidney                                                           | 0.19    | -                           | ICRP (2002) [84]; <i>Jones and Rowland-Yeo</i> (2013) [35]      |
| FQh                 | Fractional blood flow hepatic vein                                                     | 0.215   | -                           | ICRP (2002) [84]; <i>Jones and Rowland-Yeo</i> (2013) [35]      |
| Mr_tal              | Molecular weight of talinolol                                                          | 363.495 | $\frac{g}{mole}$            | CHEBI:135533                                                    |
| Fit parameter       | Description                                                                            | Value   | Unit                        |                                                                 |
| ftissue_tal         | Rate of distribution in tissues                                                        | 0.6413  | $\frac{1}{min}$             |                                                                 |
| Kp_tal              | Tissue/plasma partition coefficient                                                    | 6.6214  | -                           |                                                                 |
| KI_TALEX_k          | Urinary excretion rate                                                                 | 0.9592  | $\frac{1}{min}$             |                                                                 |
| LI_TALIM_Vmax       | $V_{max}$ of liver import                                                              | 0.01    | $\frac{mmole}{min \cdot l}$ |                                                                 |
| LI_TALEX_k          | Excretion rate of liver                                                                | 0.1501  | $\frac{1}{min}$             |                                                                 |
| Ka_dis_tal          | Dissolution of talinolol                                                               | 0.6819  | $\frac{1}{h}$               |                                                                 |
| GU_F_tal_abs        | Fraction of absorbed talinolol                                                         | 0.4548  | -                           |                                                                 |
| GU_TALABS_Vmax      | $V_{max}$ of absorption                                                                | 2.0577  | $\frac{mmol}{min \cdot l}$  |                                                                 |
| GU_TALEFL_Vmax      | $V_{max}$ of enterocytes efflux                                                        | 0.3286  | $\frac{1}{min}$             |                                                                 |
| GU_TALEX_Vmax       | $V_{max}$ of excretion                                                                 | 0.0007  | $\frac{1}{min}$             |                                                                 |
| Scan parameter      | Description                                                                            | Value   | Unit                        |                                                                 |
| GU_f_OATP2B1        | Scaling factor of OATP2B1 activity                                                     | 1       | -                           |                                                                 |
| GU_f_PG             | Scaling factor of PG activity                                                          | 1       | -                           |                                                                 |
| LI_f_OATP1B1        | Scaling factor of OATP1B1 activity                                                     | 1       | -                           |                                                                 |
| KI_f_renal_function | Scaling factor of renal function                                                       | 1       | -                           |                                                                 |
| f_cirrhosis         | Scaling factor of the severity of cirrhosis. Combination of f_shunts and f_tissue_loss | 0       | -                           |                                                                 |
| f_shunts            | Fraction of blood shunted around the liver                                             | 0       | -                           |                                                                 |
| f_tissue_loss       | Fraction of lost liver tissue                                                          | 0       | -                           |                                                                 |

### 3.2.2 Intestinal model

Talinolol can be administered either intravenously, orally as a tablet or capsule, or by intestinal infusion. After oral application of talinolol in solid form, talinolol is dissolved reaches the intestine. Here it can be absorbed via OATP2B1 or the fraction unabsorbed is excreted via the feces. Via P-gp talinolol can be exported back in the intestinal lumen.

**Simple intestinal model** First a simple model of these processes was developed with an overview of all reactions in the intestine is shown in Fig. 5.

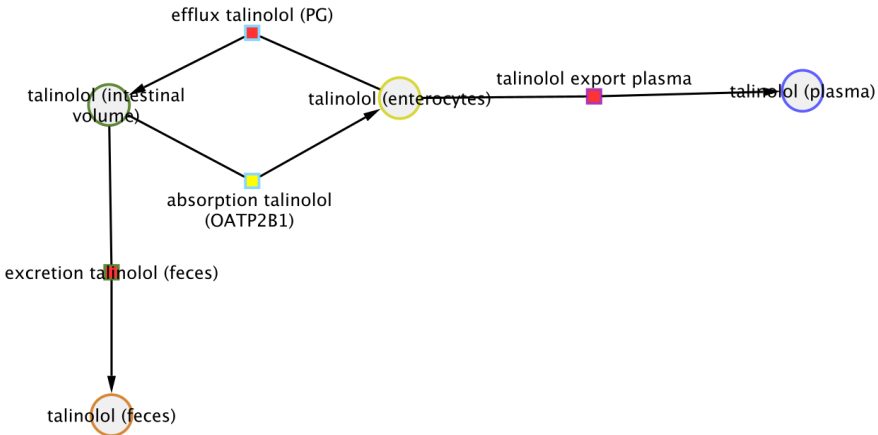


**Figure 5:** Simple intestine model. Talinolol is transported from the intestinal lumen into the enterocytes by OATP2B1. Simultaneously, a reverse transport of talinolol from the enterocytes back into the intestinal lumen via P-glycoprotein (PG) takes place. From the enterocytes talinolol can enter the systemic circulation (plasma). Unabsorbed talinolol is excreted via the feces.

The absorption of talinolol was modeled via an irreversible first-order Michaelis-Menten kinetics and is described by equation 11.

$$absorption = oatp2b1 \cdot V_{gu} \cdot \frac{TALABS\_V_{max} \cdot tal}{tal + TALABS\_K_m} \quad (11)$$

The absorption equation 11 consists of the parameters *oatp2b1*, the protein amount of OATP2B1 in the gut, *V<sub>gu</sub>*, the volume of the intestine, *TALABS\_V<sub>max</sub>*, the maximum velocity of talinolol absorption, and *TALABS\_K<sub>m</sub>*, the Michaelis-Menten constant for the absorption of talinolol.

Talinolol absorption occurs actively via OATP2B1 on the apical side into enterocytes and is represented in equation 12. The activity of OATP2B1 can vary due to genetic variants. Regulation of OATP2B1 activity is controlled by the factor *f\_OATP2B1*. A value of 1 represents normal activity, while values <1 correspond to reduced activity and values >1 to increased activity. The parameter *f\_tal\_abs* describes the fraction of talinolol which is absorbed from the intestine, which is approximately 55 % [81, 18].

$$absorption_{tal} = f\_OATP2B1 \cdot F\_tal\_abs \cdot absorption \quad (12)$$

The efflux transport via P-gp, which occurs from enterocytes back into the intestinal lumen, was described by a mass action law, as seen in equation 13. The concentration of talinolol in enterocytes is denoted by *tal\_entero*. The protein amount of P-gp, which is the responsible efflux protein for the back-transport of talinolol, is represented by the parameter *pgp*. The enzymatic activity of P-gp, denoted by the factor *f\_PG*, refers to the functionality or catalytic capability of P-gp. Similar to OATP2B1, the enzymatic activity of P-gp can be modulated. A value of 1 indicates normal activity, while values less than 1 reduce P-gp activity, and values greater than 1 increase P-gp activity.

$$efflux_{tal} = f\_PG \cdot pgp \cdot TALEFL\_V_{max} \cdot V_{gu} \cdot tal\_entero \quad (13)$$

The export of talinolol to the blood via the basal side of the enterocytes is described via equation 14, with TALEX\_V<sub>max</sub>, the maximum velocity of talinolol export.

$$excretion_{tal} = TALEX\_Vmax \cdot V_{gu} \cdot tal\_entero \quad (14)$$

The fraction of talinolol that is not absorbed in the intestine is excreted in the feces.

**Site-specific intestinal model** Talinolol can be administered via intestinal infusion, as mentioned above. In this procedure, a tube is passed into the appropriate segment of the intestine. This procedure is used to study the absorption windows of talinolol in *Gramatte et al.* (1996) [18] and *Bogman et al.* (2005) [6].

The simple intestinal model presented above was extended by dividing the intestine into different segments, i.e., duodenum, jejunum1, jejunum2, ileum1, ileum2, and colon with site specific parameters and transport rates. The segments differ in length and volume as well as in the enzymatic activity of the individual transporters, see Tab. 3 and 4. The overall equations from the simple compartmental model were used, but extended via site-specific parameters and transport equations between the different sites corresponding to movement within the intestine. An overview of the site-specific intestine model is shown in Fig. 6. This extended model allowed to study the effect of site-specific infusion of talinolol in the intestine as performed in [6, 18].

**Table 3: Overview of parameters in site-specific intestine model (GU).** The relative protein levels for P-gp and OATP2B1 and the transport rates in the intestinal compartments duodenum, jejunum\_1, jejunum\_2, ileum\_1, ileum\_2 and colon.

| Model parameter        | Description                         | Value | Unit            | References                 |
|------------------------|-------------------------------------|-------|-----------------|----------------------------|
| GU_pgp_duodenum        |                                     | 0.3   | -               | <i>Drozdzik et al.</i>     |
| GU_pgp_jejunum_1       | protein amount                      | 0.4   | -               | (2014) [10];               |
| GU_pgp_jejunum_2       | P-gp in intestine section           | 0.5   | -               | <i>Englund et al.</i>      |
| GU_pgp ileum_1         |                                     | 0.7   | -               | (2006)[12];                |
| GU_pgp ileum_2         |                                     | 1.1   | -               | <i>Bruckmueller et al.</i> |
| GU_pgp_colon           |                                     | 0.25  | -               | (2017) [7]                 |
| GU_oatp2b1_duodenum    |                                     | 0.45  | -               | <i>Drozdzik et al.</i>     |
| GU_oatp2b1_jejunum_1   | protein amount                      | 0.5   | -               | (2014) [10];               |
| GU_oatp2b1_jejunum_2   | OATP2B1 in intestine section        | 0.45  | -               | <i>Englund et al.</i>      |
| GU_oatp2b1 ileum_1     |                                     | 0.45  | -               | (2006) [12];               |
| GU_oatp2b1 ileum_2     |                                     | 0.45  | -               | <i>Bruckmueller et al.</i> |
| GU_oatp2b1_colon       |                                     | 0.5   | -               | (2017) [7]                 |
| GU_TALFLUX_DUODENUM_k  |                                     | 0.067 | $\frac{l}{min}$ |                            |
| GU_TALFLUX_JEJUNUM_1_k |                                     | 0.019 | $\frac{l}{min}$ |                            |
| GU_TALFLUX_JEJUNUM_2_k | Transport rate in intestine section | 0.019 | $\frac{l}{min}$ |                            |
| GU_TALFLUX_ILEUM_1_k   |                                     | 0.012 | $\frac{l}{min}$ |                            |
| GU_TALFLUX_ILEUM_2_k   |                                     | 0.012 | $\frac{l}{min}$ |                            |

**Table 4: Overview of anatomical parameters in site-specific intestine model (GU).** Given are length, diameter and transport velocity for the intestinal subcompartments duodenum, jejunum\_1, jejunum\_2, ileum\_1, ileum\_2 and colon [30, 56, 93].

| Compartment | Length | Diameter | Velocity                           |
|-------------|--------|----------|------------------------------------|
| duodenum    | 30 cm  | 3.7 cm   | 2 $\frac{\text{cm}}{\text{min}}$   |
| jejunum_1   | 105 cm | 2.7 cm   | 2 $\frac{\text{cm}}{\text{min}}$   |
| jejunum_2   | 105 cm | 2.7 cm   | 2 $\frac{\text{cm}}{\text{min}}$   |
| ileum_1     | 165 cm | 2.7 cm   | 2 $\frac{\text{cm}}{\text{min}}$   |
| ileum_2     | 165 cm | 2.7 cm   | 2 $\frac{\text{cm}}{\text{min}}$   |
| colon       | 135 cm | 6 cm     | 0.5 $\frac{\text{cm}}{\text{min}}$ |

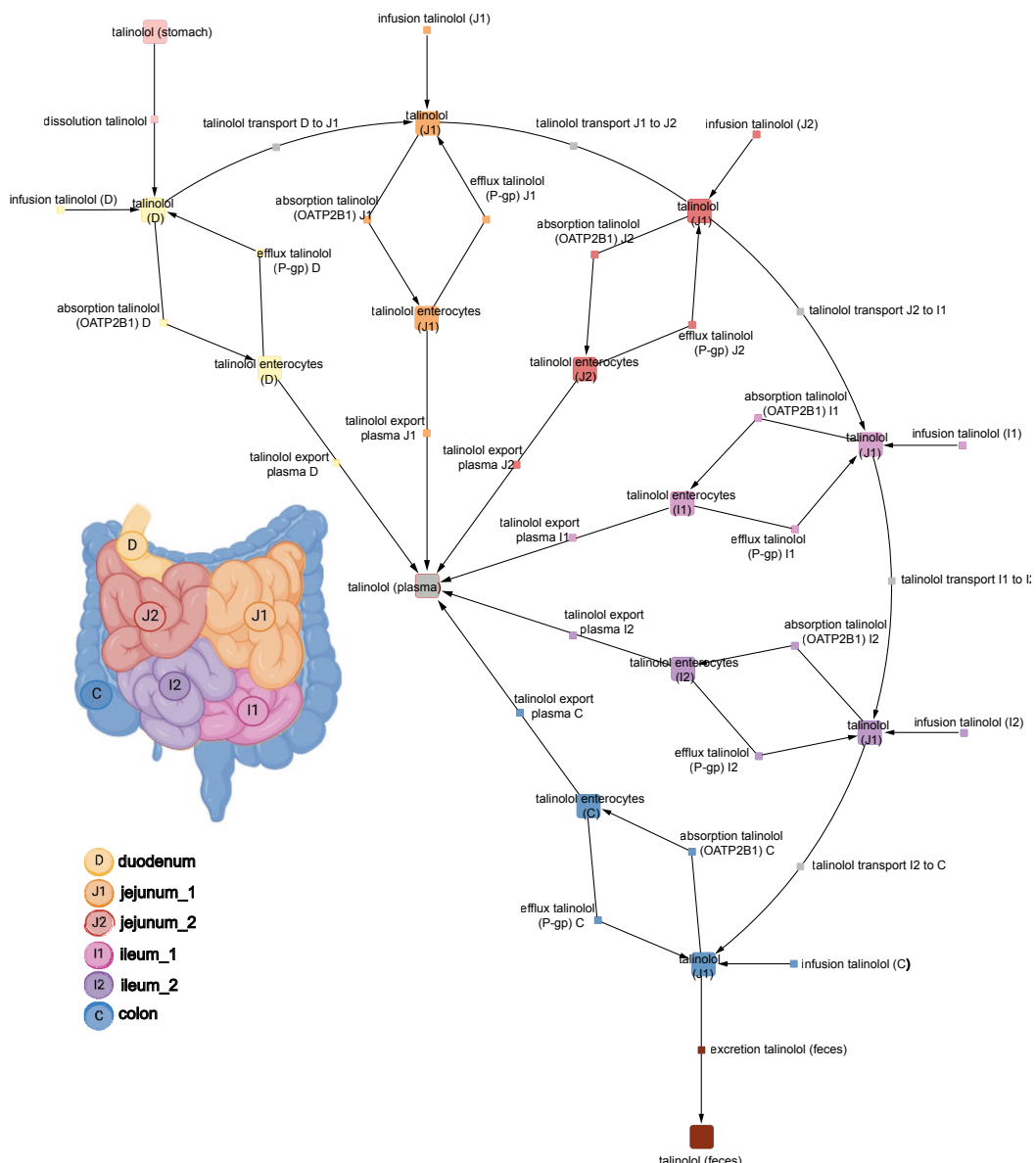


**Figure 6: Site-specific intestine model for talinolol.** The division of the intestine into duodenum (D), jejunum (J1 and J2), ileum (I1 and I2), and colon (C), allows the infusion of talinolol in specific segments. Within each segment, the model incorporates the uptake and efflux of talinolol by OATP2B1 and P-gp, respectively, into the enterocytes, as well as the transport of talinolol from the enterocytes into the bloodstream. Created with <https://biorender.com> and Cytoscape.

### 3.2.3 Kidney model

The kidney plays a significant role in the excretion of talinolol from the blood into the urine. The renal excretion of talinolol was modeled using irreversible mass-action kinetics and a simplified transport reaction which directly exports talinolol from the plasma in the kidneys into the urine, as depicted in equation 15 and Fig. 7.

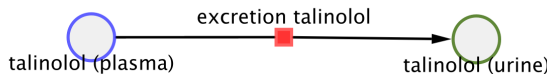


**Figure 7: Kidney model.** Renal excretion pathway of talinolol via the kidney into the urine. Created with Cytoscape.

$$\text{renal\_excretion} = f_{\text{renal\_function}} \cdot \text{TALEX\_k} \cdot V_{\text{ki}} \cdot \text{tal\_ext} \quad (15)$$

The parameters correspond to the urinary excretion rate TALEX.k, the plasma concentration tal\_ext of talinolol in the kidneys, and the kidney volume Vki. The kidney function is modulated by the parameter f\_renal\_function, which is set to 1 for normal function. Values below or above 1 allow to model impaired or enhanced renal function, respectively.

### 3.2.4 Liver model

An overview of the reactions in the liver is given in Fig. 8.



**Figure 8: Liver model.** Talinolol can be taken up by the liver via OATP1B1. No metabolism of talinolol takes place in the liver but unchanged talinolol is excretion into bile and can reach the duodenum via the enterohepatic circulation. Created with Cytoscape.

Talinolol reaches the liver either via the portal vein (e.g. after oral absorption) or via the hepatic artery. Talinolol can be taken up by the liver from the plasma into the hepatocytes via OATP1B1. Import was modeled as an irreversible Michaelis-Menten kinetics described by the following equation 16:

$$\text{import}_{\text{tal}} = f_{\text{OATP1B1}} \cdot V_{\text{li}} \cdot \frac{\text{TALIM\_Vmax} \cdot \text{tal\_ext}}{\text{tal\_ext} + \text{TALIM\_K}_m \cdot \text{tal}} \quad (16)$$

Talinolol metabolism is < 1 % and recovery of talinolol metabolites in the urine is negligible, so that no metabolic conversions were included in the liver model.

The biliary export of talinolol from the liver depends on the enzymatic activity of P-gp f\_PG and was modeled as mass-action kinetics following equation 17. Biliary export depends on TALEX.k, the rate of talinolol export, the liver volume Vli, the concentration of talinolol in the liver.

$$\text{export}_{\text{tal}} = f_{\text{PG}} \cdot V_{\text{li}} \cdot \text{TALEX\_k} \cdot \text{tal} \quad (17)$$

Talinolol reaches the lumen of the duodenum via the enterohepatic circulation where it can either be reabsorbed or excreted. Enterohepatic circulation of talinolol was described via equation 18 which depends on liver volume, talinolol concentration in bile, and the rate of enterohepatic circulation of talinolol.

$$EHC_{tal} = TALEHC\_k \cdot Vli \cdot tal_{bi} \quad (18)$$

with

$$TALEHC\_k = TALEX\_k$$

This allowed to model the enterohepatic circulation explicitly without adding additional free parameters into the model.

### 3.2.5 Model of cirrhosis and renal impairment

To study the effect of hepatic and renal impairment model changes were implemented which correspond to the respective pathophysiology.

The parameter  $f_{cirrhosis}$  describes the degree of cirrhosis in the model and can take values between 0 (no cirrhosis) and 0.95 (critical cirrhosis). As the value increases, the severity of cirrhosis increases.  $f_{cirrhosis}$  is a combination of the parameters  $f_{tissue\_loss}$  and  $f_{shunt}$ .  $f_{tissue\_loss}$  describes the proportion of liver tissue which is no longer functional (e.g. due to scarring or advanced fibrosis) and results in a decreased functional liver parenchymal volume in cirrhosis, described by equation 19.

$$Vli\_tissue = Vli \cdot (1 - f_{tissue\_loss}) \cdot (1 - Fblood) \quad (19)$$

$f_{shunts}$  describes the fraction of portal blood that is shunted via the liver. Blood which is shunted around the liver can not reach the liver. The implementation of cirrhosis is based on a recent indocyanine green model in cirrhosis [42, 43] with parameters for mild, moderate and severe cirrhosis taken from the original model.

In patients affected by cirrhosis, renal dysfunction usually also co-occurs, so called hepatorenal dysfunction. Krüger *et al.* (2001) [49], investigated the pharmacokinetics of talinolol in patients with different renal insufficiency and healthy volunteers. Impairment of renal function was modeled via the parameter  $f_{renal\_function}$  which scales all reactions in the kidney (see Sec. 3.2.3). A similar approach of modeling renal impairment allowed to study the effect of renal impairment on pravastatin recently [Pujol?].

### 3.3 Parameter fitting

The curated talinolol pharmacokinetic data was used to determine model parameters based on parameter fitting. For this purpose, selected parameters and a sub-dataset of curated time curves of healthy subjects were used with the subset of studies used for fitting indicated in Tab. 1.

The parameter fitting was performed for healthy subjects, with wildtype transporter activity and intravenous or immediate-release oral application of talinolol. The following data was excluded from parameter fitting: Studies involving controlled-release tablets, patients with renal failure, and individuals with detected P-gp mutants. Furthermore, the study by *Nguyen et al.* (2014) [59] was excluded as it was duplicate data with *Nguyen et al.* (2015) [58], and including both studies would introduce redundant information. Additionally, *Wang et al.* (2013) [87] was excluded due to exceptionally high values observed for the administered dosage. These exclusions were made to ensure that the data used for parameter fitting were representative and in line with the observed trends in talinolol pharmacokinetics.

Parameter fitting was performed as a two step procedure based on the route of administration. First, the parameters  $ftissue_{tal}$ ,  $LI\_TALEX\_k$ , and  $KI\_TALEX\_k$  were optimized using intravenous data for calibration. The optimized parameters are given in Tab. 5 with the goodness-of-fit plot given in Fig. 9. An overall good agreement between the prediction of the model and the experimental data can be observed. Only exception is a single data point from Zschiesch2002 [97].

**Table 5: Final parameters.** Fitted model parameters based on intravenous data.

| Parameter     | Description                         | Value  | Unit                        |
|---------------|-------------------------------------|--------|-----------------------------|
| ftissue_tal   | Volume of distribution              | 0.6413 | $\frac{l}{min}$             |
| Kp_tal        | Tissue/plasma partition coefficient | 6.6214 | -                           |
| KI_TALEX_k    | Rate of urinary excretion           | 0.9592 | $\frac{1}{min}$             |
| LI_TALIM_Vmax | V <sub>max</sub> of liver import    | 0.01   | $\frac{mmole}{min \cdot l}$ |
| LI_TALEX_k    | Rate of biliary excretion           | 0.1501 | $\frac{1}{min}$             |

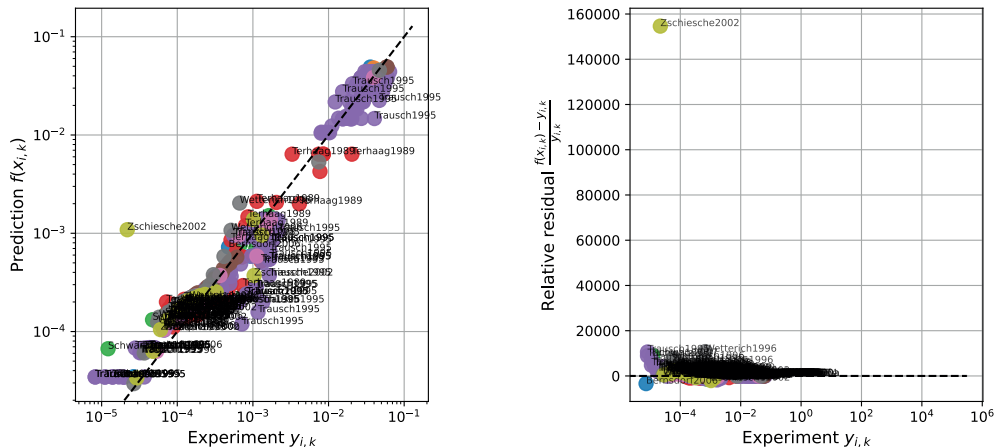


**Figure 9: Parameter fitting results.** Overview of predicted vs. experimental intravenous data and the corresponding residuals.

The parameters determined on iv data were integrated into the model and fixed for the subsequent parameter fitting based on oral data. The optimized parameters are given in Tab. 6. The goodness-of-fit plot in Fig. 10 demonstrates that the fitted model exhibits good agreement between simulated and experimental data points. Only exception are some data points from Trausch1995 [81], where the residuals show a significant discrepancy compared to the clinical data.

**Table 6: Final parameters.** Fitted model parameters based on oral data.

| Parameter      | Description                                     | Value  | Unit                        |
|----------------|-------------------------------------------------|--------|-----------------------------|
| Ka_dis_tal     | Dissolution rate of talinolol                   | 0.6819 | $\frac{1}{h}$               |
| GU_F_tal_abs   | Absorbed fraction of talinolol                  | 0.4548 | -                           |
| GU_TALABS_Vmax | V <sub>max</sub> of absorption via OATP2B1      | 2.0577 | $\frac{mmole}{min \cdot l}$ |
| GU_TALEFL_Vmax | V <sub>max</sub> of enterocytes efflux via P-gp | 0.3286 | $\frac{1}{min}$             |
| GU_TALEX_Vmax  | V <sub>max</sub> of export in plasma            | 0.0007 | $\frac{1}{min}$             |

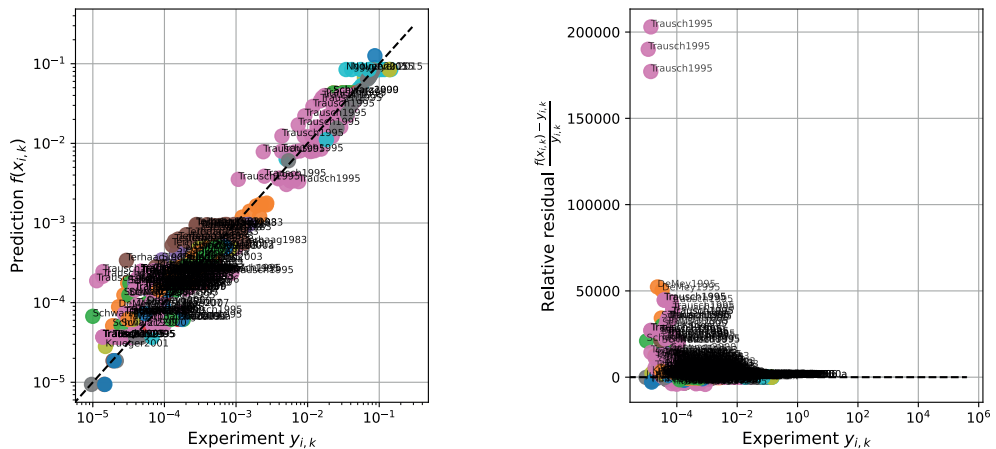


**Figure 10: Parameter fitting results.** Overview of predicted vs. experimental oral data and the corresponding residuals.

### 3.4 Model performance

The performance of the developed PBPK model of talinolol was evaluated by comparing predicted timecourses against curated time curves from clinical studies. In the following, the model performance is described according to the type of administration and tissue. In the figure legends, the administered amount and the number of subjects ( $n$ ) is provided. If experimental errors were reported these are displayed as standard deviation (SD). The solid line represents the respective simulation, while experimental data points are connected via dashed lines.

#### 3.4.1 Single dose intravenous

In nine studies, talinolol was administered intravenously as a single dose. The standard solution contained 30 mg of talinolol. An exception is one subject in *Terhaag et al.* (1989) [77], who received a 20 mg injection of talinolol.

**Plasma** Except *Giessmann et al.* (2004) [17], all studies reported time curves for talinolol concentration in plasma, see Fig. 11. Both the simulation and experimental data show a rapid increase in talinolol concentration after injection. The simulations account for the respective injection protocol. The model predictions demonstrate a very agreement with the experimental data. Only exceptions are that the study by *Terhaag et al.* (1989) [77], one subject demonstrated a  $c_{\max}$  value approximately twice as high as the simulation predicted. Another disparity is a slightly slower decline of concentration in the prediction compared to the data. This suggests a slower elimination rate of talinolol in the model, although the difference is minimal.

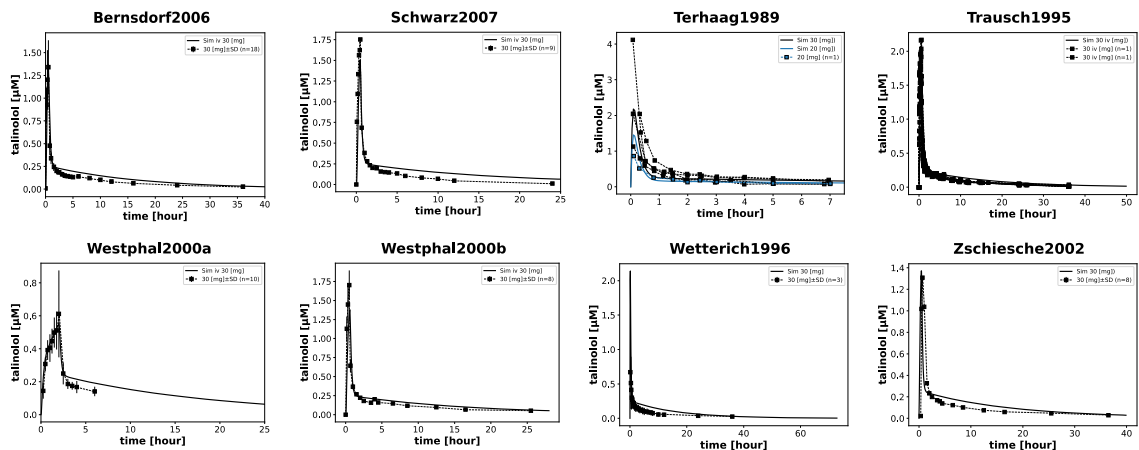


**Figure 11: Simulation experiments, single dose iv, plasma.** In these studies, each subject was treated with 30 mg of talinolol. One subject in the study, *Terhaag1989 et al.* (1989) [77], received a lower dose of 20 mg (blue) instead. The time course predicted by the model is represented by the solid line, the dashed line represents the data from the curated studies.

**Urine** The model predicts a urinary excretion of talinolol ranging between 40 and 50  $\mu\text{mole}$  (15.5 - 18.2 mg), corresponding to a recovery of 52 - 60 % of the dose Fig. 12. This is in very good agreement with the reported values of urinary recovery and model predictions agree well with the experimental data. However, it is important to acknowledge the high variability observed across different individuals in the dataset and between different studies. Furthermore, it should be noted that the model accurately captures the expected

temporal profile, with the majority of talinolol being eliminated within a few days through urine. The presented model is a mean model and does not account for the intra-individual variability.

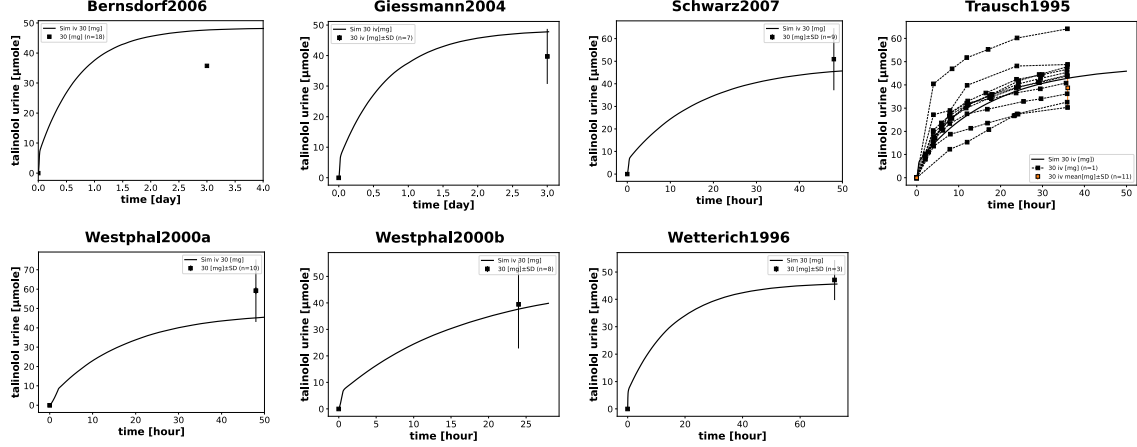


**Figure 12: Simulation experiments, single dose iv, urine.** In these studies, all subjects were treated with 30 mg of talinolol. The time course predicted by the model is represented by the solid line; the single data points are the data from the curated studies and are connected by the dashed line only when measured more than once over time.

**Feces and bile** The elimination of talinolol through feces and its pharmacokinetics in the bile are depicted in Fig. 13. Among the studies examined, only *Bernsdorf et al.* (2006) [5] provide data on talinolol excretion in feces. The simulation suggests an elimination of talinolol within the first two days in the feces, with fecal excretion being much lower than urinary excretion (3 pole corresponding only to 1.1 mg or 3.7 % of the dose). However, this finding deviates significantly from the measured value of 6.3 mg [5].

The model's predictions on the amount of talinolol excreted in the bile align more closely with the experimental data. Although the model indicates that the excretion amount varies depending on the dosage, the differences observed in the experimental data are minimal. Nevertheless, it is essential to acknowledge that the extent of talinolol excretion in bile can exhibit interindividual variability.

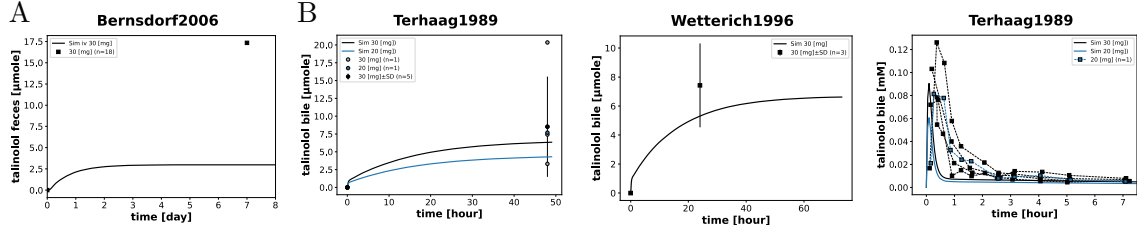


**Figure 13: Simulation experiments, single dose iv, feces (A) and bile (B).** In these studies, each subject was treated with 30 mg of talinolol. One subject in the study, *Terhaag1989 et al.* (1989) [77], received a lower dose of 20 mg (blue) instead. The time course predicted by the PKDB model is shown by the solid line; the single data points are the data from the curated studies and are connected by the dashed line only when measured more than once over time.

### 3.4.2 Single dose oral

In 27 studies, talinolol was administered orally as a singel dose in solid form. In most cases, the standard dose of 50 or 100 mg of talinolol was given in tablet form.

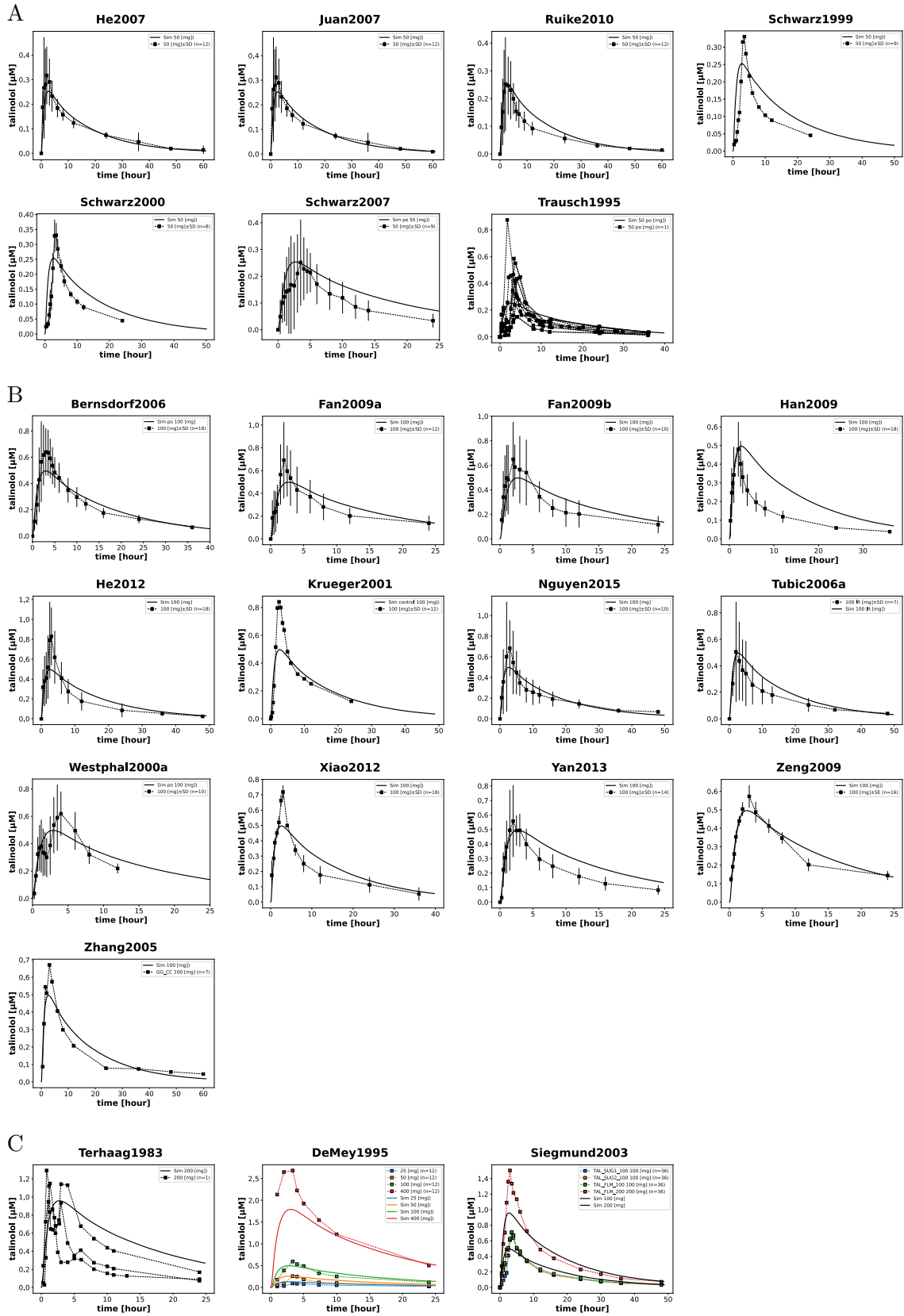


**Figure 14: Simulation experiments, single dose po, plasma.** The standard amount was 50 (A) or 100 (B) mg. In these studies, subjects received a dose of talinolol in various tablet forms, ranging from 25 to 400 mg (C). The time course predicted by the model is displayed by the solid line, and the data from the curated studies are indicated by the dashed line. The different doses are indicated by different colors.

**Plasma** The  $c_{\max}$  values for 50 mg and 100 mg of talinolol are approximately 0.25  $\mu\text{M}$  and 0.5  $\mu\text{M}$ , respectively, reached around three to four hours post-dose, aligning with the measured values. For the 200 mg dose, similar trends hold, with the  $c_{\max}$  value of 1  $\mu\text{M}$  matching the empirical data. The model exhibits a good agreement with the experimental data, as shown in Fig. 14. Furthermore, it is important to consider that, as demonstrated in *Trausch et al.* (1995) [81], the concentration of talinolol in blood can vary significantly among individuals.

The studies *DeMey et al.* (1995) [54], *Nguyen et al.* (2015) [58], and *Siegmund et al.* (2003) [70] do not yield notable findings concerning tablet formulations when compared to other studies. *DeMey et al.* (1995) [54] examines various doses ranging from 25 to 400 mg and demonstrates a dose-dependent relationship, which the model very accurately predicts up to a dose of 400 mg. However, as the talinolol dose increases, the simulation deviates more from the measured data.

No discernible differences can be observed between talinolol concentrations in plasma and serum in the model's predictions and the experimental data.

**Urine** The model predicts that administration of 50 mg and 100 mg of talinolol results in the excretion of approximately 40  $\mu\text{mol}$  and 80  $\mu\text{mol}$ , respectively, in the urine. This is not only consistent with the actual measured values but also indicates a similar rate of talinolol excretion in the urine, as illustrated in Fig. 15. Notably, a substantial degree of intraindividual variability is observed across the conducted studies with the model in good agreement with the mean data.

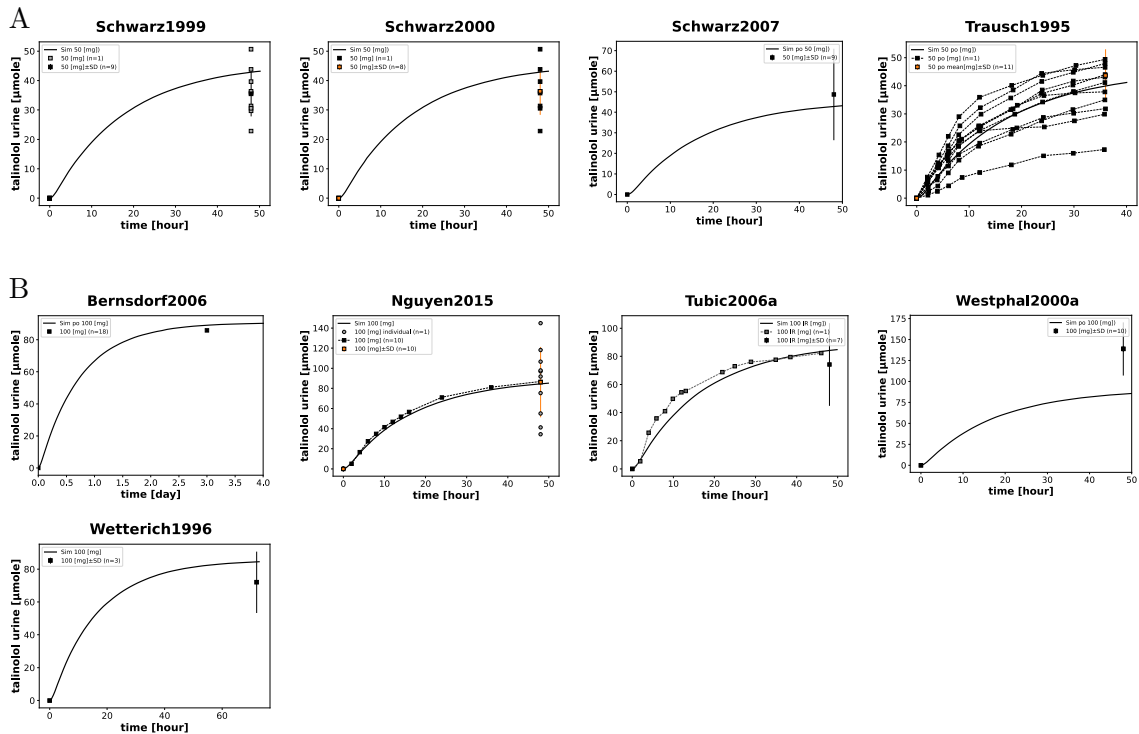


**Figure 15: Simulation experiments, single dose po, urine.** In these studies, subjects received (A) 50 or (B) 100 mg of talinolol. The solid line displays the time course predicted by the model; the single data points are the data from the curated studies and are connected by the dashed line only when measured more than once over time.

**Feces and bile** Bernsdorf et al. and Wetterich conducted studies on the excretion of talinolol via the feces and bile. Within a day, almost the entire amount of talinolol is excreted via the feces. The model predicts amounts of 120  $\mu\text{mole}$  talinolol in the feces with the data from around 90  $\mu\text{mole}$ . The excretion of talinolol through bile reaches a value of  $6.65 \pm 1.9 \text{ mg}$  after one day, which surpasses the predicted value. The comparison between curated data and simulation results is illustrated in Fig. 16. Overall some discrepancies can be observed in the amounts in feces and bile, but very large variability is observed as can be seen from the large standard deviation.

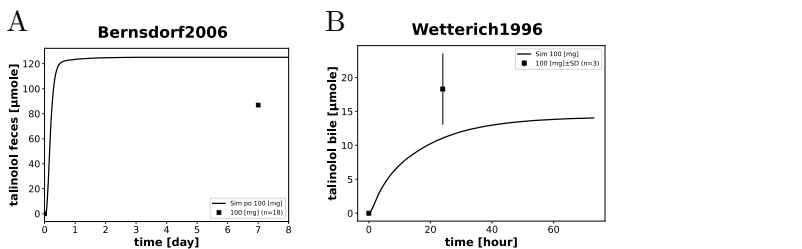


**Figure 16: Simulation experiments, single dose po, feces (A) and bile (B).** In these studies, subjects received 100 mg of talinolol. The time course predicted by the PKDB model is displayed by the solid line and the single data points are the data from the curated studies.

### 3.4.3 Multiple dose oral

Finally, the model performance after multiple doses of talinolol are presented. In general, 100 mg of talinolol was taken orally in tablet form once daily. The model with recurring daily peaks represents the concentration of talinolol in plasma and the corresponding daily amount in the urine. The curated data were plotted at the time points defined in each study, as the measurement time points varied between studies. The results of the simulation experiments with multiple administrations of talinolol in plasma and urine are depicted in Fig. 17. Importantly, none of the multiple dose data was used for model parametrization, i.e., the multiple dose predictions are all model validations.

**Plasma** Following the administration of talinolol, rapid absorption leads to a peak concentration in the bloodstream within approximately 3 hours. Subsequently, talinolol undergoes gradual elimination over the remainder of the day, resulting in a slight accumulation over multiple doses. Consequently, a minimla concentration of approximately 0.1  $\mu\text{M}$  is maintained in the subsequent days. Steady-state conditions (i.e. a stable dosing profile) are typically achieved within 48 hours.

Overall, the model's predictions shows a very good agreement a favorable agreement with the observed data, with the exception of a minor overestimation of talinolol accumulation compared to the measured values after several days.

**Urine** A large fraction of talinolol is eliminated via the urine. While the model accurately predicts the quantity of talinolol excreted in the urine after multiple days, the predicted amounts align closely with the data reported by Giessmann et al. and Krueger et al. (2001) [49].However, there is a significant deviation from the findings reported by Westphal et al. (2000b) [90], which is surprising because single dose urinary data is in very good agreement as well as plasma concentrations. The possible deviation could be due to a reporting error in the study.

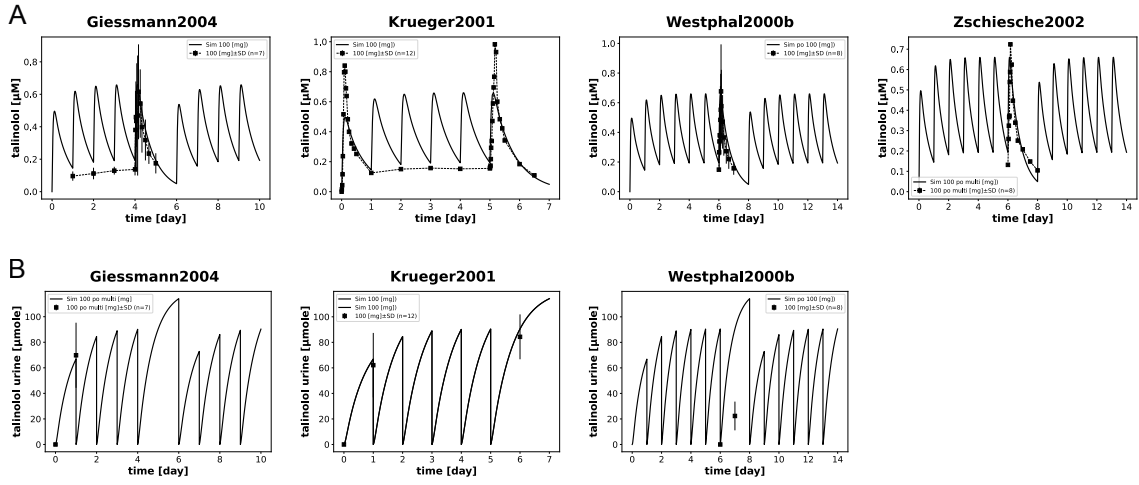


**Figure 17: Simulation experiments, multiple dose po, plasma and urine.** In these studies, subjects received 100 mg of talinolol daily. The time course predicted by the model is displayed by the solid line and the single data points are the data from the curated studies.

### 3.5 Model application

After establishing the PBPK model of talinolol, testing its performance and validating some of the predictions via multiple dose applications, we applied the model to investigate scientific questions.

Scans were performed to investigate the influence of various factors on the pharmacokinetics of talinolol, including P-gp activity, OATP1B1, OATP2B1, renal function, and site-dependent intestinal absorption of talinolol. In addition, the effects of different degrees of cirrhosis were analyzed.

In the following, the results of the individual scans after taking 100 mg talinolol orally will be presented. The corresponding scans under intravenous administration can be obtained from the supplement Sec. 6.

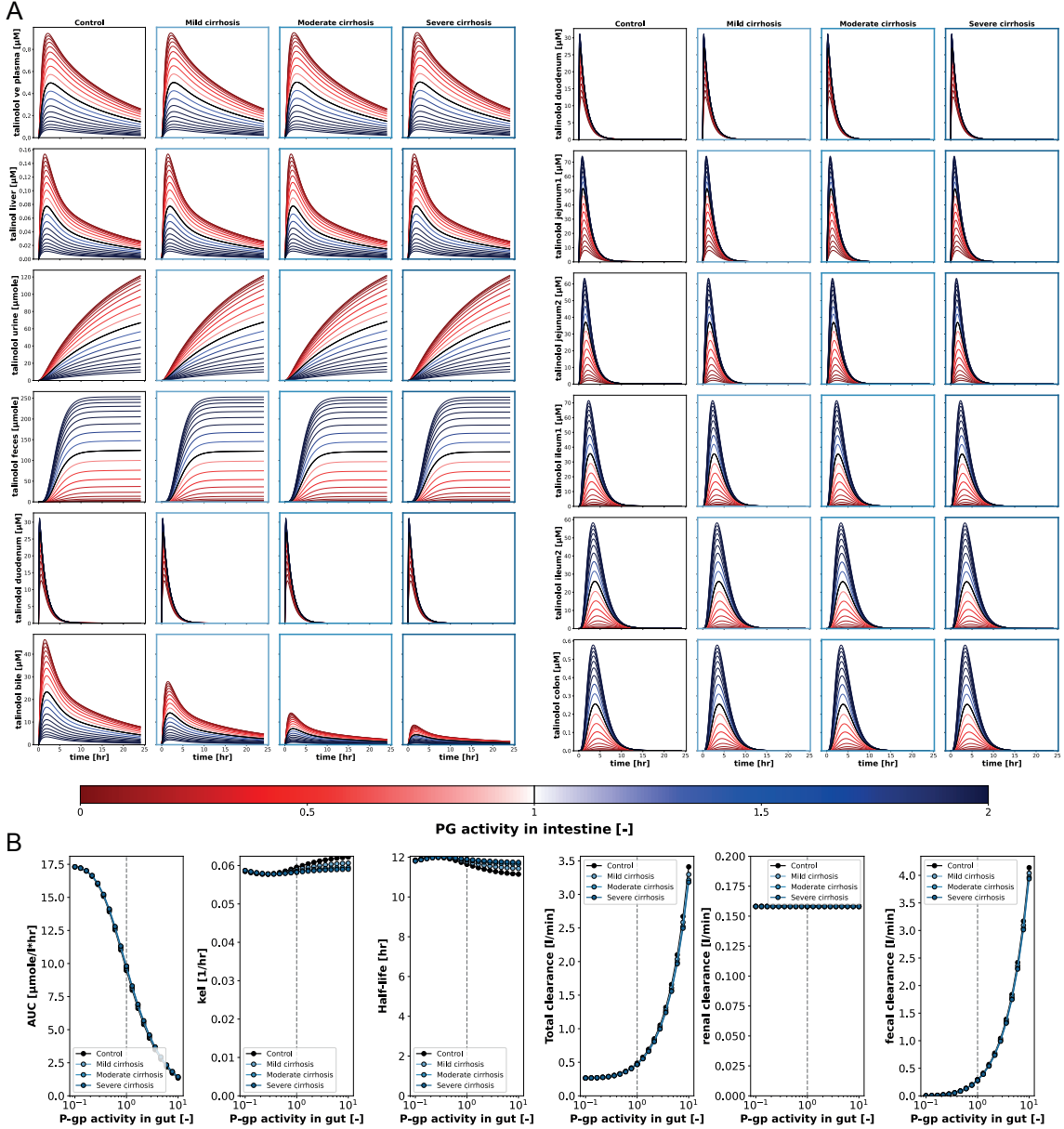
In the scan results, an increase of the investigated independent factor is depicted by the gradient of blue lines, while a reduction in the factor is represented by lines with a red gradient.

#### 3.5.1 Effect of P-glycoprotein activity

To study the effect of altered P-gp activity the corresponding factor was changed systematically and the effect on talinolol pharmacokinetics was studied.

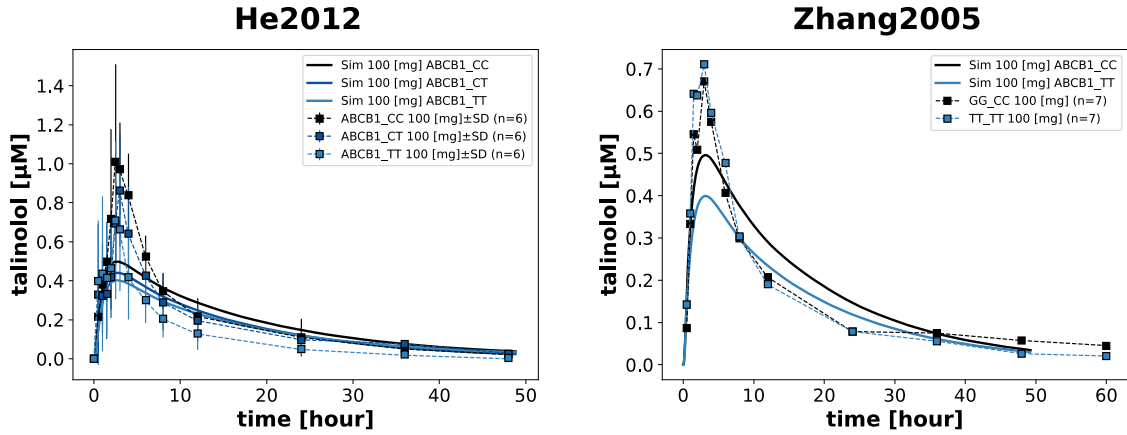
The results, as depicted in Fig. 18A, reveal a significant correlation between P-gp activity and the disposition of talinolol in the body. Decreased P-gp activity leads to elevated talinolol concentrations in plasma and liver, as well as increased excretion of talinolol in urine and bile. In contrast, talinolol concentrations in the duodenum and all other segments of the intestine, as well as the amount of talinolol excreted in feces, demonstrate a parallel relationship with P-gp activity, i.e., the larger the efflux activity the larger the respective values. Furthermore, the impact of reduced P-gp activity on talinolol concentration intensifies along the course of the intestine. Enhanced P-gp activity has limited effects on talinolol excretion in the human body and does not affect talinolol concentration in the duodenum. Furthermore, the results indicate that an increase in the severity of cirrhosis exhibits a diminishing effect on the excretion of talinolol into bile. However, no differences are observed in all other compartments.

Fig. 18B illustrates the impact of varying degrees of cirrhosis in relation to P-gp activity on several pharmacokinetic parameters, including AUC,  $k_{el}$ ,  $t_{half}$ , as well as total, renal, and fecal clearance. In the presence of cirrhosis and increased P-gp activity, there is a slight decrease or increase observed in  $k_{el}$  and  $t_{half}$ , respectively. These findings complement the previous results and highlight the influence of both cirrhosis severity and P-gp activity on talinolol pharmacokinetics. While AUC, total clearance, and fecal clearance are dependent on P-gp activity, renal clearance does not exhibit any dependence on either enzymatic activity or the presence of cirrhosis.



**Figure 18: P-gp scan.** (A) provides an overview of the effects of P-gp activity on talinolol availability in different compartments at different degrees of cirrhosis. Increased and decreased P-gp activities are marked by the blue and red gradients, respectively. (B) represents the influence of the degree of cirrhosis on the pharmacokinetic parameters AUC,  $k_{el}$ ,  $t_{half}$ , and clearance (renal, fecal, and total) at different P-gp activities and degree of cirrhosis.

The model predictions were validated by utilizing appropriate time curves from *He et al.* (2012) [26], *Zhang et al.* (2005) [96], and *Schwarz et al.* (2000) [66]. *He et al.* (2012) [26] and *Zhang et al.* (2005) [96] performed experiments with subjects with different genetic variants of P-gp who received a single oral dose of 100 mg talinolol. The experimental data were compared with the model's prediction in Fig. 19, revealing that an increased number of T alleles correlated with a reduction in AUC. The reduction in plasma concentration for the T variants are in good agreement with the observed reduction in *He et al.* (2012). In contrast, *Zhang et al.* (2005) does not report any differences between the CC and TT variants.



**Figure 19: Validation.** Comparison between the predicted talinolol plasma concentrations of different P-gp genotypes based on a model (solid line) and the experimental data (dashed line) from the studies by *He et al.* (2012) [26] and *Zhang et al.* (2005) [96] is shown. Increased P-gp activity of 20 % and 40 % was assumed for the CT and TT variants.

*Schwarz et al.* (2000) [66] studied the effect of drug-drug interactions after administering 50 mg of talinolol alone or combined with the P-gp inhibitor erythromycin. The outcomes were depicted in Fig. 20, indicating that inhibition of P-gp results in a higher  $c_{\max}$  and AUC of talinolol in plasma, which is in good agreement with the model's prediction.

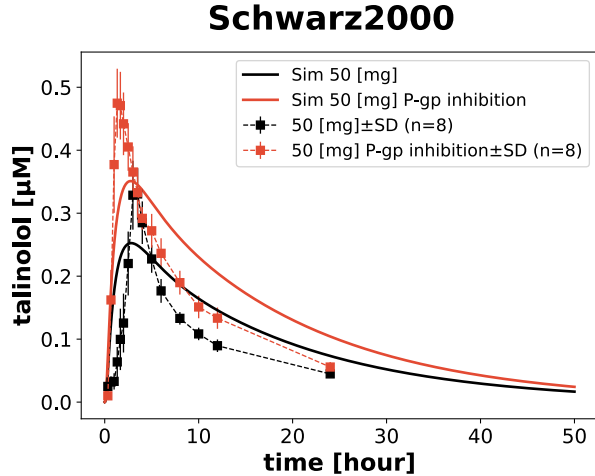


**Figure 20: Validation.** Shown is the model prediction (solid line) compared with curated time-course (dashed line) of *Schwarz et al.* (2000) [66] for the concentration of talinolol in serum. Normal P-gp activity is represented by the black line, while the red line depicts decreased P-gp activity due to inhibition by erythromycin. For the model simulation the P-gp activity was reduced to 50 %.

### 3.5.2 Effect of OATP1B1 activity

Next the effect of the hepatic uptake transporter OATP1B1 activity on the pharmacokinetics of talinolol was studied.

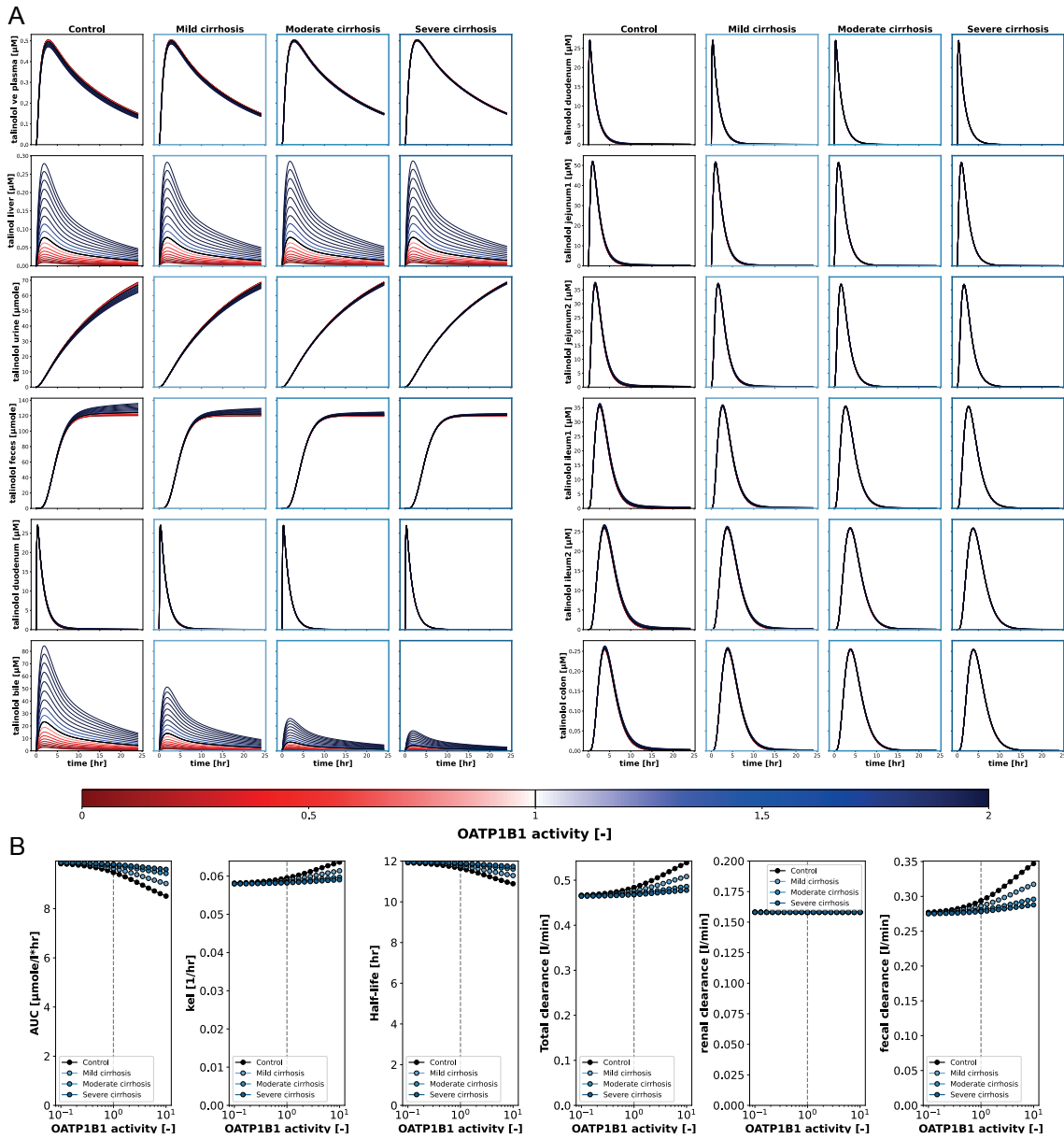


**Figure 21: OATP1B1 scan.** (A) provides an overview of the effects of OATP1B1 activity on talinolol availability in different compartments at different degrees of cirrhosis. Increased and decreased OATP1B1 activity are marked by the blue and red gradients, respectively. (B) represents the influence of the degree of cirrhosis on the pharmacokinetic parameters AUC,  $k_{el}$ ,  $t_{half}$ , and clearance (renal, fecal, and total) at different OATP1B1 activities.

The scanning results highlight that OATP1B1 activity primarily affects talinolol concentration in the liver and the excretion of talinolol into bile. Particularly, induction of OATP1B1 has a strong influence, resulting in increased concentrations and excretion of talinolol in the liver and bile. In contrast, minimal opposing effects are observed in plasma and urine. The inhibitory activity demonstrates contrasting effects on talinolol disposition in the body. However, talinolol concentrations in individual intestinal segments do not

significantly differ based on varying levels of OATP1B1 activity. Similarly, the severity of cirrhosis does not exert an influence.

With increasing severity of cirrhosis, changes are only observed in the liver, and the impact of OATP1B1 activity on talinolol disposition in the body is reduced. An overview of the scanning results is presented in Fig. 21A.

The results depicting the influence of cirrhosis on the pharmacokinetic parameters, depending on OATP1B1 activity, are shown in Fig. 21B. These findings reinforce the previously mentioned results and demonstrate that with increasing OATP1B1 activity, the severity of cirrhosis plays a role. This leads to a decrease in elimination rate, resulting in lower fecal excretion and prolonged retention of talinolol in the body. Conversely, renal clearance remains unaffected by both OATP1B1 activity and the severity of cirrhosis.

### 3.5.3 Effect of OATP2B1 activity

Next the effect of the intestinal uptake transporter OATP2B1 activity on the pharmacokinetics of talinolol was studied.

The scanning results, Fig. 22A, demonstrate that changes in the enzymatic activity of intestinal OATP2B1 are associated with alterations in all examined compartments. Augmenting OATP2B1 activity leads to a notable increase in talinolol absorption, consequently resulting in a higher proportion of talinolol being excreted in urine rather than feces. Conversely, diminishing OATP2B1 activity exerts an opposite effect, leading to a greater retention of talinolol in the intestinal tract. Notably, this effect becomes more pronounced as the distance from the duodenum increases. Furthermore, the influence of various degrees of cirrhosis on talinolol availability in individual compartments was examined. The scan outcomes reveal a significant correlation between talinolol concentration and the severity of cirrhosis. Interestingly, the concentration of talinolol and the impact of OATP2B1 activity tend to diminish as the degree of cirrhosis intensifies.

Fig. 22B illustrate the impact of cirrhosis severity on pharmacokinetic parameters, dependent on OATP2B1 activity. The results demonstrate that an increase in OATP2B1 activity leads to an elevation in the AUC of talinolol. The influence of reduced OATP2B1 activity on the elimination rate constant ( $k_{el}$ ) and half-life ( $t_{half}$ ) of talinolol in the body is contingent upon the severity of cirrhosis. In healthy conditions, OATP2B1 activity exerts minimal effects on  $k_{el}$  and  $t_{half}$ . However, as the severity of cirrhosis increases,  $k_{el}$  decreases, while  $t_{half}$  rises, for reduced OATP2B1 activity. Enhanced OATP2B1 activity is associated with decreased total and fecal clearance of talinolol. Neither OATP2B1 activity nor cirrhosis significantly impact renal clearance.

As an important side note, the effects of changes in OATP2B1 activity are opposite to changes in P-gp activity. As expected an increase in the intestinal influx transporter OATP2B1 has a similar effect as an decrease in the efflux transporter P-gp, and vice versa.

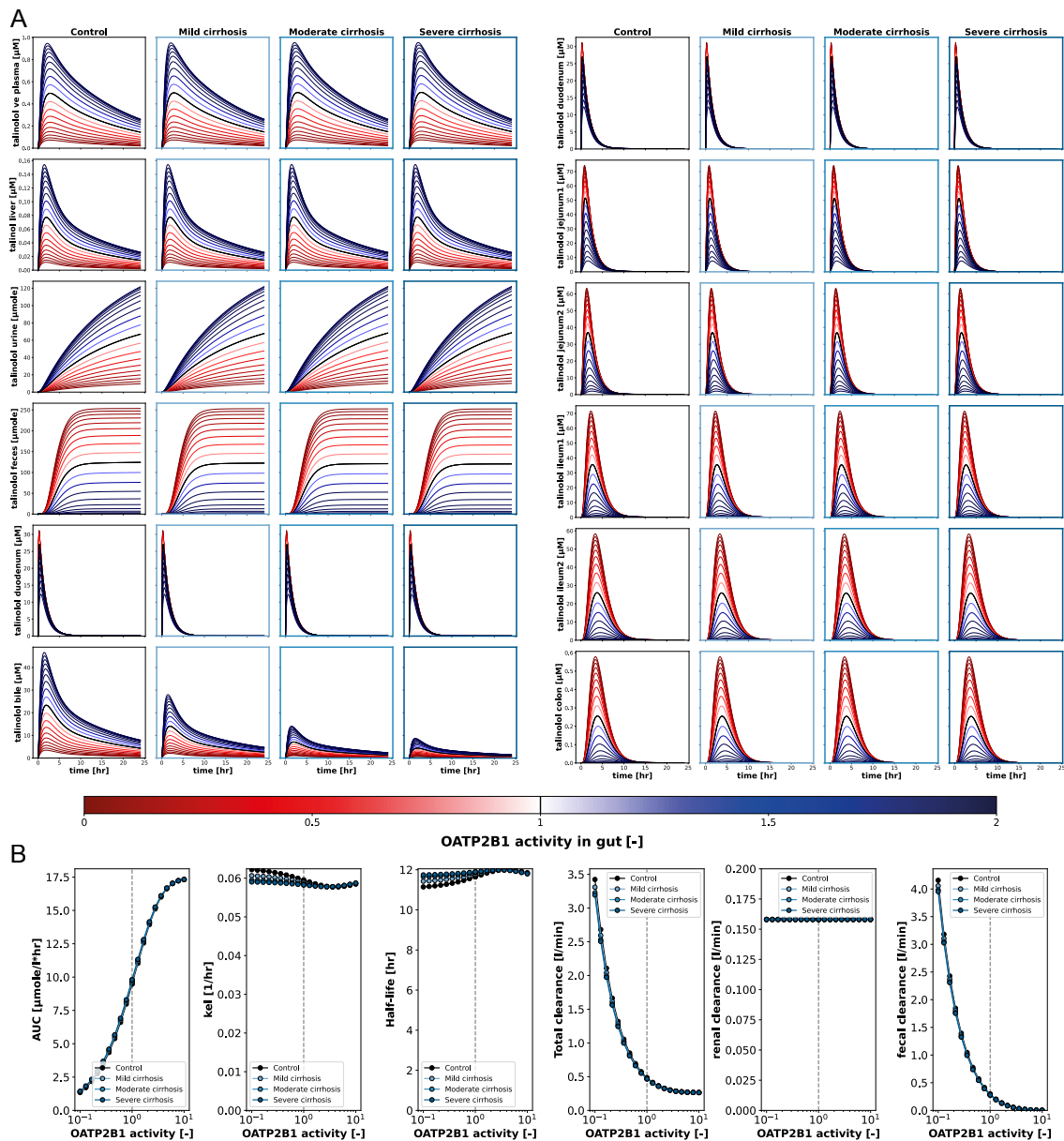


**Figure 22: OATP2B1 scan.** (A) provides an overview of the effects of OATP2B1 activity on taliolol availability in different compartments at different degrees of cirrhosis. Increased and decreased OATP2B1 activity are marked by the blue and red gradients, respectively. (B) represents the influence of the degree of cirrhosis on the pharmacokinetic parameters AUC,  $k_{\text{el}}$ ,  $\text{thalf}$ , and clearance (renal, fecal, and total) at different OATP2B1 activities.

### 3.5.4 Effect of renal function

Next the effect of renal function on the pharmacokinetics of talinolol was studied.

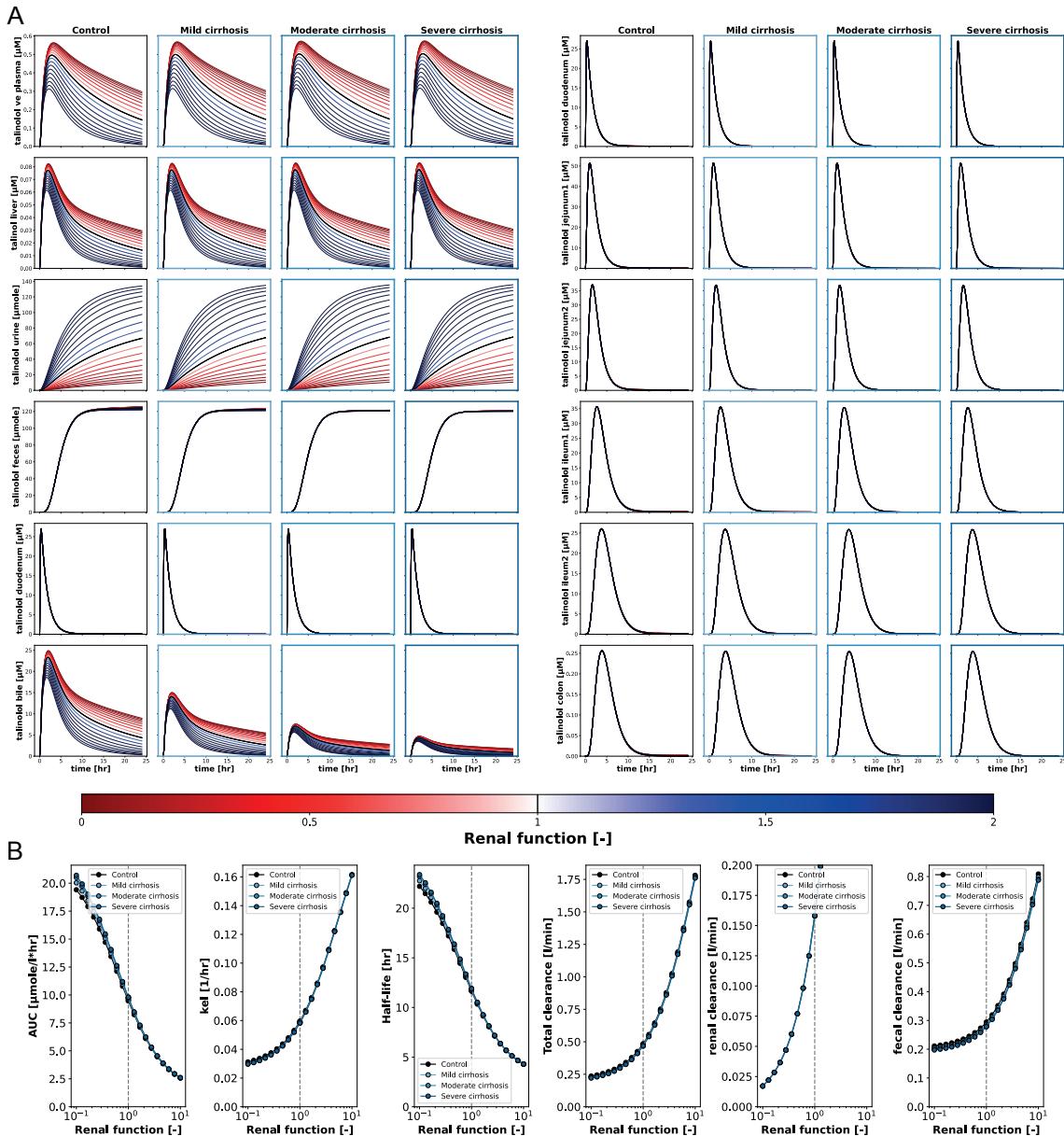


**Figure 23: Renal function scan.** (A) provides an overview of the effects of renal function on talinolol availability in different compartments at different degrees of cirrhosis. Increased and decreased renal function are marked by the blue and red gradients, respectively. (B) represents the influence of the degree of cirrhosis on the pharmacokinetic parameters AUC,  $k_{el}$ ,  $t_{half}$ , and clearance (renal, fecal, and total) dependend on renal function.

The scanning results (Fig. 23A) demonstrate that the talinolol concentration in the intestine and the amount excreted in feces remain unchanged even when renal function is altered. A decrease in renal function leads to an increase in talinolol concentration in plasma, liver, and bile, as well as a reduction in the amount of talinolol excreted in urine. Conversely, an increase in renal function has the opposite effect, resulting in a decrease in talinolol concentration in plasma, liver, and bile, along with an increase in the amount of

talinolol excreted in urine. The increase in renal function exerts a stronger effect on the disposition of talinolol compared to the decrease in renal function.

With increasing severity of cirrhosis, the impact of altered renal function on talinolol disposition is predominantly observed in the concentration of talinolol in bile, exhibiting an approximate 80 % reduction. Conversely, cirrhosis has no significant effect on the overall disposition of talinolol in the body. Fig. 23B illustrates the influence of cirrhosis severity in relation to renal function on the pharmacokinetic parameters of talinolol. The results indicate that only with impaired renal function are slight changes in AUC,  $t_{\text{half}}$ , and fecal clearance attributable to cirrhosis observed. Renal clearance, on the other hand, is solely dependent on renal function. As renal function increases,  $k_{\text{el}}$  and total, renal, and fecal clearance of talinolol also increase, while AUC and  $t_{\text{half}}$  decrease.

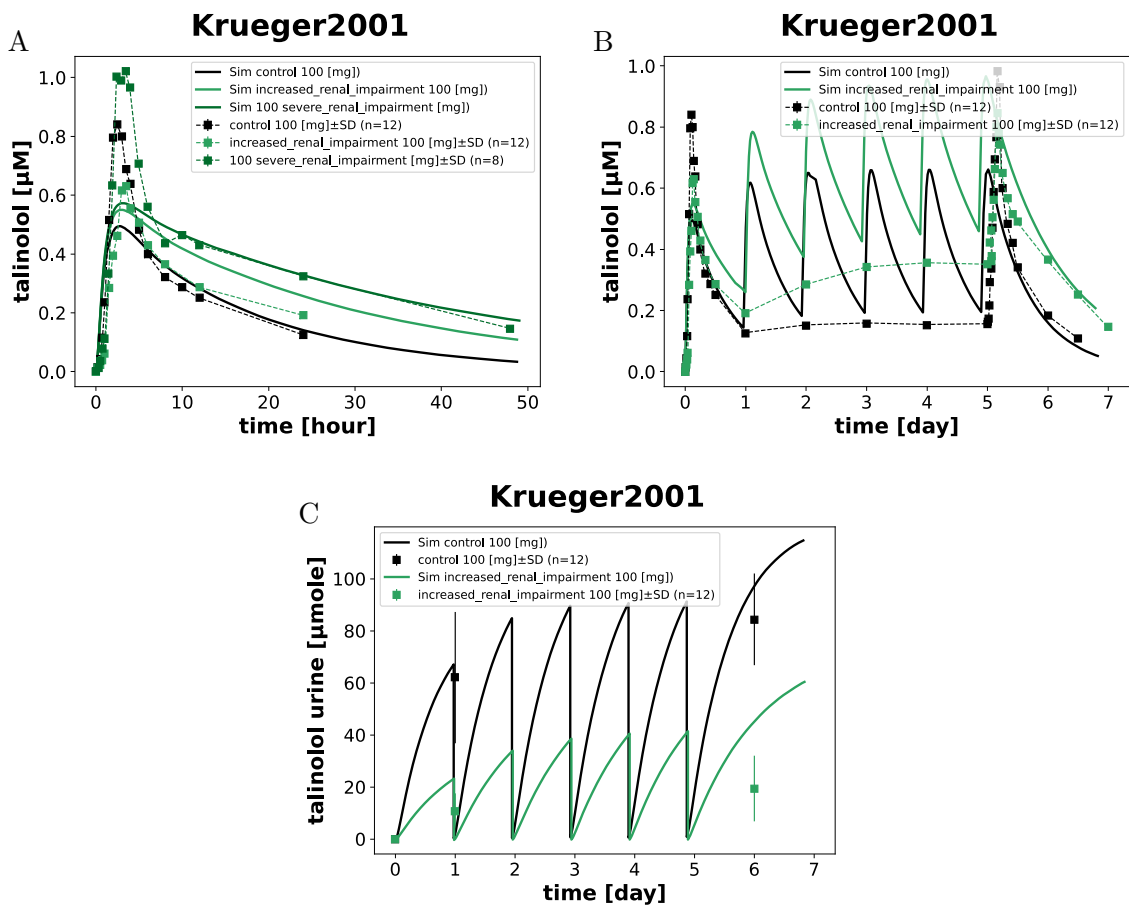


**Figure 24: Validation.** Comparison between the model prediction and the experimental data of Krueger *et al.* (2001) [49] for different degrees of renal impairment (green lines). Decreased kidney function of approx. 50 - 70 % in case of elevated or severe renal insufficiency, respectively. The time curves of talinolol in (A) plasma after a single dose, (B) multiple dose (C) in urine are presented. The time course predicted by the model is displayed by the solid line, and the data from the curated studies are indicated by the dashed line.

The model predictions for renal impairment were validated with experimental data. Krueger *et al.* (2001) [49] studied the pharmacokinetics of talinolol in 24 subjects with different creatinine clearance levels corresponding to various degrees of renal impairment after 100 mg of talinolol administration.

In Fig 24, the experimental data, with single and repeated administration of talinolol,

from plasma and urine, were compared with the model prediction. Regardless of the mode of administration, it can be seen that with increasing renal impairment, the  $c_{max}$  in plasma increases, and the amount excreted in urine decreases. Overall the model prediction is in very good agreement with the data. However, it is important to note that the model predicts a slightly lower trajectory but greater accumulation of talinolol in both plasma and urine compared to what is suggested by the experimental data.

Fig. 25 illustrates the relationship between renal clearance and creatinine clearance, which serves as a measure of renal function. In healthy subjects and those with severely impaired renal function, the average renal clearance is approximately 0.03 and  $0.15 \frac{l}{min}$ , respectively. With improved creatinine clearance, the variability of renal clearance increases. The model enables the representation of the correlation between renal clearance and renal function.

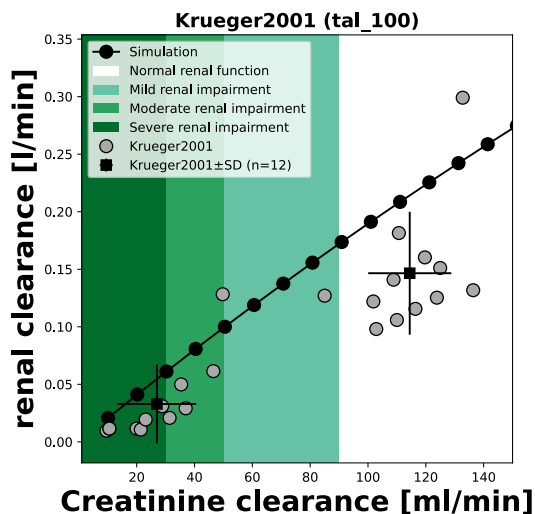


**Figure 25: Validation.** Shown is the correlation between renal clearance of talinolol and creatinine clearance in the model and the *Krueger et al.* (2001) [49] study. The degrees of renal insufficiency are shown in different green colors. The gray dots describe the subjects from the study, and the black squares are the mean $\pm$ SD of the group. The solid black line represents the model prediction.

### 3.5.5 Site-dependency of intestinal absorption

Next the effect of site-specific infusion of talinolol in the intestine on pharmacokinetics of talinolol was studied.

In addition to oral administration of talinolol in solid form, it is possible to infuse talinolol specifically into different intestinal segments. The intestinal site-dependency scan depending on the P-gp activity allows a detailed investigation of the pharmacokinetics of talinolol after administration into the individual segments, duodenum, jejunum\_1, jejunum\_2, ileum\_1, ileum\_2, and colon. The infusion is applied as an infusion at constant rate for five hours. In the investigation of the site-specific infusions, an immediate decrease in talinolol concentration is observed in plasma, liver, bile, and individual segments of the intestine following the end of infusion, except in urine and feces, which show further increase after the infusion ends due to the cumulative character of the quantities (i.e. total amount in feces and urine).

Furthermore, minimal talinolol is detected in regions prior to the infusion site, which is due to the minimal enterohepatic circulation of talinolol.

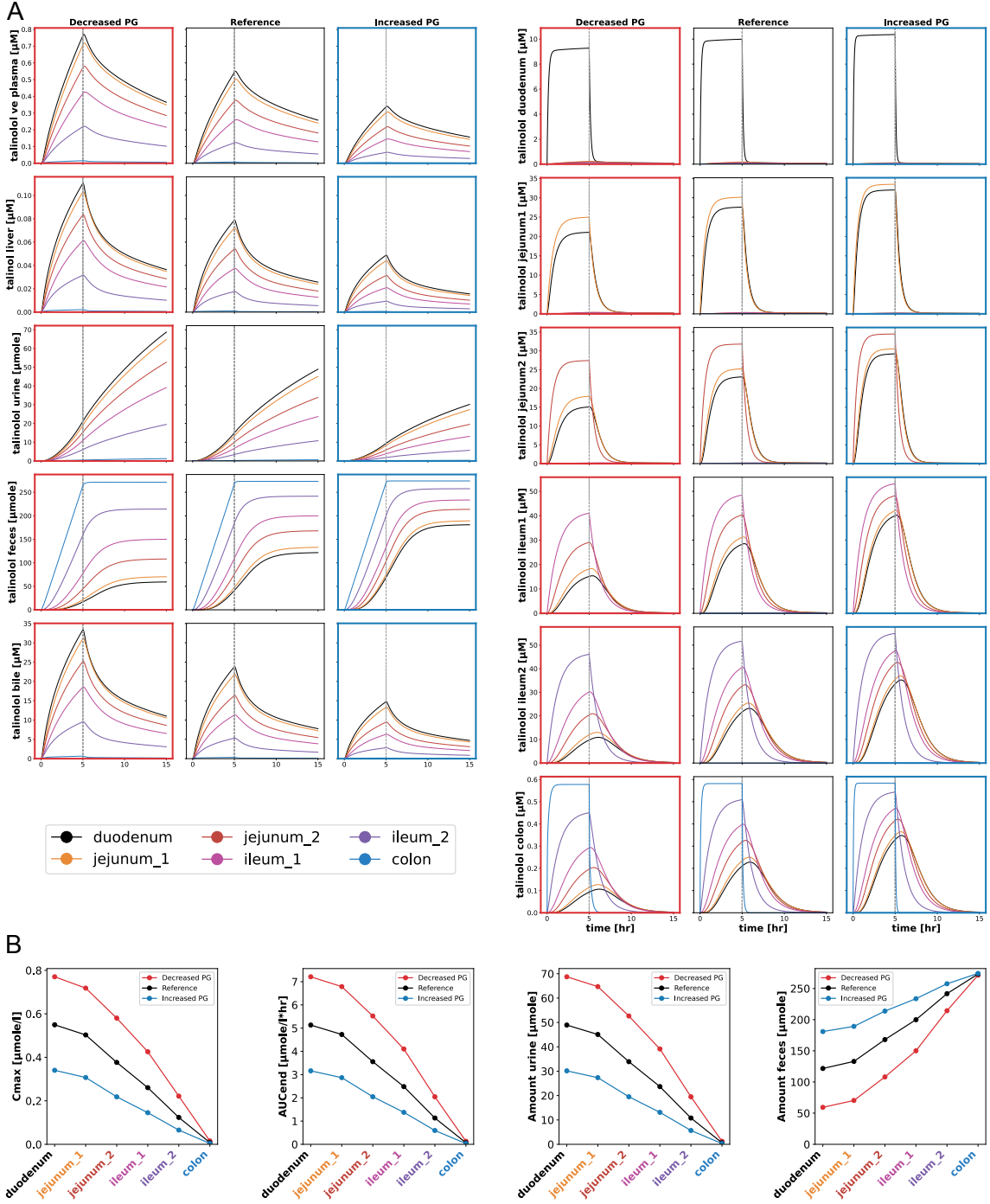


**Figure 26: Site-dependency scan.** (A) provides an overview of the effects of site-dependency intestinal infusion on talinolol availability in different compartments at different P-gp activities. Intestinal infusion in duodenum (black), jejunum\_1 (orange), jejunum\_2 (red), ileum\_1 (pink), ileum\_2 (purple), and colon (blue) are shown. (B) shows the influence of P-gp activity on pharmacokinetic parameters  $\text{AUC}_{\text{end}}$ ,  $C_{\text{max}}$ , and the amount in urine and feces depending on the localization of intestinal infusion.

Overall, the results (Fig. 26) demonstrate a decrease in talinolol concentration in plasma, urine, and bile with increasing distance from the duodenum. In contrast, the amount of talinolol in feces increases. This observation is further supported by the infusion of talinolol into the colon, where no talinolol is absorbed into the body, and 100 %

of the administered talinolol is recovered in feces. While fecal excretion remains constant during infusion into the colon, the bioavailability of talinolol decreases with both the distance from the infusion site to the duodenum and increasing P-gp activity.

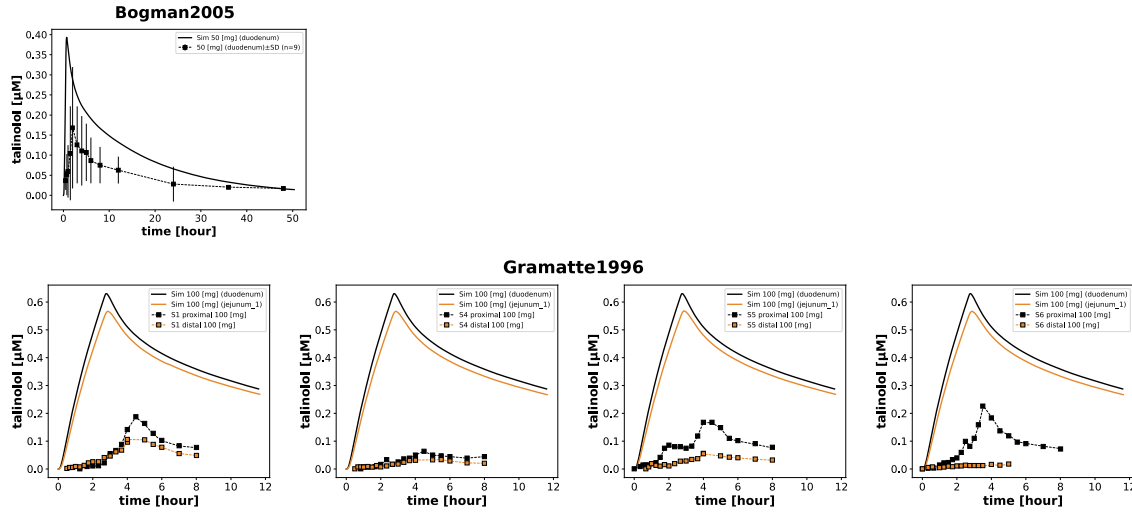


**Figure 27: Validation intestinal infusion.** Talinolol plasma concentrations after 30 min infusion in the duodenum (black line) or jejunum\_1 (orange line) are shown. The model prediction is shown by the solid line while the dashed line represents the data from the studies *Gramatte et al.* (1996) [18] and *Bogman2005 et al.* (2005) [6].

*Gramatte et al.* (1996) [18] utilized the method of intestinal infusion to investigate the absorption of talinolol along the intestine. The infusion was administered either in the duodenum or jejunum. In contrast, *Bogman et al.* (2005) [6] performed the infusion exclusively in the duodenum. Significant variations in talinolol concentrations in the serum were observed among the subjects. In all cases, less talinolol was absorbed when the infusion was initiated distal to the duodenum. Despite the model predictions not being in good agreement for the plasma concentrations, the relative decrease in talinolol plasma concentrations when varying the infusion site can be recapitulated by the model. These regioselective absorption differences were effectively described by the model.

### 3.6 Summary

Within this study, a comprehensive physiologically based pharmacokinetic (PBPK) model for talinolol was developed. Notably, the intestinal compartment of the model was subdivided, facilitating the targeted infusion of talinolol into specific segments of the intestine. This subdivision enabled an in-depth investigation of talinolol disposition in relation to the varying levels of key intestinal proteins, P-gp and OATP2B1 and the site-dependent effects in the intestine. Predictions of the developed model were rigorously compared to experimental data from a multitude of curated studies. Overall, the model showed a very good agreement with most of the experimental data covering different domains.

Additionally, the established PBPK model was utilized to investigate the impact of multiple factors on the pharmacokinetics of talinolol, including the enzymatic activity of P-gp, OATP2B1, and OATP1B1, as well as renal function, cirrhosis, and differential protein distribution within the intestine. To further validate the performance of the model, additional validation was conducted using literature data that encompassed genetic variations of P-glycoprotein (P-gp), renal impairment, and the effects of intestinal infusion of talinolol.

## 4 Discussion

### 4.1 Data

Within this work an extensive quantitative data set of talinolol was established and used to develop a PBPK model of talinolol. The data set contains information on time courses and pharmacokinetics after single and multiple oral, intravenous, and intraintestinal administrations of talinolol. To our knowledge this is the largest available resource on the pharmacokinetics of talinolol with all data freely available from PK-DB. We envision that the data set will be an important asset in further studies of talinolol.

Notably, the data have some limitations: (i) most studies were performed on healthy adult subjects, one of the exceptions being a group of patients with renal impairment [49]. (ii) The concentration-time curves of talinolol in the plasma and serum from most studies are consistent with a few exceptions [87, 67]. But the large standard deviation (if reported) indicates significant variability between individuals. The same applies to the excretion amounts of talinolol in urine and bile. (iii) very limited data was available on talinolol recovery in the feces with only *Bernsdorf et al.* (2006) [5] providing data on the excretion amount of talinolol in feces following both intravenous and oral administration. (iv) Although numerous studies have investigated the pharmacokinetics of talinolol in relation to genetic variants of P-gp, the available data on the time courses of talinolol depending on P-gp genetic variants are comparatively limited. Additionally, there is a lack of available data on the relationship between OATP2B1, OATP1B1 and the pharmacokinetic parameters of talinolol. (v) Information about talinolol pharmacokinetics in liver disease was very limited and no data for cirrhotic patients was available.

Despite this limitations, the dataset comprising 33 studies from a total of 445 subjects provides both quantitative and qualitative data to support the fitting and validation of the talinolol PBPK model.

Importantly, our model predictions provided information about possible alterations of pharmacokinetics in the cases where only minimal data was available, such as changes in OATP2B1 activity, P-gp activity, or hepatic impairment. Our simulations could therefore fill an important gap of knowledge in talinolol pharmacokinetics and motivate target experiments. Hopefully future research, will address these areas thereby allowing a more comprehensive validation of the model and understanding of talinolol.

### 4.2 Model

Based on the established dataset, a physiologically based pharmacokinetic (PBPK) model was developed to analyze the pharmacokinetics of talinolol. The model is based on five key assumptions:

1. Talinolol is absorbed irreversibly across the apical membrane of enterocytes via OATP2B1.
2. Efflux of talinolol from enterocytes into the intestinal lumen occurs irreversibly through P-gp.
3. Import of talinolol into the liver takes place irreversibly via OATP1B1.
4. No metabolism of talinolol takes place in the body.
5. Talinolol undergoes transport from the bile into the duodenum, leading to enterohepatic circulation.

No information was available about the reversibility of talinolol transport via OATP2B1, OATP1B1 and P-gp. The assumption of irreversibility was used for simplification of the model. Only minimal talinolol metabolism has been reported in the literature (< 1 %) via CYP3A4 dependent hydroxylation of talinolol [5, 62, 81, 97].

The model was fitted using single-dose intravenous and exclusively fast-release oral data. The current model is not applicable to controlled-release formulations which show markedly altered pharmacokinetics with later and lower maximal plasma concentrations. But the model could easily be extended to include such data, e.g., by adjusting the tablet dissolution and absorption rates based on the tablet formulation. Because only a small subset of the data was reported for slow-release tablets the focus of the model was on the fast-release formulations.

According to the results, the model demonstrates a strong agreement with the overall dynamics of talinolol disposition in the body, for both intravenous and single/multiple oral administrations of talinolol.

The developed model was a mean model and we did not take intra-individual variability into account, despite large variability observed in the curated data. Future model extensions will account for these variability, e.g., via nonlinear mixed effect models or sampling from underlying parameter distributions.

### Intestinal model

An important part of the model was a subdivision of the intestine into subcompartments corresponding to duodenum, ileum, jejunum, and colon which enabled to model the effect of site-specific intestinal infusion of talinolol and the effect of site-dependent inflow and efflux transporters.

The protein level of OATP2B1 remains relatively constant throughout the different intestinal segments, whereas the protein level of P-gp increases along the small intestine. This distribution of OATP2B1 as an importer and P-gp as an efflux transporter in the intestine has the consequence that the bioavailability of talinolol in plasma decreases with increasing distance from the duodenum. The model successfully described these differences. Such site-specific windows of absorption can be important determinants of drug pharmacokinetics.

Interestingly, based on the site-dependency scan (see Sec. 3.5.5), the model shows that talinolol does only appear in very small amounts in segments above the infusion site due to the uni-directional motion within the intestinal model combined with minimal enterohepatic circulation. This finding suggests that enterohepatic circulation in talinolol's disposition is relatively insignificant.

Nevertheless, it is crucial to acknowledge that the intestinal model only includes the two primary transporters P-gp and OATP2B1, which are the main transporters reported being responsible for the intestinal disposition of talinolol. The possible role of other transporters, such as OATP1A2 [68] or MRP2 [17], was not considered in the model. Gaining a more complete picture of the role of the various transporters for talinolol pharmacokinetics would be beneficial in understanding drug-drug interaction in the intestine. The model allowed to characterize the effects of OATP2B1, P-gp and OATP1B1 on talinolol pharmacokinetics, in a similar manner an extended model could be used to study the role of additional transporters.

### 4.3 Genetic variants

The present study focused on investigating the influence of the genotype of P-gp, OATP2B1, and OATP1B1 on the pharmacokinetics of talinolol.

In particular, the results concerning the P-gp genotype were interesting. However, conflicting results were reported regarding the effect of variants of P-gp. *Kim et al.* (2001) [38] demonstrated that the mutant genotype 1236 C>T, 2677 G>T, 3435 C>T (TTT) exhibited a 40 % reduction in AUC compared to the wild-type genotype (CCC). This mutation-induced change was modeled and compared with the studies of *He et al.* (2012) [26] and *Zhang et al.* (2005) [96]. The model showed good agreement with the data of *He et al.* (2012) [26]. It is worth noting that *He et al.* (2012) [26] only investigated the genetic variants of the SNP on position 3435.

The impact of OATP1B1 gene polymorphisms on talinolol pharmacokinetics was only reported by *Bernsdorf et al.* (2006) [5]. The model successfully corroborated the results by revealing a correlation between the predicted half-life of talinolol and the activity of OATP1B1, as depicted in Fig. 21B. Unfortunately, the data was very limited and no timecourse data was reported which would have allowed for a more thorough validation of our predictions. Given the limited sample size, future investigations should consider further exploring the effects of genetic variants of OATP1B1 on the pharmacokinetics of talinolol.

### 4.4 Disease

The thesis is also dedicated to the investigation of the influence of cirrhosis, a chronic liver disease, and renal impairment on the pharmacokinetics of talinolol. One of the objectives of this project was indeed to utilize the developed model to make predictions regarding the pharmacokinetics of talinolol for different stages of cirrhosis and renal function. The presented model suggest that a higher degree of cirrhosis leads to a decrease in the uptake of talinolol into the liver. This could result in a prolonged drug residence time in the body and higher plasma levels. These effects are further reinforced by the reduced activity of OATP1B1 and intestinal P-gp. The only pharmacokinetic parameter not influenced by cirrhosis is the renal clearance. To validate the model's predictions and further enhance understanding of the influence of cirrhosis on the pharmacokinetics of talinolol, future research should include studies on the pharmacokinetics of talinolol in patients with varying degrees of cirrhosis. Moreover, such studies could contribute to expanding the understanding of potential dosage adjustments when administering talinolol to patients with cirrhosis.

The model demonstrates a clear correlation between renal clearance of talinolol and renal function. Furthermore, renal function exerts a particularly strong influence on the AUC of talinolol. When compared (see Fig. 24) to *Krueger et al.* (2001) [49], who gathered an extensive pharmacokinetic dataset of talinolol in subjects with varying renal functions, the difference in AUC following single and multiple administrations of talinolol for different renal functions was accurately captured. In an even stronger concordance, the model's prediction is consistent with the observed data regarding the dependency of renal clearance on creatinine clearance, a well-established indicator of renal function.

In summary, the present work provides valuable insights into the influence of cirrhosis and renal function on the pharmacokinetics of talinolol in the human body, particularly in relation to the activity of P-gp, OATP2B1, and OATP1B1. The findings underscore the need for further research in this field to optimize the use of talinolol in patients with cirrhosis and renal insufficiency and ensure effective therapy.

## 5 Outlook

This work has demonstrated that talinolol is a suitable test substance to investigate the activity of intestinal transport proteins such as P-gp and OATP2B1, as well as the liver-specific OATP1B1.

### 5.1 Drug-drug interactions

Drug-drug interactions can cause undesirable pharmacokinetic effects that also impact the pharmacodynamics of medications. Studies have shown that the combined intake of talinolol with rifampin leads to reduced talinolol plasma concentration due to increased activity of P-gp [90, 97]. The talinolol database and curated studies encompass a variety of drug-drug interactions involving talinolol and other medications such as simvastatin [5], St. John's Wort [64], erythromycin [66], and many more. A promising avenue is to extend the existing physiologically-based pharmacokinetic (PBPK) model with models for additional substances which would allow to study and better understand these drug-drug interactions. In summary, the PBPK model of talinolol and the existing curated data provide a solid foundation for future research on drug-drug interactions with P-gp.

### 5.2 Drug formulations

The model allows accurate predictions for the pharmacokinetics of talinolol after intravenous infusion and administration of fast-release formulations. The composition of a medication formulation can have a crucial impact on the bioavailability of the drug in the body. While there are no differences in the pharmacokinetics between film-coated and sugar-coated tablets [69] or capsules [54] of talinolol, the ingestion of controlled-release tablets leads to significantly reduced bioavailability of talinolol compared to fast-release tablets ( $c_{\max}$   $43.9 \pm 11.6$  vs.  $204.5 \pm 121.8 \frac{ng}{ml}$  and AUC  $1580.9 \pm 605.1$  vs.  $2933.9 \pm 738.4 \frac{ng \cdot h}{ml}$ ) [83]. The slower dissolution of the tablet results in the release of talinolol in more distal segments of the intestine.

Overall, these findings highlight the importance of considering the specific formulation and its impact on drug bioavailability. Future research should focus on exploring the relationship between tablet formulations or site-specific intestinal infusion, and protein distribution in the intestine to enhance our understanding of the factors influencing drug absorption and bioavailability.

### 5.3 Gastrointestinal surgery

The model demonstrated that talinolol undergoes region-selective absorption, primarily mediated by the intestinal distribution of OATP2B1 and P-gp proteins, with the absorption window located in the upper region of the duodenum. However, this window can be closed by gastrointestinal interventions, such as bariatric surgery [75]. Bariatric surgery is a long-term effective method [34] for treating adipositas ( $BMI \geq 35 \frac{kg}{m^2}$ ), which affects 19 % of adults in Germany [41].

Examining the influence of gastrointestinal resection on talinolol's pharmacokinetics would not only enhance our understanding of drug absorption in post-surgical patients but also expand the applicability of the model to a broader range of patient populations. Such investigations would contribute to optimizing medication dosing and treatment strategies for individuals who have undergone gastrointestinal resection, ultimately improving therapeutic outcomes and patient care.

## Acknowledgements

I would like to express my sincere gratitude to my supervisor, Dr. Matthias König, for providing me with the opportunity to undertake this project and for his exceptional support and guidance throughout. His expertise and encouragement have been invaluable in shaping the direction of my research and thesis.

I would also like to extend my heartfelt thanks to my family and friends for their unwavering support and patience during this time. Their encouragement and understanding have been crucial in helping me stay focused and motivated.

A special acknowledgment goes to Florian Bartsch and Sophie Silberhorn, whose constant motivation and support have been instrumental in pushing me forward every day.

## 6 Supplement

### Effect of P-Glycoprotein (iv application)

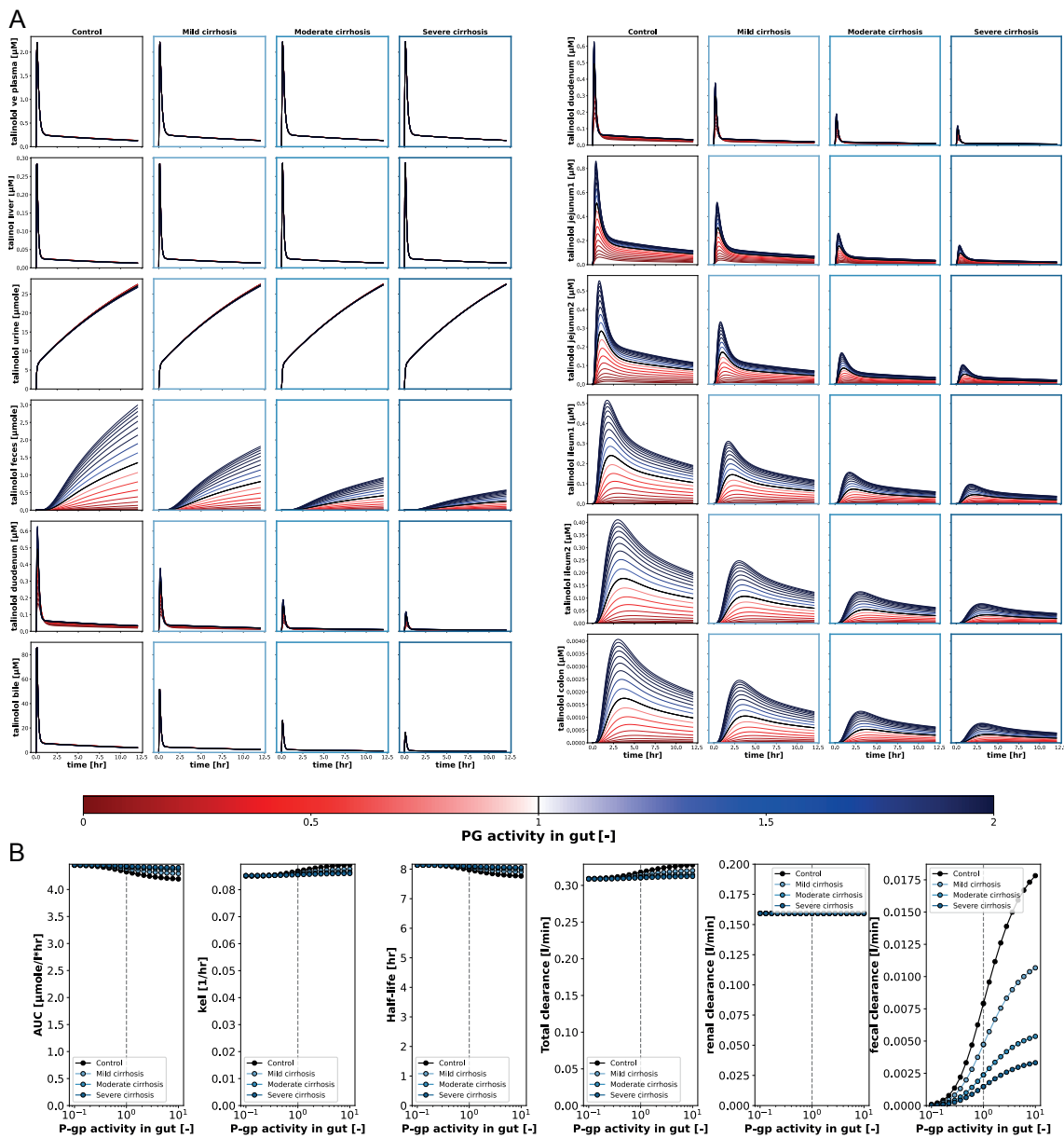


**Figure 28: P-gp scan.** (A) provides an overview of the effects of P-gp activity on talinolol availability in different compartments at different degrees of cirrhosis. Increased and decreased P-gp activities are marked by the blue and red gradients, respectively, in color. (B) represents the influence of the degree of cirrhosis on pharmacokinetic parameters of AUC,  $k_{el}$ ,  $t_{half}$ , and clearance (renal, fecal, and total) at different P-gp activities.

## Effect of OATP1B1 (iv application)

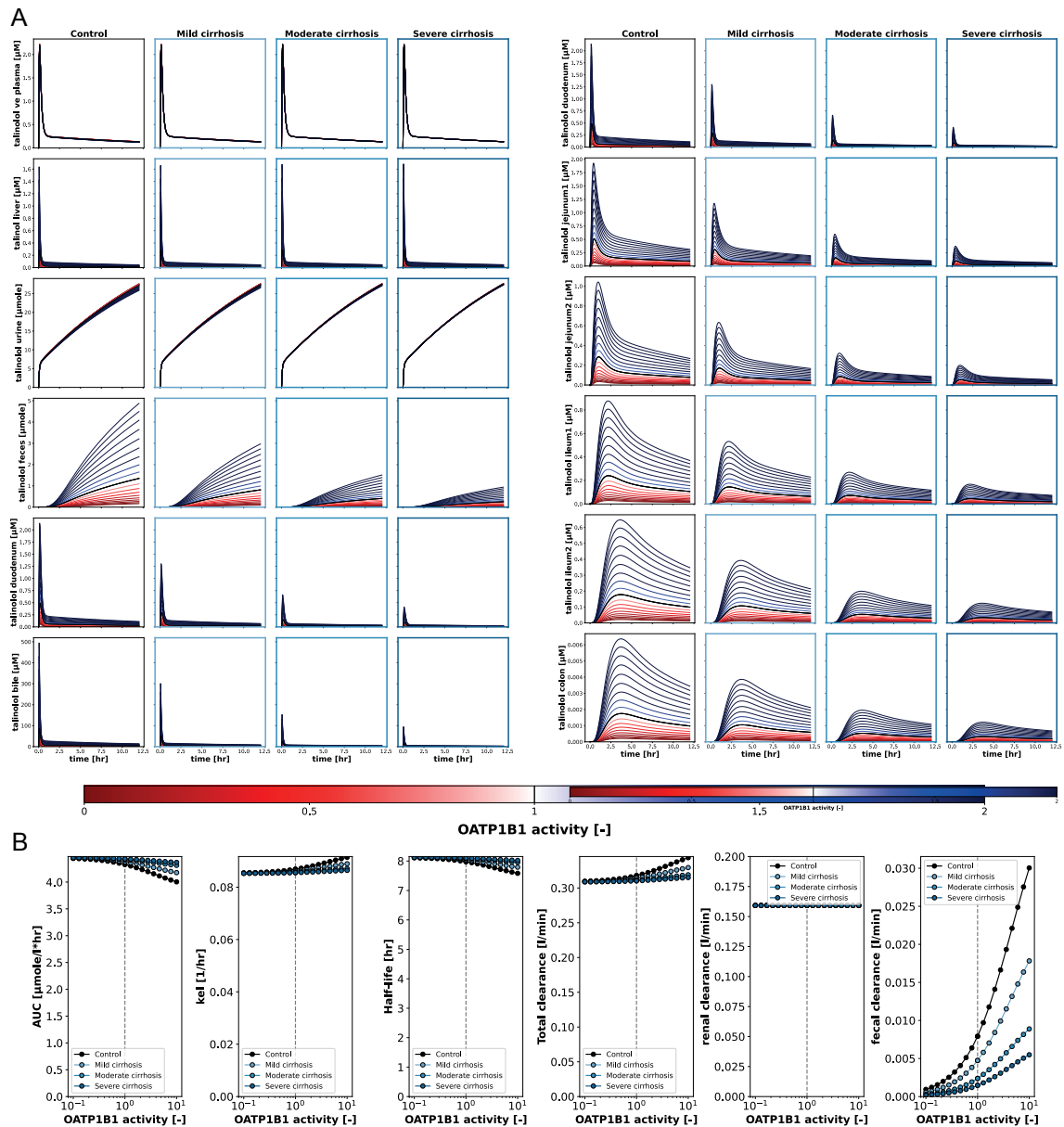


**Figure 29: OATP1B1 scan.** (A) provides an overview of how the activity of OATP1B1 affects the availability of talinolol in different compartments at various degrees of cirrhosis. The color gradients indicate increased (blue) or decreased (red) OATP1B1 activities. (B) illustrates the impact of cirrhosis severity on pharmacokinetic parameters such as AUC,  $k_{el}$ ,  $t_{half}$ , and clearance (renal, fecal, and total) at different levels of OATP1B1 activity.

## Effect of OATP2B1 (iv application)

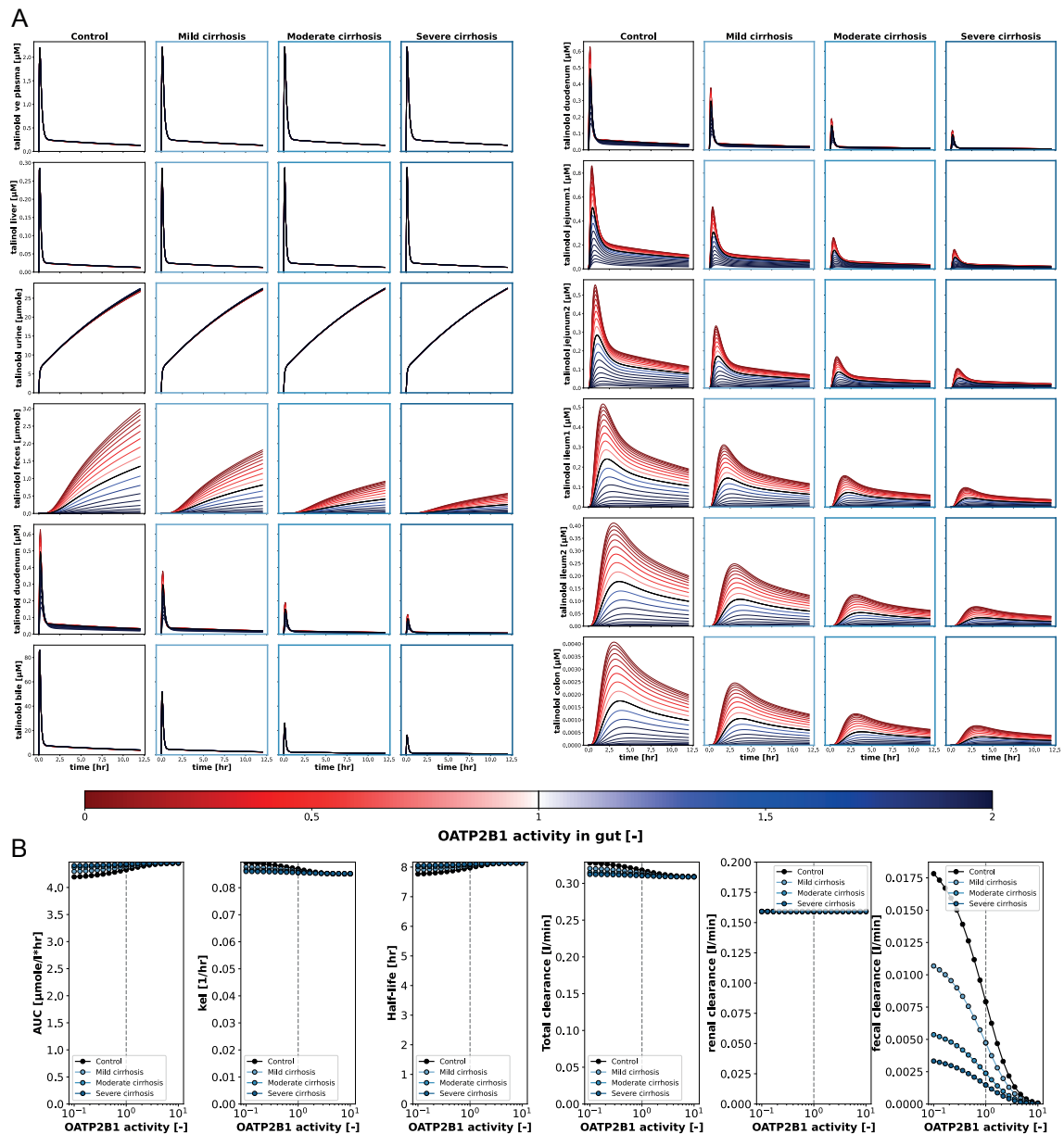


**Figure 30: OATP2B1 scan.** (A) provides an overview of the effects of OATP2B1 activity on talinolol availability in different compartments at various degrees of cirrhosis. The color gradients indicate increased (blue) or decreased (red) OATP2B1 activities. (B) illustrates the influence of cirrhosis severity on pharmacokinetic parameters such as AUC,  $k_{el}$ ,  $t_{half}$ , and clearance (renal, fecal, and total) at different levels of OATP2B1 activity.

## Effect of renal function (iv application)

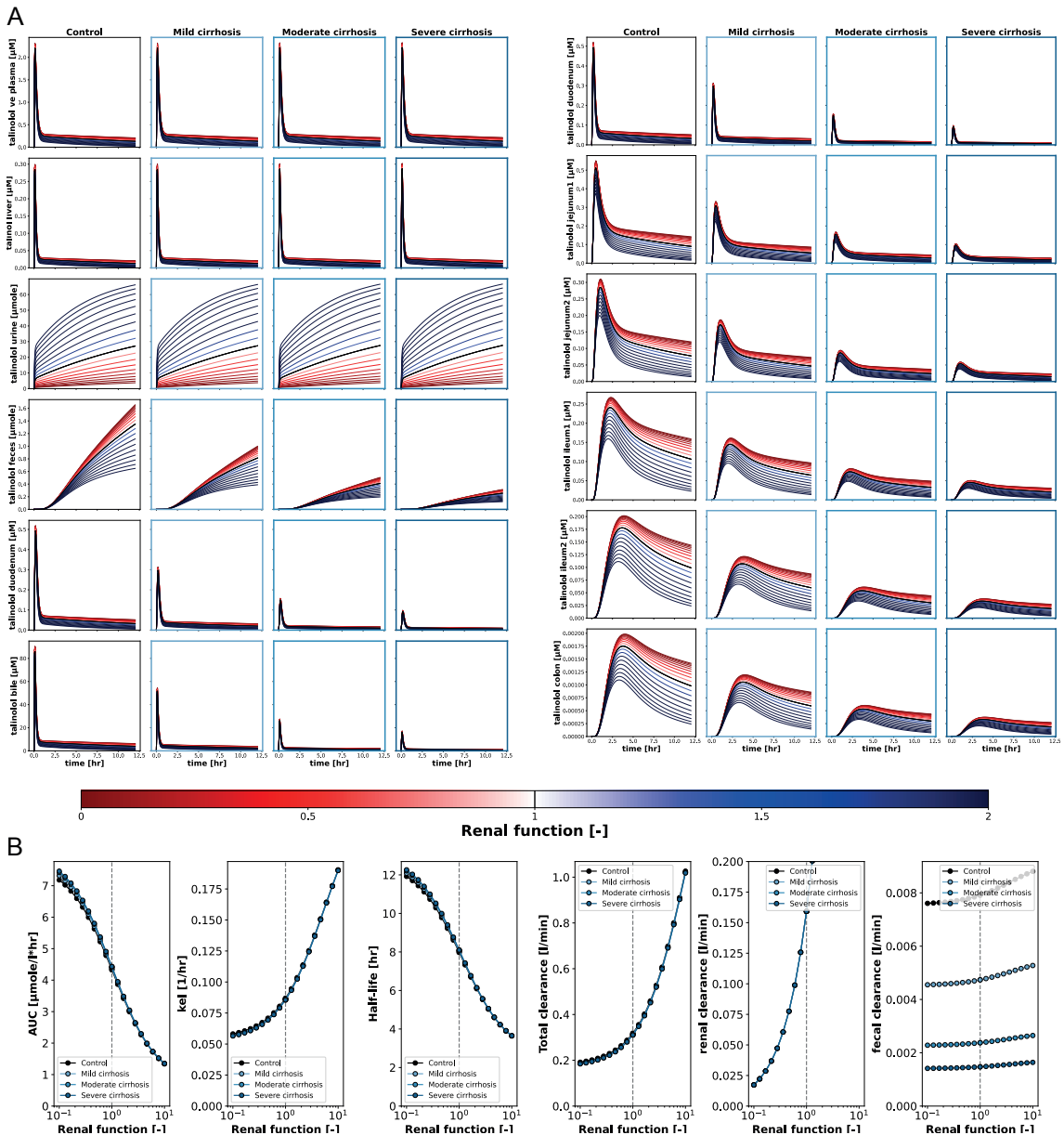


**Figure 31: Renal function scan.** (A) provides a comprehensive assessment of the influence of renal function on the availability of talinolol in different compartments across varying degrees of cirrhosis. The color-coded gradients indicate the impact of renal function on the transport and availability of talinolol. (B) presents the relationship between the severity of cirrhosis and key pharmacokinetic parameters, including AUC,  $k_{el}$ ,  $t_{half}$ , and clearance (renal, fecal, and total), considering different levels of renal function.

## Excluded data sets

The exclusion of the following datasets was based on the reasons provided in the legend.

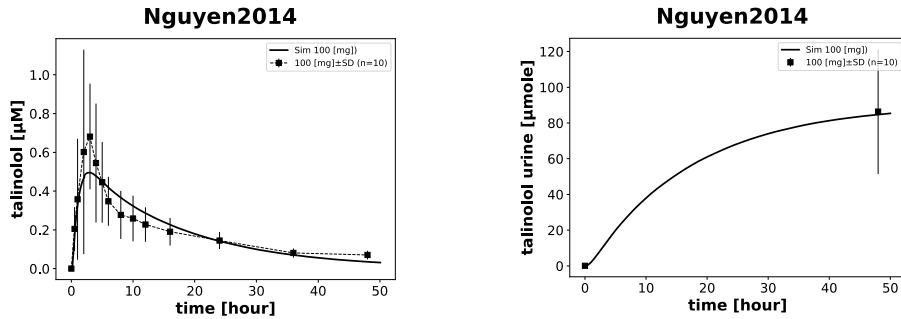


**Figure 32:** Simulation experiments Nguyen2014 [59], data was duplicate data from Nguyen2015 [58], which provided a more comprehensive dataset.

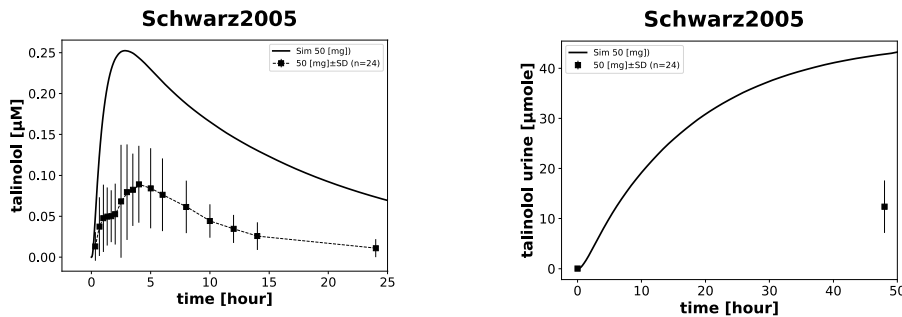


**Figure 33:** Simulation experiments Schwarz2005 [67], reported data was much too low for the given dose. Most likely slow release tablets, but no information provided in the study.

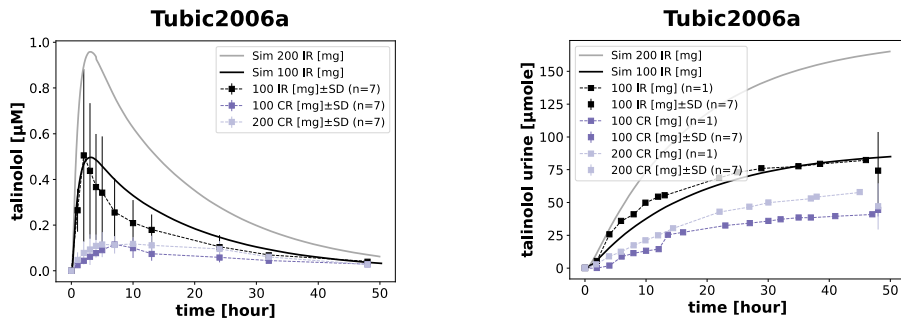


**Figure 34:** Simulation experiments Tubic2006a [83], controlled release (CR) tablets were not used. Only immediate release (IR) data was used.

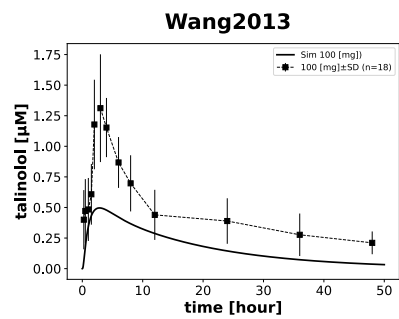


**Figure 35:** Simulation experiment Wang2013 [87], reported data was much too high for the given dose.

## References

- [1] Takaaki Abe, Masayuki Kakyo, Taro Tokui, Rie Nakagomi, Toshiyuki Nishio, Daisuke Nakai, Hideki Nomura, Michiaki Unno, Masanori Suzuki, Takeshi Naitoh, et al. “Identification of a novel gene family encoding human liver-specific organic anion transporter LST-1”. In: *Journal of Biological Chemistry* 274.24 (1999), pp. 17159–17163.
- [2] Yumiko Akamine, Masatomo Miura, Satoko Sunagawa, Hideaki Kagaya, Norio Yasui-Furukori, and Tsukasa Uno. “Influence of drug-transporter polymorphisms on the pharmacokinetics of fexofenadine enantiomers”. In: *Xenobiotica* 40.11 (2010), pp. 782–789.
- [3] Suresh V Ambudkar, Chava Kimchi-Sarfaty, Zubin E Sauna, and Michael M Gottesman. “P-glycoprotein: from genomics to mechanism”. In: *Oncogene* 22.47 (2003), pp. 7468–7485.
- [4] Monimoy Banerjee and Taosheng Chen. “Differential regulation of CYP3A4 promoter activity by a new class of natural product derivatives binding to pregnane X receptor”. In: *Biochemical pharmacology* 86.6 (2013), pp. 824–835.
- [5] Annika Bernsdorf, Thomas Giessmann, Christiane Modess, Danilo Wegner, Stefanie Igelbrink, Ute Hecker, Sierk Haenisch, Ingolf Cascorbi, Bernd Terhaag, and Werner Siegmund. “Simvastatin does not influence the intestinal P-glycoprotein and MPR2, and the disposition of talinolol after chronic medication in healthy subjects genotyped for the ABCB1, ABCC2 and SLCO1B1 polymorphisms”. In: *British journal of clinical pharmacology* 61.4 (2006), pp. 440–450.
- [6] Katrijn Bogman, Yvonne Zysset, Lukas Degen, Gérard Hopfgartner, Heike Gutmann, Jochem Alsenz, and Juergen Drewe. “P-glycoprotein and surfactants: effect on intestinal talinolol absorption”. In: *Clinical Pharmacology & Therapeutics* 77.1 (2005), pp. 24–32.
- [7] Henrike Bruckmueller, Paul Martin, Meike Kähler, Sierk Haenisch, Marek Ostrowski, Marek Drozdzik, Werner Siegmund, Ingolf Cascorbi, and Stefan Oswald. “Clinically relevant multidrug transporters are regulated by microRNAs along the human intestine”. In: *Molecular pharmaceutics* 14.7 (2017), pp. 2245–2253.
- [8] Ingolf Cascorbi. “Role of pharmacogenetics of ATP-binding cassette transporters in the pharmacokinetics of drugs”. In: *Pharmacology & therapeutics* 112.2 (2006), pp. 457–473.
- [9] Marek Drozdzik, Diana Busch, Joanna Lapczuk, Janett Müller, Marek Ostrowski, Mateusz Kurzawski, and Stefan Oswald. “Protein abundance of clinically relevant drug transporters in the human liver and intestine: a comparative analysis in paired tissue specimens”. In: *Clinical Pharmacology & Therapeutics* 105.5 (2019), pp. 1204–1212.
- [10] Marek Drozdzik, Christian Gröer, Jette Penski, Joanna Lapczuk, Marek Ostrowski, Yurong Lai, Bhagwat Prasad, Jashvant D Unadkat, Werner Siegmund, and Stefan Oswald. “Protein abundance of clinically relevant multidrug transporters along the entire length of the human intestine”. In: *Molecular pharmaceutics* 11.10 (2014), pp. 3547–3555.

- [11] Donat Dürr, Bruno Stieger, Gerd A Kullak-Ublick, Katharina M Rentsch, Hans C Steinert, Peter J Meier, and Karin Fattinger. “St John’s Wort induces intestinal P-glycoprotein/MDR1 and intestinal and hepatic CYP3A4”. In: *Clinical Pharmacology & Therapeutics* 68.6 (2000), pp. 598–604.
- [12] Gunilla Englund, Fredrik Rorsman, Anders Rönnblom, Urban Karlstrom, Lucia Lazarova, Johan Gråsjö, Andreas Kindmark, and Per Artursson. “Regional levels of drug transporters along the human intestinal tract: co-expression of ABC and SLC transporters and comparison with Caco-2 cells”. In: *European Journal of Pharmaceutical Sciences* 29.3-4 (2006), pp. 269–277.
- [13] L Fan, X-Q Mao, G-Y Tao, G Wang, F Jiang, Y Chen, Q Li, W Zhang, H-P Lei, D-L Hu, et al. “Effect of Schisandra chinensis extract and Ginkgo biloba extract on the pharmacokinetics of talinolol in healthy volunteers”. In: *Xenobiotica* 39.3 (2009), pp. 249–254.
- [14] Lan Fan, Gong-You Tao, Guo Wang, Yao Chen, Wei Zhang, Yi-Jing He, Qing Li, He-Ping Lei, Feng Jiang, Dong-Li Hu, et al. “Effects of Ginkgo biloba extract ingestion on the pharmacokinetics of talinolol in healthy Chinese volunteers”. In: *Annals of Pharmacotherapy* 43.5 (2009), pp. 944–949.
- [15] H-D Faulhaber, I Weigmann, U Lang, F Weinsberg, and B Terhaag. “Anti-anginal and anti-ischemic effects of the selective  $\beta$ -blocker talinolol in patients with stable angina pectoris.” In: *International Journal of Clinical Pharmacology & Therapeutics* 43.2 (2005).
- [16] Martin F Fromm. “Importance of P-glycoprotein at blood–tissue barriers”. In: *Trends in pharmacological sciences* 25.8 (2004), pp. 423–429.
- [17] Thomas Giessmann, Karen May, Christiane Modess, Danilo Wegner, Ute Hecker, Michael Zschiesche, Peter Dazert, Markus Grube, Eike Schroeder, Rolf Warzok, et al. “Carbamazepine regulates intestinal P-glycoprotein and multidrug resistance protein MRP2 and influences disposition of talinolol in humans”. In: *Clinical Pharmacology & Therapeutics* 76.3 (2004), pp. 192–200.
- [18] Thomas Gramatté, Reinhard Oertel, Bernd Terhaag, and Wilhelm Kirch. “Direct demonstration of small intestinal secretion and site-dependent absorption of the  $\beta$ -blocker talinolol in humans”. In: *Clinical Pharmacology & Therapeutics* 59.5 (1996), pp. 541–549.
- [19] J Grzegorzewski, F Bartsch, A Köller, and M König. “Pharmacokinetics of Caffeine: A Systematic Analysis of Reported Data for Application in Metabolic Phenotyping and Liver Function Testing. Front. Pharmacol. 12: 752826. doi: 10.3389/fphar.2021.752826”. In: *Frontiers in Pharmacology—www.frontiersin.org* 12 (2022).
- [20] Jan Grzegorzewski, Florian Bartsch, Adrian Köller, and Matthias König. “Pharmacokinetics of Caffeine: A Systematic Analysis of Reported Data for Application in Metabolic Phenotyping and Liver Function Testing”. In: *Frontiers in Pharmacology* 12 (2022). DOI: 10.3389/fphar.2021.752826. URL: <https://www.frontiersin.org/article/10.3389/fphar.2021.752826> (visited on 02/26/2022).
- [21] Jan Grzegorzewski, Janosch Brandhorst, and Matthias König. “Physiologically based pharmacokinetic (PBPK) modeling of the role of CYP2D6 polymorphism for metabolic phenotyping with dextromethorphan”. In: *bioRxiv* (2022).

- [22] Y Han, D Guo, Y Chen, Z-R Tan, and H-H Zhou. “Effect of continuous silymarin administration on oral talinolol pharmacokinetics in healthy volunteers”. In: *Xenobiotica* 39.9 (2009), pp. 694–699.
- [23] Iain S Haslam, K Jones, T Coleman, and NL Simmons. “Rifampin and digoxin induction of MDR1 expression and function in human intestinal (T84) epithelial cells”. In: *British journal of pharmacology* 154.1 (2008), pp. 246–255.
- [24] KO Haustein and K Fritzsche. “On the pharmacokinetics of talinolol, a new beta 1-receptor blocking agent.” In: *International Journal of Clinical Pharmacology, Therapy, and Toxicology* 19.9 (1981), pp. 392–395.
- [25] Juan He, Bernd Terhaag, Li-Ying Yang, Bi-Kui Zhang, Fen-Li Su, Yun-Gui Zhu, Juan Song, Jing Tang, Xiao-Lei Liu, and Wen-Xing Peng. “Determination of talinolol in human plasma by high performance liquid chromatography–electrospray ionization mass spectrometry: Application to pharmacokinetic study”. In: *Journal of Chromatography B* 853.1-2 (2007), pp. 275–280.
- [26] X He, L Mo, Z-Y Li, Z-R Tan, Y Chen, and D-S Ouyang. “Effects of curcumin on the pharmacokinetics of talinolol in human with ABCB1 polymorphism”. In: *Xenobiotica* 42.12 (2012), pp. 1248–1254.
- [27] Irving P Herman. *Physics of the human body*. Springer, 2016.
- [28] SOOHPJAITIMU Hoffmeyer, Oliver Burk, Oliver Von Richter, Hans P Arnold, Jürgen Brockmöller, Andreas Johne, Ingolf Cascorbi, Thomas Gerloff, Ivar Roots, Michel Eichelbaum, et al. “Functional polymorphisms of the human multidrug-resistance gene: multiple sequence variations and correlation of one allele with P-glycoprotein expression and activity in vivo”. In: *Proceedings of the National Academy of Sciences* 97.7 (2000), pp. 3473–3478.
- [29] Masanori Horinouchi, Toshiyuki Sakaeda, Tsutomu Nakamura, Yoshinori Morita, et al. “Significant genetic linkage of MDR1 polymorphisms at positions 3435 and 2677: functional relevance to pharmacokinetics of digoxin”. In: *Pharmaceutical research* 19.10 (2002), p. 1581.
- [30] G Hounnou, C Destrieux, J Desme, P Bertrand, and S Velut. “Anatomical study of the length of the human intestine”. In: *Surgical and radiologic anatomy* 24.5 (2002), p. 290.
- [31] Michael Hucka, Frank T Bergmann, Claudine Chaouiya, Andreas Dräger, Stefan Hoops, Sarah M Keating, Matthias König, Nicolas Le Novère, Chris J Myers, Brett G Olivier, et al. “The Systems Biology Markup Language (SBML): Language Specification for Level 3 Version 2 Core Release 2”. In: *Journal of Integrative Bioinformatics* (2019). DOI: [10.1515/jib-2019-0021](https://doi.org/10.1515/jib-2019-0021).
- [32] Ichiro Ieiri, Yohei Doi, Kazuya Maeda, Tomohiro Sasaki, Miyuki Kimura, Takeshi Hirota, Takeshi Chiyoda, Mayuko Miyagawa, Shin Irie, Kazuhide Iwasaki, et al. “Microdosing clinical study: pharmacokinetic, pharmacogenomic (SLCO2B1), and interaction (grapefruit juice) profiles of celiprolol following the oral microdose and therapeutic dose”. In: *The Journal of Clinical Pharmacology* 52.7 (2012), pp. 1078–1089.

- [33] Junko Imanaga, Tsutomu Kotegawa, Hiromitsu Imai, Kimiko Tsutsumi, Tsuneaki Yoshizato, Tetsuji Ohyama, Yoshiyuki Shirasaka, Ikumi Tamai, Tomonori Tateishi, and Kyoichi Ohashi. “The effects of the SLCO2B1 c. 1457C>T polymorphism and apple juice on the pharmacokinetics of fexofenadine and midazolam in humans”. In: *Pharmacogenetics and genomics* 21.2 (2011), pp. 84–93.
- [34] Gunn Signe Jakobsen, Milada Cvancarova Småstuen, Rune Sandbu, Njord Nordstrand, Dag Hofsø, Morten Lindberg, Jens Kristoffer Hertel, and Jørn Hjelmesæth. “Association of bariatric surgery vs medical obesity treatment with long-term medical complications and obesity-related comorbidities”. In: *Jama* 319.3 (2018), pp. 291–301.
- [35] HM Jones and Karen Rowland-Yeo. “Basic concepts in physiologically based pharmacokinetic modeling in drug discovery and development”. In: *CPT: pharmacometrics & systems pharmacology* 2.8 (2013), pp. 1–12.
- [36] He Juan, Bernd Terhaag, Zang Cong, Zhang Bi-Kui, Zhu Rong-Hua, Wang Feng, Su Fen-Li, Song Juan, Tang Jing, and Peng Wen-Xing. “Unexpected effect of concomitantly administered curcumin on the pharmacokinetics of talinolol in healthy Chinese volunteers”. In: *European journal of clinical pharmacology* 63.7 (2007), pp. 663–668.
- [37] Sarah M. Keating, Dagmar Waltemath, Matthias König, Fengkai Zhang, Andreas Dräger, Claudine Chaouiya, Frank T. Bergmann, Andrew Finney, Colin S. Gillespie, Tomáš Helikar, Stefan Hoops, Rahuman S. Malik-Sheriff, Stuart L. Moodie, Ion I. Moraru, Chris J. Myers, Aurélien Naldi, Brett G. Olivier, Sven Sahle, James C. Schaff, Lucian P. Smith, Maciej J. Swat, Denis Thieffry, Leandro Watanabe, Darren J. Wilkinson, Michael L. Blinov, Kimberly Begley, James R. Faeder, Harold F. Gómez, Thomas M. Hamm, Yuichiro Inagaki, Wolfram Liebermeister, Allyson L. Lister, Daniel Lucio, Eric Mjolsness, Carole J. Proctor, Karthik Raman, Nicolas Rodriguez, Clifford A. Shaffer, Bruce E. Shapiro, Joerg Stelling, Neil Swainston, Naoki Tanimura, John Wagner, Martin Meier-Schellersheim, Herbert M. Sauro, Bernhard Palsson, Hamid Bolouri, Hiroaki Kitano, Akira Funahashi, Henning Hermjakob, John C. Doyle, Michael Hucka, and S.B.M.L. Level 3 Community members. “SBML Level 3: An Extensible Format for the Exchange and Reuse of Biological Models.” In: *Molecular systems biology* 16.8 (Aug. 2020), e9110. doi: 10.15252/msb.20199110. ppublish.
- [38] Richard B Kim, Brenda F Leake, Edna F Choo, George K Dresser, Samir V Kubba, Ute I Schwarz, Amanda Taylor, Hong-Guang Xie, Joel McKinsey, Sheng Zhou, et al. “Identification of functionally variant MDR1 alleles among European Americans and African Americans”. In: *Clinical Pharmacology & Therapeutics* 70.2 (2001), pp. 189–199.
- [39] Jonny Kinzi, Markus Grube, and Henriette E Meyer Zu Schwabedissen. “OATP2B1—the underrated member of the organic anion transporting polypeptide family of drug transporters?” In: *Biochemical Pharmacology* 188 (2021), p. 114534.
- [40] Daisuke Kobayashi, Takashi Nozawa, Kozue Imai, Jun-ichi Nezu, Akira Tsuji, and Ikumi Tamai. “Involvement of human organic anion transporting polypeptide OATP-B (SLC21A9) in pH-dependent transport across intestinal apical membrane”. In: *Journal of pharmacology and experimental therapeutics* 306.2 (2003), pp. 703–708.

- [41] Robert Koch-Institut. *Dashboard zu Gesundheit in Deutschland aktuell - GEDA 2019/2020*. 2022. DOI: 10.25646/9362. URL: [https://public.tableau.com/app/profile/robert.koch.institut/viz/Gesundheit\\_in\\_Deutschland\\_aktuell/GEDA\\_20192020-EHIS](https://public.tableau.com/app/profile/robert.koch.institut/viz/Gesundheit_in_Deutschland_aktuell/GEDA_20192020-EHIS) (visited on 07/14/2023).
- [42] Adrian Köller, Jan Grzegorzewski, and Matthias König. “Physiologically based modeling of the effect of physiological and anthropometric variability on indocyanine green based liver function tests”. In: *Frontiers in physiology* (2021), p. 2043.
- [43] Adrian Köller, Jan Grzegorzewski, Hans-Michael Tautenhahn, and Matthias König. “Prediction of survival after partial hepatectomy using a physiologically based pharmacokinetic model of indocyanine green liver function tests”. In: *Frontiers in physiology* 12 (2021), p. 730418.
- [44] Jörg König, Yunhai Cui, Anne T Nies, and Dietrich Keppler. “A novel human organic anion transporting polypeptide localized to the basolateral hepatocyte membrane”. In: *American Journal of Physiology-Gastrointestinal and Liver Physiology* 278.1 (2000), G156–G164.
- [45] Matthias König. *Matthiaskoenig/Sbmlsim: 0.1.14 - SBML Simulation Made Easy*. <https://zenodo.org/record/5531088>. Computer Software. Accessed: 2022-08-23. Sept. 2021. DOI: 10.5281/zenodo.5531088.
- [46] Matthias König. *Sbmlutils: Python Utilities for SBML*. <https://zenodo.org/record/6599299>. Computer Software. Accessed: 2022-08-23. Oct. 2021. DOI: 10.5281/zenodo.5546603.
- [47] Matthias König, Andreas Dräger, and Hermann-Georg Holzhütter. “CySBML: A Cytoscape Plugin for SBML”. In: *Bioinformatics (Oxford, England)* 28.18 (2012), pp. 2402–2403. DOI: 10.1093/bioinformatics/bts432. pmid: 22772946.
- [48] Matthias König and Nicolas Rodriguez. *Matthiaskoenig/Cy3sbml: Cy3sbml-v0.3.0 - SBML for Cytoscape*. <https://zenodo.org/record/3451319>. Computer Software. Accessed: 2022-08-23. Sept. 2019. DOI: 10.5281/zenodo.3451319.
- [49] M Krueger, H Achenbach, B Terhaag, H Haase, K Richter, R Oertel, and R Preiss. “Pharmacokinetics of oral talinolol following a single dose and during steady state in patients with chronic renal failure and healthy volunteers.” In: *International journal of clinical pharmacology and therapeutics* 39.2 (2001), pp. 61–66.
- [50] Gerd A Kullak-Ublick, Manfred G Ismail, Bruno Stieger, Lukas Landmann, Robert Huber, Flavia Pizzagalli, Karin Fattinger, Peter J Meier, and Bruno Hagenbuch. “Organic anion-transporting polypeptide B (OATP-B) and its functional comparison with three other OATPs of human liver”. In: *Gastroenterology* 120.2 (2001), pp. 525–533.
- [51] Alli Laitinen and Mikko Niemi. “Frequencies of single-nucleotide polymorphisms of SLCO1A2, SLCO1B3 and SLCO2B1 genes in a Finnish population”. In: *Basic & clinical pharmacology & toxicology* 108.1 (2011), pp. 9–13.
- [52] Catia Marzolini, Erik Paus, Thierry Buclin, and Richard B Kim. “Polymorphisms in human MDR1 (P-glycoprotein): recent advances and clinical relevance”. In: *Clinical Pharmacology & Therapeutics* 75.1 (2004), pp. 13–33.
- [53] Yvonne Meier, Jyrki J Eloranta, Jutta Darimont, Manfred G Ismail, Christian Hiller, Michael Fried, Gerd A Kullak-Ublick, and Stephan R Vavricka. “Regional distribution of solute carrier mRNA expression along the human intestinal tract”. In: *Drug metabolism and Disposition* 35.4 (2007), pp. 590–594.

- [54] Christian de Mey, V Schroeter, R Butzer, P Jahn, K Weisser, U Wetterich, B Terhaag, E Mutschler, H Spahn-Langguth, and D Palm. “Dose-effect and kinetic-dynamic relationships of the beta-adrenoceptor blocking properties of various doses of talinolol in healthy humans.” In: *Journal of cardiovascular pharmacology* 26.6 (1995), pp. 879–878.
- [55] Henriette E Meyer zu Schwabedissen, Markus Grube, and Heyo K Kroemer. “Pharmacogenetics of drug transporters”. In: *Pharmacogenetics and Individualized Therapy* (2012), pp. 101–148.
- [56] Stéphane Mouly and Mary F Paine. “P-glycoprotein increases from proximal to distal regions of human small intestine”. In: *Pharmaceutical research* 20 (2003), pp. 1595–1599.
- [57] Takeo Nakanishi and Ikumi Tamai. “Genetic polymorphisms of OATP transporters and their impact on intestinal absorption and hepatic disposition of drugs”. In: *Drug metabolism and pharmacokinetics* 27.1 (2012), pp. 106–121.
- [58] MA Nguyen, P Staubach, I Tamai, and P Langguth. “High-dose short-term administration of naringin did not alter talinolol pharmacokinetics in humans”. In: *European Journal of Pharmaceutical Sciences* 68 (2015), pp. 36–42.
- [59] MA Nguyen, P Staubach, S Wolffram, and P Langguth. “Effect of single-dose and short-term administration of quercetin on the pharmacokinetics of talinolol in humans—implications for the evaluation of transporter-mediated flavonoid–drug interactions”. In: *European Journal of Pharmaceutical Sciences* 61 (2014), pp. 54–60.
- [60] Masuhiro Nishimura and Shinsaku Naito. “Tissue-specific mRNA expression profiles of human phase I metabolizing enzymes except for cytochrome P450 and phase II metabolizing enzymes”. In: *Drug metabolism and pharmacokinetics* 21.5 (2006), pp. 357–374.
- [61] Takashi Nozawa, Miki Nakajima, Ikumi Tamai, Kumiko Noda, Jun-ichi Nezu, Sai Yoshimichi, Akira Tsuji, and Tsuyoshi Yokoi. “Genetic polymorphisms of human organic anion transporters OATP-C (SLC21A6) and OATP-B (SLC21A9): allele frequencies in the Japanese population and functional analysis”. In: *Journal of Pharmacology and Experimental Therapeutics* 302.2 (2002), pp. 804–813.
- [62] R Oertel, K Richter, B Trausch, A Berndt, T Gramatte, and W Kirch. “Elucidation of the structure of talinolol metabolites in man determination of talinolol and hydroxylated talinolol metabolites in urine and analysis of talinolol in serum”. In: *Journal of Chromatography B: Biomedical Sciences and Applications* 660.2 (1994), pp. 353–363.
- [63] Zhao Ruike, Cao Junhua, and Peng Wenxing. “In vitro and in vivo evaluation of the effects of duloxetine on P-gp function”. In: *Human Psychopharmacology: Clinical and Experimental* 25.7-8 (2010), pp. 553–559.
- [64] UI Schwarz, H Hanso, R Oertel, S Miehlke, E Kuhlisch, H Glaeser, M Hitzl, GK Dresser, RB Kim, and W Kirch. “Induction of intestinal P-glycoprotein by St John’s wort reduces the oral bioavailability of talinolol”. In: *Clinical Pharmacology & Therapeutics* 81.5 (2007), pp. 669–678.
- [65] Ute I Schwarz, Thomas Gramatté, Jutta Krappweis, Annette Berndt, Reinhard Oertel, Oliver von Richter, and Wilhelm Kirch. “Unexpected effect of verapamil on oral bioavailability of the  $\beta$ -blocker talinolol in humans”. In: *Clinical Pharmacology & Therapeutics* 65.3 (1999), pp. 283–290.

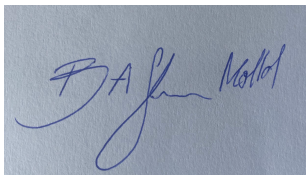
- [66] Ute I Schwarz, Thomas Gramatté, Jutta Krappweis, Reinhard Oertel, and Wilhelm Kirch. “P-glycoprotein inhibitor erythromycin increases oral bioavailability of talinolol in humans.” In: *International journal of clinical pharmacology and therapeutics* 38.4 (2000), pp. 161–167.
- [67] Ute I Schwarz, Diana Seemann, Reinhard Oertel, Stephan Miehlke, Eberhard Kuhlich, Martin F Fromm, Richard B Kim, David G Bailey, and Wilhelm Kirch. “Grapefruit juice ingestion significantly reduces talinolol bioavailability”. In: *Clinical Pharmacology & Therapeutics* 77.4 (2005), pp. 291–301.
- [68] Yoshiyuki Shirasaka, Erika Kuraoka, Hildegard Spahn-Langguth, Takeo Nakanishi, Peter Langguth, and Ikumi Tamai. “Species difference in the effect of grapefruit juice on intestinal absorption of talinolol between human and rat”. In: *Journal of Pharmacology and Experimental Therapeutics* 332.1 (2010), pp. 181–189.
- [69] Werner Siegmund, Karen Ludwig, Georg Engel, Michael Zschiesche, Gerd Franke, Anna Hoffmann, Bernd Terhaag, and Werner Weitsches. “Variability of intestinal expression of P-glycoprotein in healthy volunteers as described by absorption of talinolol from four bioequivalent tablets”. In: *Journal of pharmaceutical sciences* 92.3 (2003), pp. 604–610.
- [70] Werner Siegmund, Karen Ludwig, Thomas Giessmann, Peter Dazert, Eike Schroeder, Bernhard Sperker, Rolf Warzok, Heyo K Kroemer, and Ingolf Cascorbi. “The effects of the human MDR1 genotype on the expression of duodenal P-glycoprotein and disposition of the probe drug talinolol”. In: *Clinical pharmacology & therapeutics* 72.5 (2002), pp. 572–583.
- [71] Giovanni de Simone, Richard Devereux, Stephen R Daniels, GianFrancesco Mureddu, Mary J Roman, Thomas R Kimball, Rosanna Greco, Sandra Witt, and Franco Contaldo. “Stroke volume and cardiac output in normotensive children and adults: assessment of relations with body size and impact of overweight”. In: *Circulation* 95.7 (1997), pp. 1837–1843.
- [72] Nicola F Smith, William D Figg, and Alex Sparreboom. “Role of the liver-specific transporters OATP1B1 and OATP1B3 in governing drug elimination”. In: *Expert opinion on drug metabolism & toxicology* 1.3 (2005), pp. 429–445.
- [73] Endre T Somogyi, Jean-Marie Bouteiller, James A Glazier, Matthias König, J Kyle Medley, Maciej H Swat, and Herbert M Sauro. “libRoadRunner: A High Performance SBML Simulation and Analysis Library”. In: *Bioinformatics (Oxford, England)* 31.20 (2015), pp. 3315–3321. DOI: 10.1093/bioinformatics/btv363.
- [74] Beatrice Amelie Stemmer Mallol and Matthias König. *Physiologically based pharmacokinetic (PBPK) model of talinolol*. Version 0.9.2. July 2023. DOI: 10.5281/zenodo.8150144. URL: <https://doi.org/10.5281/zenodo.8150144>.
- [75] Cordula Stillhart, Katarina Vučićević, Patrick Augustijns, Abdul W Basit, Hannah Batchelor, Talia R Flanagan, Ina Gesquiere, Rick Greupink, Daniel Keszthelyi, Mikko Koskinen, et al. “Impact of gastrointestinal physiology on drug absorption in special populations - An UNGAP review”. In: *European Journal of Pharmaceutical Sciences* 147 (2020), p. 105280.
- [76] Ikumi Tamai, Jun-ichi Nezu, Hiroshi Uchino, Yoshimichi Sai, Asuka Oku, Miyuki Shimane, and Akira Tsuji. “Molecular identification and characterization of novel members of the human organic anion transporter (OATP) family”. In: *Biochemical and biophysical research communications* 273.1 (2000), pp. 251–260.

- [77] B Terhaag, Th Gramatte, K Richter, J Voss, and K Feller. “The biliary elimination of the selective beta-receptor blocking drug talinolol in man.” In: *International journal of clinical pharmacology, therapy, and toxicology* 27.4 (1989), pp. 170–172.
- [78] B Terhaag, K Richter, and H Pötter. “Pharmacokinetics of talinolol (Cordanum) in man after oral administration”. In: *Die Pharmazie* 38.8 (1983), pp. 568–569.
- [79] Franz Thiebaut, Takashi Tsuru, Hirofumi Hamada, Michael M Gottesman, IRA Pastan, and Mark C Willingham. “Cellular localization of the multidrug-resistance gene product P-glycoprotein in normal human tissues.” In: *Proceedings of the National Academy of Sciences* 84.21 (1987), pp. 7735–7738.
- [80] Rommel G Tirona, Brenda F Leake, Gracia Merino, and Richard B Kim. “Polymorphisms in OATP-C: identification of multiple allelic variants associated with altered transport activity among European-and African-Americans”. In: *Journal of Biological Chemistry* 276.38 (2001), pp. 35669–35675.
- [81] Beate Trausch, R Oertel, K Richter, and T Gramatte. “Disposition and bioavailability of the  $\beta$ 1-adrenoceptor antagonist talinolol in man”. In: *Biopharmaceutics & drug disposition* 16.5 (1995), pp. 403–414.
- [82] Matthew D Troutman and Dhiren R Thakker. “Efflux ratio cannot assess P-glycoprotein-mediated attenuation of absorptive transport: asymmetric effect of P-glycoprotein on absorptive and secretory transport across Caco-2 cell monolayers”. In: *Pharmaceutical research* 20 (2003), pp. 1200–1209.
- [83] Marija Tubic, Daniel Wagner, Hildegard Spahn-Langguth, Christine Weiler, Roland Wanitschke, Wulf Otto Böcher, and Peter Langguth. “Effects of controlled-release on the pharmacokinetics and absorption characteristics of a compound undergoing intestinal efflux in humans”. In: *European journal of pharmaceutical sciences* 29.3-4 (2006), pp. 231–239.
- [84] Jack Valentin. “Basic anatomical and physiological data for use in radiological protection: reference values: ICRP Publication 89”. In: *Annals of the ICRP* 32.3-4 (2002), pp. 1–277.
- [85] Arthur J Vander, James H Sherman, and Dorothy S Luciano. “Human physiology: the mechanisms of body function”. In: *(No Title)* (2001).
- [86] Li Wang, Carol Collins, Edward J Kelly, Xiaoyan Chu, Adrian S Ray, Laurent Salphati, Guangqing Xiao, Caroline Lee, Yurong Lai, Mingxiang Liao, et al. “Transporter expression in liver tissue from subjects with alcoholic or hepatitis C cirrhosis quantified by targeted quantitative proteomics”. In: *Drug Metabolism and Disposition* 44.11 (2016), pp. 1752–1758.
- [87] SY Wang, KM Duan, Y Li, Y Mei, H Sheng, H Liu, X Mei, W Ouyang, HH Zhou, and ZQ Liu. “Effect of quercetin on P-glycoprotein transport ability in Chinese healthy subjects”. In: *European journal of clinical nutrition* 67.4 (2013), pp. 390–394.
- [88] Ciaran Welsh, Jin Xu, Lucian Smith, Matthias König, Kiri Choi, and Herbert M. Sauro. *libRoadRunner 2.0: A High-Performance SBML Simulation and Analysis Library*. 2022. DOI: 10.48550/arXiv.2203.01175. arXiv: 2203.01175 [cs, q-bio]. URL: <http://arxiv.org/abs/2203.01175> (visited on 08/26/2022).

- [89] Kristin Westphal, Anita Weinbrenner, Thomas Giessmann, Marko Stuhr, Gerd Franke, Michael Zschiesche, Reinhard Oertel, Bernd Terhaag, Heyo K Kroemer, and Werner Siegmund. “Oral bioavailability of digoxin is enhanced by talinolol: evidence for involvement of intestinal P-glycoprotein”. In: *Clinical Pharmacology & Therapeutics* 68.1 (2000), pp. 6–12.
- [90] Kristin Westphal, Anita Weinbrenner, Michael Zschiesche, Gerd Franke, Manfred Knoke, Reinhard Oertel, Peter Fritz, Oliver Von Richter, Rolf Warzok, Thomas Hachenberg, et al. “Induction of P-glycoprotein by rifampin increases intestinal secretion of talinolol in human beings: a new type of drug/drug interaction”. In: *Clinical Pharmacology & Therapeutics* 68.4 (2000), pp. 345–355.
- [91] Ulrike Wetterich, Hildegard Spahn-Langguth, Ernst Mutschler, Bernd Terhaag, Wolfgang Rösch, and Peter Langguth. “Evidence for intestinal secretion as an additional clearance pathway of talinolol enantiomers: concentration-and dose-dependent absorption in vitro and in vivo”. In: *Pharmaceutical research* 13 (1996), pp. 514–522.
- [92] C-Q Xiao, R Chen, J Lin, G Wang, Y Chen, Z-R Tan, and H-H Zhou. “Effect of genistein on the activities of cytochrome P450 3A and P-glycoprotein in Chinese healthy participants”. In: *Xenobiotica* 42.2 (2012), pp. 173–178.
- [93] “3 - Biomechanics of the Digestive System”. In: *Integrated Nano-Biomechanics*. Ed. by Takami Yamaguchi, Takuji Ishikawa, and Yohsuke Imai. Micro and Nano Technologies. Boston: Elsevier, 2018, pp. 71–99. DOI: <https://doi.org/10.1016/B978-0-323-38944-0.00003-6>. URL: <https://www.sciencedirect.com/science/article/pii/B9780323389440000036>.
- [94] Miao Yan, Ping-Fei Fang, Huan-De Li, Ping Xu, Yi-Ping Liu, Feng Wang, Hua-Lin Cai, and Qin-You Tan. “Lack of effect of continuous glycyrrhizin administration on the pharmacokinetics of the P-glycoprotein substrate talinolol in healthy volunteers”. In: *European journal of clinical pharmacology* 69.3 (2013), pp. 515–521.
- [95] Y Zeng, F-Y He, Y-J He, L-L Dai, L Fan, and H-H Zhou. “Effect of bifendate on the pharmacokinetics of talinolol in healthy subjects”. In: *Xenobiotica* 39.11 (2009), pp. 844–849.
- [96] Wei-Xia Zhang, Guo-Lin Chen, Zhi-Rong Tan, Jie Liu, Gan Zhou, Dong-Li Hu, Hong-Hao Zhou, et al. “MDR1 genotype do not influence the absorption of a single oral dose of 100 mg talinolol in healthy Chinese males”. In: *Clinica chimica acta* 359.1-2 (2005), pp. 46–52.
- [97] Michael Zschiesche, Girum Lakew Lemma, Klaus-Jürgen Klebingat, Gerd Franke, Bernd Terhaag, Anna Hoffmann, Thomas Gramatté, Heyo K Kroemer, and Werner Siegmund. “Stereoselective disposition of talinolol in man”. In: *Journal of pharmaceutical sciences* 91.2 (2002), pp. 303–311.

## Eigenständigkeitserklärung

Hiermit erkläre ich, dass ich die vorliegende Arbeit selbständig verfasst habe und sämtliche Quellen, einschließlich Internetquellen, die unverändert oder abgewandelt wiedergegeben werden, insbesondere Quellen für Texte, Grafiken, Tabellen und Bilder, als solche kenntlich gemacht habe. Ich versichere, dass ich die vorliegende Abschlussarbeit noch nicht für andere Prüfungen eingereicht habe. Mir ist bekannt, dass bei Verstößen gegen diese Grundsätze ein Verfahren wegen Täuschungsversuchs bzw. Täuschung gemäß der fachspezifischen Prüfungsordnung und/oder der Fächerübergreifenden Satzung zur Regelung von Zulassung, Studium und Prüfung der Humboldt-Universität zu Berlin (ZSP-HU) eingeleitet wird.

A handwritten signature in blue ink, appearing to read "BA Stemmer Mallol".

Berlin, den 15. Juli 2023, Beatrice Amelie Stemmer Mallol